MARIA EDUARDA TESSER

EFEITOS DE NANOPARTÍCULAS METÁLICAS BIOGÊNICAS (AG, TIO2, FE) PARA DUAS ESPÉCIES DULCÍCOLAS:

O BIVALVE ANODONTITES TRAPESIALIS E O TELEÓSTEO PROCHILODUS LINEATUS

Londrina
2021

MARIA EDUARDA TESSER

EFEITOS DE NANOPARTÍCULAS METÁLICAS BIOGÊNICAS (AG, TIO2, FE) PARA DUAS ESPÉCIES DULCÍCOLAS:

O BIVALVE ANODONTITES TRAPESIALIS E O TELEÓSTEO PROCHILODUS LINEATUS

Dissertação apresentada ao Programa de Pós-Graduação em Ciências Fisiológicas da Universidade Estadual de Londrina, como requisito parcial para a obtenção do título de Mestre.

Orientadora: Prof.ª Dr.ª Claudia Bueno dos Reis Martinez

Londrina
2021

Ficha de identificação da obra elaborada pelo autor, através do Programa de Geração Automática do Sistema de Bibliotecas da UEL

T338e Tesser, Maria Eduarda.

Efeitos de nanopartículas metálicas biogênicas (Ag, TiO_2, Fe) para duas espécies dulcícolas: o bivalve *Anodontites trapesialis* e o teleósteo *Prochilodus lineatus* / Maria Eduarda Tesser. - Londrina, 2021.
112 f.

Orientador: Claudia Bueno dos Reis Martinez.
Dissertação (Mestrado em Ciências Fisiológicas) - Universidade Estadual de Londrina, Centro de Ciências Biológicas, Programa de Pós-Graduação em Ciências Fisiológicas, 2021.
Inclui bibliografia.

1. Fisiologia animal comparada - Tese. 2. Ecotoxicologia de agrotóxicos alternativos - Tese. 3. Ecotoxicologia de nanopartículas metálicas - Tese. 4. Biomarcadores de contaminação aquática - Tese. I. Martinez, Claudia Bueno dos Reis. II. Universidade Estadual de Londrina. Centro de Ciências Biológicas. Programa de Pós-Graduação em Ciências Fisiológicas. III. Título.

CDU 574

MARIA EDUARDA TESSER

EFEITOS DE NANOPARTÍCULAS METÁLICAS BIOGÊNICAS (AG, TIO2, FE) PARA DUAS ESPÉCIES DULCÍCOLAS:

O BIVALVE ANODONTITES TRAPESIALIS E O TELEÓSTEO PROCHILODUS LINEATUS

Dissertação apresentada ao Programa de Pós-Graduação em Ciências Fisiológicas da Universidade Estadual de Londrina, como requisito parcial para a obtenção do título de Mestre.

BANCA EXAMINADORA

_____

Dr.ª Claudia Bueno dos Reis Martinez
Universidade Estadual de Londrina – UEL

_____

Dr.ª Jimena Cazenave
Universidad Nacional del Litoral – UNL
Argentina

_____

Dr.ª Susana Patrícia Mendes Loureiro
Universidade de Aveiro – UA
Portugal

Londrina, 31 de agosto de 2021.

AGRADECIMENTOS

À Universidade Estadual de Londrina (UEL).

Ao Programa de Pós-Graduação em Ciências Fisiológicas (PGCIF).

À Coordenação de Aperfeiçoamento de Pessoal de Nível Superior (CAPES), pela concessão da bolsa de Mestrado.

Ao Conselho Nacional de Desenvolvimento Científico e Tecnológico (CNPq) e à *Fundação de Amparo à Pesquisa do Estado de São Paulo* (FAPESP), pelo financiamento desta pesquisa.

À Dr.ª Jimena Cazenave e à Dr.ª Susana Loureiro, pela disponibilidade em participar da minha banca examinadora. Ao Dr. Carlos Eduardo Delfino Vieira (Universidade Estadual do Norte do Paraná, UENP) e à Dr.ª Mariana Machado Lauer (UEL), por também se disponibilizarem como membros suplentes.

À minha banca de qualificação, Dr. Halley Caixeta de Oliveira (UEL) e Dr.ª Renata de Lima (Universidade de Sorocaba, UNISO), pelas contribuições a este trabalho.

À Dr.ª Renata de Lima, pela parceria científica para a avaliação ecotoxicológica das nanopartículas sintetizadas pelo seu grupo de pesquisa, e por ter sido sempre solícita. À Dr.ª Mariana Guilger Casagrande, à Dr.ª Tatiane Pasquoto Stigliani e à M.ª Nathalia Bilesky-José, também da UNISO, pela síntese e caracterização das nanopartículas utilizadas neste trabalho, e pelo suporte quando precisei.

À Dr.ª Claudia Bueno dos Reis Martinez, pela orientação acadêmica e pessoal. Claudia, é uma honra ser orientada por você, que ao mesmo tempo que é uma pesquisadora de excelência, é humana, ética, e acredita no potencial dos seus alunos e se preocupa com eles. Agradeço pela convivência leve e por ter conhecido você, que sempre será um exemplo para mim.

Ao Dr. Wagner Ezequiel Risso (UEL) e Dr. Adalto Bianchini (Universidade Federal do Rio Grande, FURG), pela ajuda com as análises de metais.

Ao Laboratório de Ecofisiologia Animal (LEFA), pelo imenso aprendizado e oportunidade de conhecer a pesquisa científica.

Aos integrantes do LEFA, pela ajuda nas amostragens e análises.

Tesser, Maria Eduarda. **Efeitos de nanopartículas metálicas biogênicas (Ag, TiO2, Fe) para duas espécies dulcícolas: o bivalve Anodontites trapesialis e o teleósteo Prochilodus lineatus.** 2021. 112 f. Dissertação (Mestrado em Ciências Fisiológicas) – Universidade Estadual de Londrina, Londrina, 2021.

RESUMO

Nanopartículas de prata, de dióxido de titânio e de ferro, sintetizadas a partir do fungo Trichoderma harzianum, possuem uso agrícola promissor. No entanto, possíveis efeitos devem ser avaliados em animais aquáticos, os quais podem entrar em contato com contaminantes agrícolas. Assim, o objetivo deste trabalho foi avaliar os efeitos subletais da exposição de curto período (24 h) a nanopartículas de prata (AgNP), de dióxido de titânio (TiO2NP) e de ferro (FeNP), sintetizadas com T. harzianum, para o bivalve Anodontites trapesialis e para o teleósteo Prochilodus lineatus, ambas espécies dulcícolas e nativas. Foram realizados experimentos independentes para cada espécie. Bivalves adultos ou teleósteos juvenis foram divididos em quatro grupos: grupo controle, mantido apenas em água; grupo exposto às AgNP; grupo exposto às TiO2NP; e grupo exposto às FeNP. Os bivalves expostos às AgNP acumularam prata e apresentaram diminuição de sódio e cloreto na hemolinfa, enquanto as exposições às TiO2NP e às FeNP levaram ao acúmulo de titânio e de ferro, respectivamente, sem evidências de efeitos adicionais. Para teleósteos, as AgNP provocaram acúmulo de prata, alterações histológicas nas brânquias, aumento de glicose, lactato e potássio plasmáticos, diminuição de cálcio plasmático, diminuição na contagem de leucócitos circulantes e redução da concentração de glutationa (GSH) e da atividade da glutationa S-transferase (GST) no fígado. As TiO2NP provocaram acúmulo de titânio, diminuição de cálcio plasmático, diminuição da GST e aumento de glicogênio no fígado. As FeNP provocaram acúmulo de Fe em todos os tecidos e fluidos avaliados (brânquias, fígado, rim posterior, cérebro, músculo, plasma e bile), aumento na contagem de leucócitos circulantes, diminuição de GSH e aumento de lipoperoxidação (LPO) nas brânquias, diminuição da GST e aumento de glicogênio no fígado. As alterações histológicas nas brânquias se relacionam com o aumento de glicose, lactato e K+ plasmáticos, indicando o comprometimento das trocas gasosas associado às AgNP. Nesse grupo, a diminuição de GSH pode estar relacionada à ligação da prata com grupamentos sulfidrila. Por outro lado, nos teleósteos expostos às FeNP, a diminuição de GSH e aumento da LPO evidencia estresse oxidativo nas brânquias, e o acúmulo de Fe em diversos tecidos indica biodisponibilidade do Fe quando na forma de FeNP. Todas as NPs levaram à diminuição da GST no fígado, o que pode comprometer a biotransformação. Entre os tecidos, as brânquias foram o principal órgão-alvo da toxicidade das AgNP e FeNP, enquanto que o fígado foi o principal órgão-alvo das TiO2NP. Todas as nanopartículas provocaram acúmulo de metal no rim posterior, plasma, e hemolinfa, o que aponta para a sensibilidade desse tecido e fluidos ao acúmulo. O bivalve A. trapesialis apresentou potencial de bioacumulação, mas se mostrou menos sensível às nanopartículas do que o teleósteo P. lineatus. Os resultados indicam que as nanopartículas não se mostraram seguras nas concentrações avaliadas. As AgNP provocaram o maior número de efeitos, o que sugere que são mais prejudiciais do que as TiO2NP e FeNP, dentro das condições avaliadas. Mais estudos são necessários para o uso seguro de nanopartículas

biológicas na agricultura.

Palavras-chave: ecotoxicologia; agrotóxico; síntese verde; biomarcadores; estresse oxidativo; osmorregulação; histopatologia; mexilhão; peixe.

Tesser, Maria Eduarda. **Effects of biogenic metallic nanoparticles (Ag, TiO2, Fe) for two freshwater species: the bivalve Anodontites trapesialis and the teleost Prochilodus lineatus.** 2021. 112 p. Master's Dissertation (Masters in Physiological Sciences) – State University of Londrina, Londrina, 2021.

ABSTRACT

Silver, titanium dioxide and iron nanoparticles synthesized from the fungus Trichoderma harzianum have promising agricultural use. However, possible effects should be evaluated in aquatic animals, which may encounter agricultural contaminants. Thus, the objective of this work was to evaluate the sublethal effects of short-term exposure (24 h) to silver (AgNP), titanium dioxide (TiO2NP) and iron (FeNP) nanoparticles synthesized with T. harzianum on the bivalve Anodontites trapesialis and on the teleost Prochilodus lineatus, both freshwater and native species. Independent experiments were carried out for each species. Adult bivalves or juvenile teleosts were divided into four groups: control group, kept only in water; group exposed to AgNP; group exposed to TiO2NP; and group exposed to FeNP. Bivalves exposed to AgNP accumulated silver and showed a decrease in sodium and chloride in the hemolymph, while exposures to TiO2NP and FeNP led to the accumulation of titanium and iron, respectively, without evidence of additional effects. For teleosts, AgNP caused silver accumulation, histological changes in the gills, increased plasma glucose, lactate and potassium, decreased plasma calcium, decreased circulating white blood cell count and reduced glutathione (GSH) and glutathione S-transferase (GST) activity in the liver. TiO2NP caused titanium accumulation, decreased plasma calcium, decreased GST and increased liver glycogen. FeNP caused Fe accumulation in all tissues and fluids evaluated (gill, liver, posterior kidney, brain, muscle, plasma, and bile), increased circulating leukocyte count, decreased glutathione and increased lipoperoxidation (LPO) in the gills, decreased GST and increased liver glycogen. Histological changes in the gills were related to the increase in plasma glucose, lactate and K+, indicating impairment in gas exchange associated with AgNP. In this group, the decrease in GSH may be related to silver binding with sulfhydryl groups. On the other hand, in teleosts exposed to FeNP, the decrease in GSH and increase in LPO evidence oxidative stress in the gills, and the accumulation of Fe in various tissues indicate bioavailability of Fe as FeNP. All NPs lead to a decrease in GST in the liver, which can compromise biotransformation. Among tissues, the gills were the main target organ for AgNP and FeNP toxicity, while the liver was the main target organ for TiO2NP. All nanoparticles caused metal accumulation in the posterior kidney, plasma, and hemolymph, which points to the sensitivity of this tissue and fluids to bioaccumulation. The bivalve A. trapesialis showed bioaccumulation potential, but was less sensitive to nanoparticles than the teleost P. lineatus. The results indicate that nanoparticles were not safe at the concentrations evaluated. AgNP caused most effects, which suggests that they are more harmful than TiO2NP and FeNP, under the conditions evaluated. More studies are needed for the safe use of biological nanoparticles in agriculture.

Key words: ecotoxicology; pesticide; green synthesis; biomarkers; oxidative stress; osmoregulation; histopathology; mussel; fish.

SUMÁRIO

1 INTRODUÇÃO GERAL

1.1 Expansão Agrícola e o Uso de Agrotóxicos

Segurança alimentar designa a situação em que todas as pessoas, em todos os momentos, têm acesso físico, social e econômico à comida suficiente, segura e nutritiva, que atenda suas necessidades nutricionais e preferências alimentares (FAO, 2003). Entretanto, atualmente 2 bilhões de pessoas não possuem segurança alimentar (FAO, 2020).

A produção mundial de alimentos é suficiente para 10 bilhões de pessoas (HOLT-GIMÉNEZ et al., 2012), muito mais do que a população mundial atual de 7,8 bilhões. No entanto, o desperdício de alimentos e sua má distribuição fazem com que a alta produção não resulte em alimento para todos (FAO, 2020; GODFRAY et al., 2010). Aliado a isso, a mudança climática impacta negativamente a produtividade agrícola (NASTIS; MICHAILIDIS; CHATZITHEODORIDIS, 2012) e, à medida que o século 21 avança em direção a uma população de 11 bilhões de pessoas, avança a pressão para a produção de mais alimentos.

Uma maior expansão da agricultura deve ocorrer na América do Sul e na África Subsaariana. Entretanto, a expansão da agricultura ameaça os ecossistemas, a biodiversidade e a obtenção de serviços ecossistêmicos (LAURANCE; SAYER; CASSMAN, 2014). Nesse cenário, a agricultura deve ser ainda mais eficiente para que a quantidade de terra adicional necessária seja menor. Em nações em desenvolvimento, muitas áreas apresentam agricultura relativamente ineficiente por falta de acesso a tecnologias agrícolas já existentes (SAYER; CASSMAN, 2013). O acesso a essas tecnologias, o desenvolvimento de novas tecnologias e políticas que promovam uma produção de alimentos eficiente e sustentável são cruciais para que calamidades ambientais sejam evitadas (LAURANCE; SAYER; CASSMAN, 2014).

As tecnologias para agricultura são diversas (TILMAN et al., 2002), mas o uso de agrotóxicos se destaca. No Brasil, a venda total de agrotóxicos totalizou 620 mil toneladas em 2019, o que representa um aumento de 12,97% nas vendas internas em relação ao ano de 2018, e um aumento de 282% em relação ao ano de 2000 (IBAMA, 2021a). Em 2019, os agrotóxicos mais comercializados foram

formulados à base dos seguintes ingredientes ativos, em ordem decrescente de vendas: glifosato, 2,4-D, mancozebe, acefato, atrazina, clorotalonil, dicloreto de paraquate, malationa, enxofre e corpirifós.

O uso de agrotóxicos se reflete na sua detecção nas águas superficiais (BRODEUR et al., 2020; PÉREZ et al., 2021; VIEIRA et al., 2016, 2019). Os agrotóxicos chegam ao ambiente aquático pela aplicação direta para o controle de plantas aquáticas, pelo descarte inadequado, ou após serem aplicados nas culturas agrícolas, por processos que dissipam essas substâncias do local de aplicação. Esses processos consistem, em linhas gerais, na deriva de gotículas, escoamento superficial, lixiviação e absorção pelos organismos (SOLOMON et al., 2013). A proximidade de zonas agrícolas aos corpos d'água, muitas vezes sem a presença das matas ciliares e das vegetações protetoras de nascentes, também favorece a chegada de agrotóxicos ao ambiente aquático (TOMITA; BEYRUTH, 2002).

O risco ecológico de agrotóxicos para a biota aquática pode ser avaliado a partir do conhecimento da concentração de determinados agrotóxicos no corpo de água de interesse, e dos efeitos tóxicos que esses agrotóxicos exercem sobre organismos aquáticos, avaliados a partir de estudos em laboratório. A partir de metodologias de análise de risco ecológico, Pérez et al. (2021) não encontraram risco agudo, mas encontraram uma faixa de baixo a alto risco crônico para a biota aquática em uma bacia na região dos Pampas, na Argentina, sendo que a atrazina e seus metabólitos, o glifosato e o acetocloro foram os principais resíduos de agrotóxicos que contribuíram para o aumento do risco.

Além da avaliação de risco ecológico, outra ferramenta para a análise dos efeitos da contaminação aquática consiste no biomonitoramento. O biomonitoramento ativo é capaz de esclarecer os efeitos de misturas de agrotóxicos em situações reais de exposição, em que há variações físico-químicas da água e na concentração de contaminantes ao longo do tempo. Nesse sentido, Vieira et al. (2019) confinaram indivíduos de *Prochilodus lineatus*, uma espécie de teleósteo dulcícola da região Neotropical, em um local de referência, menos suscetível à entrada de contaminantes, e em um local experimental, localizado próximo a culturas agrícolas. A partir de uma análise de múltiplos biomarcadores ao longo de 120 dias, os autores descobriram que o estado de saúde geral dos peixes confinados no local experimental diminuiu em relação aos peixes confinados no local de referência, o

que pôde ser associado à presença de agrotóxicos.

A partir dos estudos citados, evidencia-se que os agrotóxicos ameaçam os ecossistemas aquáticos, e seu uso deve ser substituído, ou pelo menos reduzido, com urgência. Nesse contexto, torna-se necessário o desenvolvimento de formulações que aumentem a eficiência agrícola ao mesmo tempo que apresentem menor impacto ecológico do que os agrotóxicos convencionais. Um crescente número de pesquisas tem buscado o desenvolvimento de tais formulações (BONOMO et al., 2020; RODRIGUES et al., 2021).

1.2 Uso de *Trichoderma* SPP. Como Uma Estratégia Para a Agricultura Sustentável

Trichoderma constitui um gênero cosmopolita de fungos filamentosos, de vida-livre e decompositores, os quais habitam solos, raízes e folhas (HARMAN et al., 2004; KREDICS et al., 2014). Além de apresentarem vida-livre, também podem estabelecer mutualismo facultativo (ou oportunista) com diversas plantas. Esses fungos beneficiam a planta hospedeira de muitas formas, incluindo proteção contra patógenos, tais como fungos parasitas (HOWELL, 2003), indução de resistência a doenças (SALDAJENO et al., 2014), aumento da imunidade (CONTRERAS-CORNEJO et al., 2014), promoção do crescimento (STEWART; HILL, 2014), aumento da disponibilidade e absorção de nutrientes (SINGH et al., 2014), e degradação de xenobióticos (COCAIGN et al., 2013; SMITH, 1995). Devido a esses benefícios, os fungos do gênero *Trichoderma* são comercializados e utilizados na agricultura como biofungicidas e biofertilizantes (CUMAGUN, 2014). De fato, os produtos microbiológicos mais produzidos e comercializados no Brasil em 2019, para aplicação na agricultura e em outros setores, foram os fungos do gênero *Trichoderma* (*T. asperellum*, *T. harzianum* e *T. koningiopsis)*, com uma produção de 109.310,32 kg (IBAMA, 2021a).

As espécies de *Trichoderma* atuam contra doenças fúngicas em plantas pelos mecanismos de competição, antibiose e micoparasitismo. A competição se dá pela ocupação do substrato e obtenção de nutrientes; a antibiose consiste no antagonismo entre um organismo e as substâncias metabólicas produzidas por outro; e o micoparasitismo é descrito como a interação parasita com

um fungo hospedeiro (HARMAN et al., 2004; HOWELL, 2003). A antibiose ocorre pela produção, por *Trichoderma*, de antimicrobianos (KESWANI et al., 2014), ao passo que o micoparasitismo se dá pela síntese de enzimas líticas como as quitinases, as quais clivam as ligações glicosídicas da quitina, um componente da parede celular de fungos (LORITO et al., 1993), bem como celulases (degradam a celulose), β-glucanases (degradam o polissacarídeo glucano) e proteases (SINGH et al., 2014).

Assim, o uso de fungos do gênero *Trichoderma* como forma de controle biológico representa uma alternativa ao uso de agrotóxicos convencionais, e constitui uma importante ferramenta para a agricultura sustentável. Contudo, o uso de *Trichoderma spp*. apresenta algumas limitações, como sua sensibilidade à luz ultravioleta, necessidade de alta umidade e baixa estabilidade térmica, o que resulta na diminuição de sua biodisponibilidade e biopersistência nas lavouras (FRACETO et al., 2019). Pesquisas recentes têm mostrado que tais limitações podem ser contornadas com o uso de novas tecnologias de aplicação, como a microencapsulação (MARUYAMA et al., 2020) e a síntese de nanopartículas metálicas (GUILGER et al., 2017).

1.3 Nanotecnologia e Nanopartículas Metálicas Biogênicas

A Organização Internacional para Padronização (*International Organization for Standardization*, ISO) define nanomaterial como o “material com qualquer dimensão externa na nanoescala ou tendo estrutura interna ou estrutura de superfície na nanoescala”, e nanoescala como “a faixa de comprimento de 1 nm a 100 nm aproximadamente” (ISO, 2015a, tradução nossa). Assim, a própria definição de nanoescala reconhece que a faixa de comprimento pode estar fora dos limites precisos. O documento citado também escreve que “os efeitos biológicos dependentes do tamanho, especificamente as interações célula-partícula e as interações ambientais relacionadas à nanotecnologia, envolvem estruturas abaixo de 1 nm e acima de 100 nm” (ISO, 2015a, tradução nossa), além de ressaltar a influência de outras propriedades físicas e químicas, além do tamanho, sobre as interações biológicas e ambientais de nanomateriais. A definição de termos possui o intuito de facilitar a comunicação. À medida que a nanotecnologia evolui, seus

termos e definições também evoluirão (ISO, 2015a).

Ainda de acordo com a ISO, os nanomateriais incluem os nano-objetos e os materiais nano-estruturados. Os nano-objetos são materiais com uma, duas ou três dimensões externas na nanoescala, ao passo que os materiais nano-estruturados possuem uma estrutura interna ou superficial em nanoescala (ISO, 2015a). As nanopartículas são nano-objetos que possuem as três dimensões externas em nanoescala (ISO, 2015b).

As nanopartículas podem ser constituídas por apenas carbono ou por moléculas orgânicas mais complexas, bem como podem ser formadas por metais e óxidos de metais (EALIAS; SARAVANAKUMAR, 2017). As nanopartículas metálicas são o foco deste trabalho, e por isso serão discutidas a seguir.

A síntese de nanopartículas metálicas pode ser dividida em *top-down* e *bottom-up*. A abordagem *top-down* reduz o tamanho de um material, ao passo que a abordagem *bottom-up* consiste na construção de nanopartículas a partir de elementos menores, como átomos e moléculas (WANG; XIA, 2004). Nesta última, podem ser utilizados agentes redutores e estabilizantes. Esses agentes podem ser processos físicos (como altas pressões e temperaturas), químicos (pelo uso de reagentes) (GAWANDE et al., 2016), ou tais agentes podem ser obtidos de extratos de organismos vivos, como plantas, bactérias e fungos, o que constitui a síntese biogênica ou biológica. A síntese biogênica possui vantagens em relação à síntese física e química por apresentar menor custo e menor geração de resíduos tóxicos (FRACETO et al., 2019; SINGH et al., 2016).

O uso de fungos na síntese biogênica de nanopartículas metálicas apresenta como vantagens a sua fácil manipulação, possibilidade de produção em larga escala e baixo custo de produção (GUILGER et al., 2017). Os fungos produzem nanopartículas por mecanismos intracelulares, no qual o metal precursor é internalizado pelo organismo, ou extracelulares, no qual o metal precursor é adicionado ao filtrado aquoso contendo biomoléculas derivadas do fungo (GUILGER-CASAGRANDE; LIMA, 2019). A síntese extracelular é a mais comumente empregada (GUILGER-CASAGRANDE; LIMA, 2019), e é também o método utilizado neste trabalho.

Diversas biomoléculas foram sugeridas como agentes redutores na síntese extracelular de nanopartículas metálicas. Em especial, aponta-se o papel da enzima nitrato redutase, dependente de NADPH/NADH (GUILGER-CASAGRANDE;

LIMA, 2019; KUMAR; MAMIDYALA, 2011). Contudo, a síntese de nanopartículas de prata já foi observada com a utilização de apenas NADPH, sem a participação da enzima nitrato redutase. Ainda, a adição de nitrato redutase causou uma diminuição na taxa de reação e aumento na distribuição de tamanho das partículas (HIETZSCHOLD et al., 2019). Outras enzimas citadas são as redutases dependentes de α-NADPH (ANIL KUMAR et al., 2007) e moléculas quinonas transportadoras de elétrons (*electron shuttle quinones*) (KAUSHAL, 2018; PRASAD, 2019).

Além de agentes redutores, algumas biomoléculas fúngicas encontradas no filtrado agem como estabilizantes (GUILGER-CASAGRANDE; LIMA, 2019). Durante a síntese biogênica, a formação de nanopartículas ocorre simultaneamente com a formação de um *capping*, isto é, um recobrimento da superfície da nanopartícula. Esse *capping* é formado por biomoléculas derivadas do organismo vivo utilizado durante a síntese, e atua como um estabilizante, bem como pode alterar a atividade e toxicidade das nanopartículas (GUILGER et al., 2017). Essas biomoléculas podem ser proteínas ou resíduos de aminoácidos que se ligam ao metal e à superfície por resíduos de cisteína ou por grupos amino e carboxila livres (GUILGER-CASAGRANDE et al., 2019).

1.4 Nanopartículas Metálicas Sintetizadas Utilizando-se *Trichoderma harzianum*

Nanopartículas de prata foram sintetizadas utilizando-se filtrados aquosos de *T. harzianum* com o objetivo de controlar o fitopatógeno *Sclerotinia sclerotiorum*, fungo causador do mofo branco da soja. Em seu primeiro trabalho (GUILGER et al., 2017), os autores avaliaram os efeitos provocados pelas nanopartículas biogênicas, nanopartículas de prata comerciais e por *T. harzianum* sobre o crescimento micelial e sobre a formação de novos escleródios em meios de cultura contendo *S. sclerotiorum*. As nanopartículas biogênicas controlaram o crescimento micelial do fitopatógeno com maior eficiência quando comparado às nanopartículas comerciais e ao tratamento com *T. harzianum*. Ainda, na maior concentração ($3{,}1 \times 10^{11}$ NPs mL^{-1}), as nanopartículas biogênicas impediram a formação de novos escleródios, ao passo que novos escleródios foram formados nas culturas tratadas com nanopartículas comerciais e *T. harzianum*. Finalmente,

este trabalho também expôs *T. harzianum* às nanopartículas biogênicas, tendo concluído que as nanopartículas não afetam o desenvolvimento do fungo, e, assim, podem ser utilizadas em conjunto com formulações de *T. harzianum* na agricultura.

Em um trabalho posterior (GUILGER-CASAGRANDE et al., 2019), os autores sintetizaram nanopartículas de prata utilizando *T. harzianum* cultivado com e sem o estímulo enzimático da parede celular de *S. sclerotiorum* (AgNP-TS e AgNP-T, respectivamente). Ambas as nanopartículas impediram o crescimento micelial e a formação de novos escleródios, porém as culturas expostas às AgNP-TS apresentaram o menor diâmetro micelial em relação às culturas expostas às AgNP-T. Guilger et al. (2019) assinalam que a maior eficiência das AgNP-TS sobre o crescimento micelial de *S. sclerotiorum* pode estar relacionado ao menor tamanho encontrado para essas nanopartículas em relação às AgNP-T, bem como devido ao estímulo da parede celular de *S. sclerotiorum*. Os autores suspeitaram que tal estímulo faria com que *T. harzianum* secretasse enzimas hidrolíticas com ação inibitória sobre o desenvolvimento de *S. sclerotiorum*. Devido a isso, avaliaram e detectaram a atividade das enzimas hidrolíticas β-1,3-glucanase, N-acetilglucosaminidase (NAGase), quitinase e protease ácida nos filtrados de *T. harzianum* com e sem estímulo, bem como nas dispersões finais de nanopartículas de prata sintetizas em ambos os filtrados (AgNP-TS e AgNP-T). Em todas as situações, encontraram a maior atividade para a enzima NAGase, seguida pela β-1,3-glucanase, quitinase e protease ácida. Quando comparadas em cada situação, as atividades das enzimas NAGase e a quitinase apresentaram maior atividade nas dispersões finais de AgNP-TS em relação às dispersões finais de AgNP-T. Nesse sentido, destaca-se um possível papel de ambas as enzimas no controle de *S. sclerotiorum*.

É importante notar que, no trabalho recém citado (GUILGER-CASAGRANDE et al., 2019), a concentração de nanopartículas foi reduzida 100 vezes em relação ao trabalho anterior (GUILGER et al., 2017), sendo, agora, 3×10^9 NPs mL^{-1}. Visto que a menor concentração ainda proporcionou o controle do fitopatógeno, os autores sugerem que a concentração de 3×10^9 NPs mL^{-1} seja a utilizada no campo.

Se as nanopartículas biogênicas são capazes de controlar o micro-organismo desejado, qual será o seu efeito sobre organismos não-alvo suscetíveis ao entrar em contato com as nanopartículas, como, por exemplo, a microbiota do

solo? Para responder a essa pergunta, Guilger et al. (2017) trataram amostras de solo com as nanopartículas de prata biogênicas e, após 15, 30, 90 e 180 dias, quantificaram genes específicos de bactérias envolvidas no ciclo do nitrogênio. Os autores encontraram diferenças evidentes no número total de bactérias e em sua distribuição somente após 90 e 180 dias. Esses achados foram interpretados como um efeito da liberação de íons prata (Ag^{+}), os quais teriam afetado a microbiota do solo de forma mais tardia devido à proteção fornecida pelo *capping* presente nas nanopartículas. De fato, quando as nanopartículas foram analisadas por espectroscopia de raios X por dispersão em energia (EDS), acoplada à microscopia eletrônica de varredura (MEV), verificou-se um pico característico da prata, confirmando a presença do metal nas nanopartículas (GUILGER et al., 2017). Assim, constatou-se que as nanopartículas de prata sintetizadas a partir de *T. harzianum* são formadas por um interior metálico constituído por prata elementar (Ag^{0}), e estabilizadas por um *capping* de biomoléculas secretas pelo fungo empregado, dentre as quais já foram identificadas as enzimas hidrolíticas β-1,3-glucanase, NAGase, quitinase e protease ácida.

Se os íons de prata foram sugeridos como uma fonte potencial de toxicidade das nanopartículas, é possível utilizar outros metais precursores? As nanopartículas formadas por outros metais promoveriam menos efeitos em organismos não-alvo, em relação às nanopartículas de prata biogênicas? A partir dessas questões, nanopartículas de titânio e de ferro foram sintetizadas utilizando-se *T. harzianum*.

As nanopartículas de titânio foram sintetizadas a partir de três diferentes precursores: óxido de titânio (II), óxido de titânio (IV) anatase e óxido de titânio (IV) rutilo. Cada precursor foi adicionado a dois tipos de filtrado aquoso de *T. harzianum*: um em que o fungo foi cultivado com o estímulo da parede celular de *S. sclerotiorum*, e outro sem o estímulo. Assim, foram sintetizadas seis dispersões finais de nanopartículas. Ao final da síntese, foi detectada a existência de conídios e micélios de *T. harzianum* em todas as dispersões (PASQUOTO-STIGLIANI, 2019).

Em seguida, o crescimento do micélio e a formação de novos escleródios foram avaliados em meios de cultura de *S. sclerotiorum* tratados com as nanopartículas na concentração de 1×10^{8} NPs mL^{-1}. As nanopartículas sintetizadas a partir do óxido de titânio (II) e óxido de titânio (IV) rutilo sem estímulo tiveram melhor atividade no controle do fitopatógeno. Em relação aos efeitos em organismos

não-alvo, a germinação, crescimento e vigor de plantas de feijão não foram afetados pela exposição às nanopartículas. Por outro lado, raízes de cebola (*Allium cepa)* expostas a nanopartículas de óxido de titânio (IV) rutilo sem estímulo apresentaram aumento no índice de alterações cromossômicas.

Diferente das nanopartículas de prata, a formação das nanopartículas de titânio não ocorre por mecanismos de oxirredução. Os autores propõem que o mecanismo para a síntese das nanopartículas de titânio biogênicas consista na dispersão do óxido de titânio em conteúdo enzimático de *T. harzianum*, e posterior adsorção de proteínas do fungo na superfície das partículas (PASQUOTO-STIGLIANI, 2019).

Por fim, as nanopartículas de ferro foram sintetizadas a partir de cloreto de ferro ($FeCl_3$). Após a síntese, a análise por difração de raios-X indicou que as nanopartículas consistiam principalmente em hematita (α-Fe_2O_3). As nanopartículas não alteraram a viabilidade celular e não levaram a alterações no índice mitótico. Na concentração de 5×10^7 NPs mL^{-1}, foram capazes de aumentar a proliferação de *T. harzianum*, o que levou à inibição do patógeno *S. sclerotiorum*, sem afetar a germinação das sementes (BILESKY-JOSÉ et al., 2021).

1.5 Efeitos da Poluição para Animais Aquáticos

A partir do momento em que as nanopartículas biológicas discutidas neste trabalho passarem a serem utilizadas na agricultura, é possível que uma parcela desse produto chegue aos corpos de água. Estima-se que a concentração de nanopartículas de prata e de ferro em águas superficiais esteja na ordem de nanogramas por litro, enquanto que a concentração de nanopartículas de dióxido de titânio chega a 1,6 $\mu g\ L^{-1}$ em rios (GOTTSCHALK; SUN; NOWACK, 2013; WANG et al., 2016).

No Brasil, a avaliação ambiental de agrotóxicos é uma exigência para seu registro, sendo composta pela avaliação do potencial de periculosidade ambiental (PPA) e avaliação de risco ambiental (ARA) (IBAMA, 2021b). Apesar do mérito dessas ferramentas e do avanço que a ARA representa no contexto nacional, o presente trabalho se preocupa com *endpoints* em níveis de organização biológica mais baixos do que os adotados pela ARA.

Adicionalmente, o Brasil não dispõe de legislação acerca de nanomateriais. O entendimento dos impactos de nanomateriais nos ecossistemas e na saúde humana é um dos tópicos de pesquisa prioritários para alcançar a sustentabilidade ambiental na América Latina (FURLEY et al., 2018). Nesse contexto, a compreensão dos efeitos biológicos de nanopartículas é essencial para sua regulamentação.

Diante do exposto, os subtópicos a seguir descrevem alguns dos principais efeitos, no nível de indivíduo, que podem decorrer da exposição a poluentes no ambiente aquático, com ênfase em teleósteos e bivalves dulcícolas. Esses efeitos consistem em mudanças bioquímicas, celulares, fisiológicas e comportamentais, as quais podem ser consideradas biomarcadores da contaminação aquática, por serem mensuráveis e indicarem exposição ou efeitos da contaminação (DEPLEDGE, 1994). Os biomarcadores são medidos em nível individual, mas podem ser preditivos de efeitos no nível populacional (COSSU-LEGUILLE; VASSEUR, 2013).

1.5.1 Efeitos Hematológicos

As análises hematológicas e plasmáticas são ferramentas de rotina utilizadas para monitorar o estado fisiológico de peixes. O sangue é um tecido composto principalmente pelas células vermelhas (eritrócitos), células brancas (leucócitos), e pelo líquido extracelular que circunda essas células, o plasma. Os peixes possuem quatro principais tipos de leucócitos no sangue: os linfócitos, envolvidos na imunocompetência; os trombócitos, responsáveis pela coagulação sanguínea; os granulócitos, como os eosinófilos, neutrófilos e basófilos, cuja função não está bem estabelecida; e os monócitos, os quais são células fagocíticas (FARRELL, 2011). As análises hematológicas podem incluir a quantificação de hemoglobina, determinação do hematócrito e contagem do número de eritrócitos, bem como o cálculo de índices hematimétricos obtidos a partir da relação entre essas variáveis. Além disso, é possível incluir a contagem total e diferencial de leucócitos. Os poluentes podem afetar as variáveis hematológicas de muitas formas, por exemplo, em decorrência de sua ação citotóxica sobre as células sanguíneas, como é o caso de nanopartículas de óxido de cobre (CHEN; KANG; LING, 2013),

pelo comprometimento da hematopoiese, como após exposição à dioxina (BELAIR; PETERSON; HEIDEMAN, 2001), e como uma resposta compensatória ao estresse respiratório, como após a exposição ao cobre (MAZON et al., 2002).

Adicionalmente, como variáveis plasmáticas tais como pH, composição eletrolítica (concentração de Na^+, Cl^-, Ca^{+2}, K^+, dentre outros) e pressões parciais de oxigênio e dióxido de carbono estão sobre controle homeostático, sua alteração é indicativa de perda da homeostase. Condições em que há perda da homeostase incluem patologias, a exposição a poluentes e a resposta de estresse (FARRELL, 2011).

1.5.2 Resposta de Estresse

A resposta de estresse é uma adaptação que permite ao animal responder imediatamente de forma generalizada à uma ameaça ou situação desafiadora (HILL; WYSE; ANDERSON, 2008). Em vertebrados, a resposta de estresse pode ser dividida em três categorias, de acordo com os níveis de organização biológica afetados. Durante a resposta primária, há aumento na concentração plasmática de catecolaminas (adrenalina e noradrenalina) e de corticoides (como o cortisol). A resposta secundária compreende os efeitos fisiológicos desses hormônios, e a resposta terciária inclui alterações fisiológicas e comportamentais que podem ser restaurativas, adaptativas ou patológicas. Somente a iniciação de cada resposta é temporalmente sequencial, ao passo que a duração de cada resposta resulta em sobreposição temporal (BOUYOUCOS et al., 2021; WENDELAAR BONGA, 2011). Assim como os vertebrados, os invertebrados também experienciam a resposta de estresse pela liberação de fatores neuroendócrinos. Em moluscos, a resposta de estresse se inicia com a liberação de noradrenalina na hemolinfa. Em ostras, a noradrenalina é liberada por células semelhantes a cromafins localizadas no coração. Assim como em vertebrados, os fatores neuroendócrinos liberados em invertebrados durante a resposta de estresse também atuam na mobilização de reservas energéticas (ADAMO, 2012).

O efeito da resposta de estresse sobre o metabolismo energético é uma de suas principais características adaptativas. Em vertebrados, as catecolaminas fornecem substratos energéticos pela quebra do glicogênio em

glicose no fígado e músculo, e pela liberação de ácidos graxos a partir do tecido adiposo. Os corticoides reforçam as ações das catecolaminas e têm efeitos metabólicos adicionais que facilitam a liberação de fontes de energia na circulação. Esses efeitos incluem o catabolismo de proteínas, a gliconeogênese, e o catabolismo de gorduras (HILL; WYSE; ANDERSON, 2008). A quantificação de cortisol na circulação sanguínea é o parâmetro de estresse mais utilizado em peixes (WENDELAAR BONGA, 2011). Além disso, a resposta de estresse pode ser compreendida por análises relacionadas ao metabolismo energético, como a quantificação de glicose na circulação e quantificação de glicogênio em tecidos.

Ademais, as catecolaminas otimizam a função cardiorrespiratória e asseguram o fornecimento adequado de oxigênio aos tecidos. Em peixes, a adrenalina aumenta o volume sistólico, a frequência cardíaca, o fluxo sanguíneo no cérebro, músculos e brânquias, e a permeabilidade branquial. A noradrenalina aumenta o número de células vermelhas por meio da contração esplênica e a afinidade da hemoglobina pelo O_2. No entanto, o aumento da permeabilidade branquial acarreta a diluição do plasma em teleósteos dulcícolas. Em peixes, o cortisol atua duplamente como glicocorticoide e mineralocorticoide. O cortisol restaura o balanço hidromineral pelo estímulo da proliferação e diferenciação de células ricas em mitocôndrias (CRM) nas brânquias, e pelo aumento da atividade da enzima Na^+/K^+-ATPase em brânquias, intestino (teleósteos marinhos) e rim (WENDELAAR BONGA, 2011).

1.5.3 Captação Iônica, Osmorregulação e Neurotoxicidade

A água doce é um ambiente hiposmótico em relação aos animais que nela habitam. Essa condição faz com que os animais dulcícolas constantemente ganhem água por osmose, ao mesmo tempo que perdem íons passivamente. A osmolaridade do líquido extracelular é mantida pela absorção de íons da água por transporte ativo e eliminação de água por meio de uma urina diluída (EVANS, 2011).

A osmolaridade nos fluidos corporais de teleósteos e bivalves varia conforme a espécie (EVANS, 2011; PORTO MARTINS MEDEIROS, 2019), mas, em geral, os bivalves dulcícolas mantém valores mais baixos de osmolaridade em relação a outros invertebrados e teleósteos dulcícolas (CUMMINGS; GRAF, 2015;

GRIFFITH, 2017). Assim como para os animais dulcícolas em geral, a osmolaridade do líquido extracelular de teleósteos e bivalves é conferida principalmente pelos íons sódio (Na^+) e cloreto (Cl^-). A absorção desses íons se dá principalmente por células especializadas localizadas nas brânquias, denominadas ionócitos, células ricas em mitocôndrias (CRM), ou células de cloreto. Os ionócitos possuem uma membrana apical (em contato com a água), e uma membrana basolateral (em contato com o sangue ou hemolinfa). A captação de Na^+ depende da atividade da enzima Na^+/K^+-ATPase, presente na membrana basolateral da célula. Essa enzima ativamente transporta Na^+ para o fluido circulatório em troca de íons potássio (K^+) criando o gradiente eletroquímico para a absorção apical de Na^+ por canais de Na^+. O excesso K^+ é regulado por canais de vazamento de K^+. A captação de Na^+ também depende da atuação da enzima H^+-ATPase, que, ao bombear H^+ para o meio externo, aumenta o gradiente elétrico que favorece a entrada de Na^+ por canais de Na^+. A captação de Na^+ também se dá pelo antiporte Na^+/H^+ (CUMMINGS; GRAF, 2015; GRIFFITH, 2017; HWANG, 2011).

A absorção de Cl^- ocorre em troca de bicarbonato (HCO_3^-). Tanto o HCO_3^- quanto o H^+ são produtos do metabolismo do animal, resultantes da atuação da enzima anidrase carbônica, que catalisa a hidrólise do gás carbônico (CO_2). Assim, a absorção de Na^+ pelo antiporte Na^+/H^+ e a absorção de cloreto pelo antiporte Cl^-/HCO_3^- estão ligadas à atividade da enzima anidrase carbônica, e ao balanço ácido-base (GRIFFITH, 2017; HWANG, 2011).

A absorção de cálcio (Ca^{+2}) em animais dulcícolas também depende de transporte ativo. Em teleósteos, a tomada desse íon ocorre nas brânquias e intestino, ao passo que, para bivalves, ainda que transportadores de Ca^{+2} tenham sido encontrados nas brânquias e no manto, o papel de cada tecido na absorção desse íon ainda não está bem estabelecido (PONDER; LINDBERG; PONDER, 2019). A absorção de Ca^{+2} é particularmente substancial em bivalves, os quais utilizam esse mineral na formação das conchas. A formação da concha também depende da atividade da enzima anidrase carbônica, a qual afeta o equilíbrio entre o íon carbonato (CO_3^{-2}) e o HCO_3^-, o que afeta a conversão entre carbonato de cálcio ($CaCO_3$) e o Ca^{+2} (GRIFFITH, 2017).

Nos ionócitos branquiais de teleósteos, a captação de Ca^{+2} ocorre através de um canal de Ca^{+2} na membrana apical, seguida pelo transporte ativo de Ca^{+2} através da membrana basolateral pela Ca^{+2}-ATPase e pelo antiporte Na^+/Ca^{+2},

o qual opera a partir do gradiente eletroquímico gerado pela Na^+/K^+-ATPase. Em bivalves, o transporte de Ca^{+2} também depende de canais de Ca^{+2} e da Ca^{+2}-ATPase, porém há também um antiporte H^+/Ca^{+2}, o qual depende de H^+ resultante da ação da anidrase carbônica (GRIFFITH, 2017).

A captação de íons pode ser afetada por poluentes, sendo um alvo frequente de metais. Muitos metais são captados pelo organismo por vias de absorção iônica, por meio do mimetismo iônico. Alguns exemplos são o cobre e a prata, os quais mimetizam o Na^+, e o zinco, chumbo, cádmio e cobalto, que mimetizam o Ca^{+2}. A captação desses metais pode resultar em morte pela deficiência de Na^+ e Ca^{+2}, por exemplo (WOOD, 2011). A captação iônica também pode ser comprometida pela inibição das enzimas de transporte. A Na^+/K^+-ATPase pode ser inibida por metais e agrotóxicos em concentrações ambientalmente relevantes (NIKINMAA, 2014a). Em alguns casos, a inibição da enzima Na^+/K^+-ATPase é o principal mecanismo de toxicidade aguda (GROSELL, 2011; WOOD, 2012).

A inibição do transporte ativo através das membranas pode ocorrer em outros órgãos além dos envolvidos na captação iônica, se o poluente for absorvido e distribuído. Essa inibição afeta todos os processos fisiológicos que dependem das diferenças de gradientes iônicos, como a propagação dos impulsos nervosos. Adicionalmente, poluentes podem afetar a transmissão sináptica modificando a atividade da enzima acetilcolinesterase (AChE) (NIKINMAA, 2014a). A inibição dessa enzima é considerada um biomarcador de efeito específico da exposição a poluentes neurotóxicos, sendo inicialmente descrita para os agrotóxicos organofosforados e carbamatos (COSSU-LEGUILLE; VASSEUR, 2013). No entanto, alterações na atividade da AChE também foram descritas após exposição de teleósteos a nanopartículas (MIRANDA et al., 2016).

1.5.4 Desintoxicação, Estresse Oxidativo e Genotoxicidade

Após sua absorção, um poluente pode ser modificado, redistribuído e eliminado (NEWMAN; CLEMENTS, 2008). A biotransformação é um processo enzimático de duas fases nas quais moléculas orgânicas lipofílicas são transformadas em moléculas hidrofílicas, o que permite sua eliminação do

organismo pela excreção. A fase 1 de biotransformação adiciona grupos polares a moléculas orgânicas ou expõe aqueles já contidos na molécula por meio de reações de oxidação, redução ou hidrólise. O grupo mais importante de enzimas da fase 1 são as enzimas do citocromo P450 (abreviado como CYP). Na fase 2, a polaridade da molécula é aumentada pela conjugação com moléculas polares endógenas, geralmente para formar íons orgânicos que podem ser excretados em solução aquosa. As glutationa S-transferases (GSTs) são um exemplo de família de enzimas da fase 2. As GSTs catalisam a conjugação da glutationa (GSH) com moléculas eletrofílicas, o que faz com que algumas isoformas da enzima também atuem como defesas antioxidantes. Os metabólitos da fase 2 são geralmente menos tóxicos do que a molécula original, mas as reações de fase 1 podem resultar em metabólitos mais tóxicos, um processo denominado bioativação. Além da bioativação, outros fatores impedem a desintoxicação, como a produção de espécies reativas de oxigênio (ERO) durante a reação enzimática (NIKINMAA, 2014b).

Além da possibilidade de ser um subproduto da biotransformação, a produção de ERO também pode ser induzida pelo xenobiótico em si. Metais com valências variadas, como ferro, cobre, manganês e cromo, induzem a produção de ERO pela reação de Fenton (MARTINEZ; SIMONATO ROCHA; MELETTI, 2021). Além da produção de ERO, poluentes podem afetar o estado redox das células pela inibição de enzimas antioxidantes, alteração na cadeia transportadora de elétrons e diminuição na concentração de glutationa (GROSELL, 2011).

O estado em que a produção de ERO excede a sua eliminação, levando a um aumento na concentração de ERO em estado estacionário, denomina-se estresse oxidativo. O estresse oxidativo causa danos a componentes celulares, como lipídeos, proteínas e o DNA, e afeta o metabolismo celular, bem como os mecanismos normais de sinalização celular. O estado redox normal é mantido pela regulação da produção e eliminação das ERO, sendo que a eliminação se dá pela atuação de sistemas antioxidantes. Exemplos de antioxidantes não enzimáticos são a vitamina C (ácido ascórbico) e vitamina E (tocoferol), polifenóis e a glutationa (GSH). Os antioxidantes enzimáticos e outras enzimas envolvidas no metabolismo da glutationa incluem a superóxido dismutase (SOD), catalase, glutationa peroxidase (GPx) e glutationa redutase (GR). A SOD catalisa a dismutação do radical superóxido ($O_2^{\bullet-}$) em oxigênio molecular (O_2) e peróxido de hidrogênio (H_2O_2). Por sua vez, a catalase catalisa a decomposição do H_2O_2 em H_2O e O_2, e a GPx utiliza a

GSH para reduzir H_2O_2 em H_2O. O *pool* de glutationa (GSH) é mantido pela GR, que reduz a glutationa oxidada (GSSG) em GSH usando NADPH. O *pool* de NADPH é mantido pela redução do $NADP^+$ por diversas enzimas (LUSHCHAK, 2016).

Os poluentes podem diretamente ou indiretamente (alterando o estado redox) provocar danos ao DNA, induzindo a formação de micronúcleos e de alterações nucleares. Micronúcleo é um corpo extranuclear formado por fragmentos de cromossomos danificados ou por cromossomos inteiros. A presença de micronúcleos em esfregaços sanguíneos é considerada um biomarcador de genotoxicidade, e sua análise pode ser complementada pela identificação de alterações eritrocíticas nucleares (CARRASCO; TILBURY; MYERS, 1990; CARROLA et al., 2014).

1.5.5 Efeitos Histológicos

Os efeitos em níveis bioquímicos e celulares podem culminar em efeitos teciduais. Não obstante, alterações teciduais também podem provocar mudanças bioquímicas e fisiológicas. No contexto da Ecotoxicologia, a histopatologia, isto é, o exame microscópico do tecido, é uma ferramenta sensível para acessar os efeitos tóxicos da exposição a poluentes (CAMARGO; MARTINEZ, 2007; PEREIRA NAVARRO LINS et al., 2017; WINKALER et al., 2001). Esses efeitos podem inclusive serem relacionados à saúde e aptidão dos indivíduos, o que permite uma maior extrapolação de efeitos para populações e comunidades. De fato, a histopatologia é considerada um elo entre os ensaios moleculares, bioquímicos e celulares, e estudos que envolvem organismos ou populações inteiras (CHIANG; AU, 2013).

Em peixes, os tecidos mais comumente utilizados para avalição histopatológica são as brânquias, fígado e rim (WOLF; WOLFE, 2005). A análise desses três tecidos é capaz de fornecer informações valiosas, no entanto, como as brânquias estão em contato direto com o ambiente aquático, elas são mais vulneráveis. As brânquias possuem múltiplas funções: respiração, osmorregulação, equilíbrio ácido-base e excreção. Alterações histológicas podem tanto comprometer esses processos, quanto serem respostas adaptativas que os possibilitam, frente a desafios impostos por poluentes (CAMARGO; MARTINEZ, 2007; CARMO et al., 2018).

1.5.6 Bioacumulação

Quando um agente tóxico não é suficientemente excretado pelo organismo, este pode acumular-se em diversos órgãos, processo denominado de bioacumulação. A análise da concentração de um contaminante em diferentes órgãos pode fornecer bases para a compreensão dos mecanismos de absorção, distribuição e eliminação do contaminante em um organismo (NEWMAN; CLEMENTS, 2008).

1.6 Modelos Biológicos

Os moluscos bivalves são bons modelos biológicos porque são encontrados em abundância e são facilmente coletados e mantidos em laboratório. Além disso, esses animais são frequentemente citados e utilizados pela sua capacidade de filtração da água e potencial de bioacumulação de compostos, resultante do hábito alimentar de filtração de suspensões, presente na maioria das espécies de bivalves (FARRIS; HASSEL, 2007). Esse hábito alimentar faz com que os bivalves filtrem grandes volumes de água e entrem em contato com o material dissolvido, partículas em suspensão, sedimento e micro-organismos, como bactérias e microalgas. As brânquias são ciliadas e direcionam as partículas de alimento para a boca, o que faz com que o alimento entre no sistema digestório e seja digerido na glândula digestiva (CUMMINGS; GRAF, 2015). Nesse processo, nanopartículas podem ser internalizadas por células da glândula digestiva, as quais são adaptadas para a endocitose de partículas de alimento na dimensão de nanoescala, visto que esse é o principal mecanismo pelo qual os bivalves absorvem nutrientes. Devido a isso, os bivalves têm sido descritos como organismos-alvo para a toxicidade de nanopartículas (CANESI et al., 2012; ROCHA et al., 2015).

Por outro lado, os teleósteos são modelos utilizados e recomendados desde o início da Ecotoxicologia, em meados do século XX. Naquele momento, o principal foco de estudo era o processo de biomagnificação, e alguns peixes foram considerados modelos de topo da cadeia trófica (VASSEUR, 2021). Além de ocuparem diferentes níveis tróficos, outras caracteríticas os fazem modelos biológicos adequados até a atualidade, tais como o conhecimento de sua biologia, sua sensibilidade a mudanças no ambiente aquático, e possibilidade de entrar em

contato com contaminantes por diferentes vias de exposição (água e alimento) (YANCHEVA et al., 2015).

Diante da relevância do uso de bivalves e teleósteos em estudos de Ecotoxicologia, e considerando a preferência pelo uso de espécies nativas para a proteção dos nossos ecossistemas (FURLEY et al., 2018), o mexilhão *Anodontites trapesialis* e o teleósteo *Prochilodus lineatus* (Figura 1), ambos dulcícolas e nativos, podem ser considerados modelos biológicos adequados ao presente estudo. Além disso, ambas as espécies já se mostraram sensíveis a metais (LOAYZA-MURO; ELÍAS-LETTS, 2007; OLIVEIRA et al., 2018a, 2018b).

A espécie *A. trapesialis* (Lamarck, 1819) possui a seguinte classificação sistemática:

Reino: Animalia
Filo: Mollusca
Classe: Bivalvia
Subclasse: Autobranchia
Infraclasse: Heteroconchia
Subterclasse: Palaeoheterodonta
Ordem: Unionida
Superfamília: Etherioidea
Família: Mycetopodidae
Subfamília: Anodontitinae
Gênero: *Anodontites*
Espécie: *Anodontites trapesialis*

A espécie *P. lineatus* (Valenciennes, 1837) possui a seguinte classificação sistemática:

Reino: Animalia
Filo: Chordata
Classe: Actinopterygii
Ordem: Characiformes
Família: Prochilodontidae
Gênero: *Prochilodus*
Espécie: *Prochilodus lineatus*

Figura 1 – (A) Adulto de *Anodontites trapesialis* e (B) juvenil de *Prochilodus lineatus*.

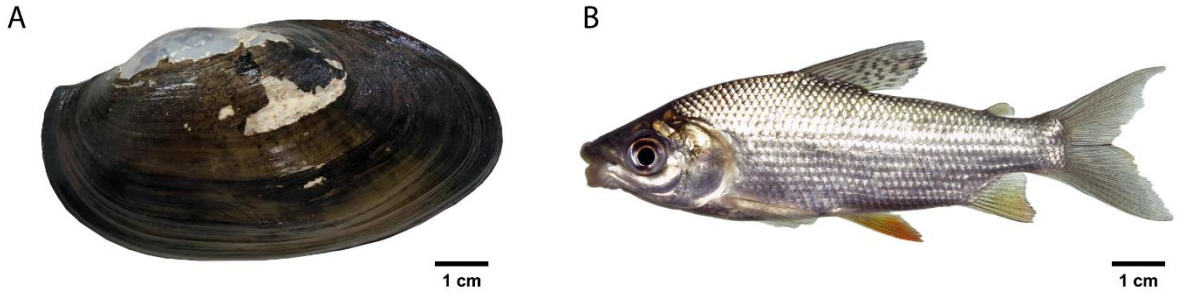

Fonte: (A) O próprio autor. (B) Museu de Zoologia da UEL (MZUEL).

2 HIPÓTESES DESTE ESTUDO

1) As nanopartículas metálicas biogênicas (AgNP, TiO_2NP e FeNP) provocarão efeitos subletais nas duas espécies avaliadas.
2) Os efeitos provocados por cada tipo de nanopartícula (AgNP, TiO_2NP ou FeNP) apresentarão similaridades e discrepâncias entre si, sendo as discrepâncias relacionadas à toxicidade do metal que compõe a nanopartícula.
3) Os efeitos provocados pelas nanopartículas apresentarão similaridades e discrepâncias entre as espécies de bivalve e de teleósteo. No entanto, não será possível distinguir a espécie mais suscetível às nanopartículas, pois serão observados efeitos em ambas.
4) Os animais acumularão prata após exposição às AgNP, com base em estudos na literatura com concentrações similares, mesmo que com nanopartículas de prata distintas.
5) Os animais não acumularão titânio após exposição às TiO_2NP, pois mesmo que as TiO_2NP estejam biodisponíveis, seria necessária uma concentração maior para resultar em bioacumulação.
6) Os animais não acumularão ferro após exposição às FeNP, pois mesmo que as FeNP estejam biodisponíveis, seria necessária uma concentração maior para resultar em bioacumulação.

3 OBJETIVOS

3.1 OBJETIVO GERAL

Avaliar os efeitos subletais da exposição de curto período a nanopartículas de prata, de dióxido de titânio rutilo e de ferro, sintetizadas com o fungo *T. harzianum,* para animais aquáticos.

3.2 OBJETIVOS ESPECÍFICOS

a) Verificar se as nanopartículas são seguras, nas concentrações e tempo de exposição proposto, para o bivalve *A. trapesialis* e para o teleósteo *P. lineatus*.

b) Avaliar o potencial e padrão de bioacumulação de metais nas espécies estudadas, após exposição às nanopartículas.

c) Obter uma visão integrada, em nível de organismo, dos efeitos biológicos das nanopartículas.

d) Identificar os tecidos mais suscetíveis, em ambas as espécies, aos efeitos das nanopartículas, no curto tempo de exposição proposto.

e) Indicar semelhanças e diferenças entre as respostas de cada espécie estudada à exposição às nanopartículas.

f) Comparar a sensibilidade de cada espécie às nanopartículas, considerando-se as concentrações propostas.

g) Definir *endpoints* adequados para a exposição de bivalves e teleósteos às nanopartículas estudadas.

REFERÊNCIAS BIBLIOGRÁFICAS

ADAMO, S. A. The effects of the stress response on immune function in invertebrates: An evolutionary perspective on an ancient connection. **Hormones and Behavior**, v. 62, n. 3, p. 324–330, 2012.

ANIL KUMAR, S. et al. Nitrate reductase-mediated synthesis of silver nanoparticles from $AgNO_3$. **Biotechnology Letters**, v. 29, n. 3, p. 439–445, 2007.

BELAIR, C. D.; PETERSON, R. E.; HEIDEMAN, W. Disruption of erythropoiesis by dioxin in the zebrafish. **Developmental Dynamics**, v. 222, n. 4, 2001.

BILESKY-JOSÉ, N. et al. Biogenic α-Fe_2O_3 Nanoparticles Enhance the Biological Activity of *Trichoderma* against the Plant Pathogen *Sclerotinia sclerotiorum*. **ACS Sustainable Chemistry and Engineering**, v. 9, n. 4, p. 1669–1683, 2021.

BONOMO, M. M. et al. Biochemical and genotoxic biomarkers and cell cycle assessment in the zebrafish liver (ZF-L) cell line exposed to the novel metal-insecticide magnesium-hespiridin complex. **Chemosphere**, v. 250, p. 126416, 2020.

BOUYOUCOS, I. A. et al. Ancient fishes and the functional evolution of the corticosteroid stress response in vertebrates. **Comparative Biochemistry and Physiology Part A: Molecular & Integrative Physiology**, v. 260, p. 111024, out. 2021.

BRODEUR, J. C. et al. The problem with implementing fish farms in agricultural regions: A trial in a pampean pond highlights potential risks to both human and fish health. **Chemosphere**, v. 262, p. 128408, 2020.

CAMARGO, M. M. P.; MARTINEZ, C. B. R. Histopathology of gills , kidney and liver of a Neotropical fish caged in an urban stream. v. 5, n. 3, p. 327–336, 2007.

CANESI, L. et al. Bivalve molluscs as a unique target group for nanoparticle toxicity. **Marine Environmental Research**, v. 76, p. 16–21, 2012.

CARMO, T. L. L. et al. Mitochondria-rich cells adjustments and ionic balance in the Neotropical fish Prochilodus lineatus exposed to titanium dioxide nanoparticles. **Aquatic Toxicology**, v. 200, p. 168–177, 2018.

CARRASCO, K. R.; TILBURY, K. L.; MYERS, M. S. Assessment of the Piscine Micronucleus Test as an in situ Biological indicator of Chemical Contaminant Effects. **Canadian Journal of Fisheries and Aquatic Sciences**, v. 47, n. 11, p. 2123–2136, 1990.

CARROLA, J. et al. Frequency of micronuclei and of other nuclear abnormalities in erythrocytes of the grey mullet from the Mondego, Douro and Ave estuaries-Portugal. **Environmental Science and Pollution Research**, v. 21, n. 9, p. 6057–6068, 2014.

CHEN, L. Q.; KANG, B.; LING, J. Cytotoxicity of cuprous oxide nanoparticles to fish blood cells: Hemolysis and internalization. **Journal of Nanoparticle Research**, v. 15, n. 3, 2013.

CHIANG, M. W.-L.; AU, D. W.-T. Histopathological Approaches in Ecotoxicology. In: FÉRARD, J.-F.; BLAISE, C. (Eds.). **Encyclopedia of Aquatic Ecotoxicology**. Dordrecht: Springer Netherlands, 2013. p. 597–614.

COCAIGN, A. et al. Biotransformation of Trichoderma spp. and their tolerance to aromatic amines, a major class of pollutants. **Applied and Environmental Microbiology**, v. 79, n. 15, p. 4719–4726, 2013.

CONTRERAS-CORNEJO, H. A. et al. Enhanced Plant Immunity Using Trichoderma. In: GUPTA, V. et al. (Eds.). **Biotechnology and Biology of Trichoderma**. 1. ed. Oxford: Elsevier, 2014. p. 495–504.

COSSU-LEGUILLE, C.; VASSEUR, P. Aquatic Biomarkers. In: FÉRARD, J.-F.; BLAISE, C. (Eds.). . **Encyclopedia of Aquatic Ecotoxicology**. Dordrecht: Springer Netherlands, 2013. p. 49–66.

CUMAGUN, C. J. R. Advances in Formulation of Trichoderma for Biocontrol. In: **Biotechnology and Biology of Trichoderma**. Oxford: Elsevier, 2014. p. 527–531.

CUMMINGS, K. S.; GRAF, D. L. Class Bivalvia. In: THORP, J. H.; ROGERS, D. C. (Eds.). . **Thorp and Covich's Freshwater Invertebrates: Ecology and General Biology**. 4. ed. London: Academic Press, 2015. v. 1p. 423–506.

DEPLEDGE, M. H. The Rational Basis for the Use of Biomarkers as Ecotoxicological

Tools. In: FOSSI, M. C.; LEONZI, C. (Eds.). . **Nondestructive Biomarkers in Vertebrates**. 1. ed. Boca Raton, FL: CRC Press, 1994. p. 271–295.

EALIAS, A. M.; SARAVANAKUMAR, M. P. A review on the classification, characterisation, synthesis of nanoparticles and their application. **IOP Conference Series: Materials Science and Engineering**, v. 263, n. 3, 2017.

EVANS, D. H. **Osmoregulation in Fishes: An Introduction**Academic Press, , 2011. (Nota técnica).

FAO. Trade Reforms and Food Security: conceptualizing the Linkages. Rome, 2003.

FAO, IFAD, UNICEF, WFP e WHO. The State of Food Security and Nutrition in the World 2020: transforming food systems for affordable healthy diets. Rome, 2020.

FARRELL, A. P. **Cellular Composition of the Blood**Elsevier, , 2011. (Nota técnica).

FARRIS, J. L.; HASSEL, J. H. VAN (EDS.). **Freshwater Bivalve Ecotoxicology**. 1. ed. New York, NY: CRC Press, Taylor & Francis Group, 2007.

FRACETO, L. F. et al. Uso de micro e nanotecnologia com *Trichoderma*. In: MEYER, M. C.; MAZARO, S. M.; SILVA, J. C. AD (Eds.). . ***Trichoderma*: uso na agricultura**. Brasília, DF, Brazil: Embrapa, 2019. p. 297–314.

FURLEY, T. H. et al. Toward sustainable environmental quality: Identifying priority research questions for Latin America. **Integrated Environmental Assessment and Management**, v. 14, n. 3, p. 344–357, 2018.

GAWANDE, M. B. et al. Cu and Cu-Based Nanoparticles: Synthesis and Applications in Catalysis. **Chemical Reviews**, v. 116, n. 6, p. 3722–3811, 2016.

GODFRAY, H. C. J. et al. Food security: The challenge of feeding 9 billion people. **Science**, v. 327, n. 5967, p. 812–818, 2010.

GOTTSCHALK, F.; SUN, T.; NOWACK, B. Environmental concentrations of engineered nanomaterials: Review of modeling and analytical studies. **Environmental Pollution**, v. 181, p. 287-300, 2013.

GRIFFITH, M. B. Toxicological perspective on the osmoregulation and ionoregulation

physiology of major ions by freshwater animals: Teleost fish, crustacea, aquatic insects, and Mollusca. **Environmental Toxicology and Chemistry**, v. 36, n. 3, p. 576–600, 2017.

GROSELL, M. Copper. In: WOOD, C. M.; FARRELL, A. P.; BRAUNER, C. J. (Eds.). . **Homeostasis and Toxicology of Essential Metals**. Fish Physiology. 1. ed. Oxford: Academic Press, 2011. v. 31p. 53–133.

GUILGER-CASAGRANDE, M. et al. Biosynthesis of silver nanoparticles employing *Trichoderma harzianum* with enzymatic stimulation for the control of *Sclerotinia sclerotiorum*. **Scientific Reports**, v. 9, n. 1, p. 14351, 2019.

GUILGER-CASAGRANDE, M.; LIMA, R. DE. Synthesis of Silver Nanoparticles Mediated by Fungi: A Review. **Frontiers in Bioengineering and Biotechnology**, v. 7, p. 287, 2019.

GUILGER, M. et al. Biogenic silver nanoparticles based on Trichoderma harzianum: Synthesis, characterization, toxicity evaluation and biological activity. **Scientific Reports**, v. 7, p. 1–13, 2017.

HARMAN, G. E. et al. *Trichoderma* species - Opportunistic, avirulent plant symbionts. **Nature Reviews Microbiology**, v. 2, n. 1, p. 43–56, 2004.

HIETZSCHOLD, S. et al. Does Nitrate Reductase Play a Role in Silver Nanoparticle Synthesis? Evidence for NADPH as the Sole Reducing Agent. **ACS Sustainable Chemistry and Engineering**, v. 7, n. 9, p. 8070–8076, 2019.

HILL, R. W.; WYSE, G. A.; ANDERSON, M. **Animal Physiology.** 3. Ed. Sunderland, Massachusetts: Sinauer Associates, 2012. 800p.g

HOLT-GIMÉNEZ, E. et al. We Already Grow Enough Food for 10 Billion People... and Still Can’t End Hunger. **Journal of Sustainable Agriculture**, v. 36, n. 6, p. 595–598, 2012.

HOWELL, C. R. Mechanisms employed by *Trichoderma* species in the biological control of plant diseases: The history and evolution of current concepts. **Plant Disease**, v. 87, n. 1, p. 4–10, 2003.

HWANG, P. P. **Mechanisms of Ion Transport in Freshwater Fishes**, 2011. (Nota técnica).

IBAMA (Instituto Brasileiro do Meio Ambiente e dos Recursos Naturais Renováveis), 2021a. Relatórios de comercialização de agrotóxicos. 19 jul. de 2021. Disponível em: http://www.ibama.gov.br/agrotoxicos/relatorios-de-comercializacao-de-agrotoxicos. Acesso em: 14 out. de 2021.

IBAMA (Instituto Brasileiro do Meio Ambiente e dos Recursos Naturais Renováveis), 2021b. Avaliação ambiental para registro de agrotóxicos, seus componentes e afins de uso agrícola. 11 maio de 2021. Disponível em: http://www.ibama.gov.br/avaliacao-e-destinacao/quimicos-e-biologicos/avaliacao-ambiental-para-registro-de-agrotoxicos-seus-componentes-e-afins-de-uso-agricola. Acesso em: 14 out. de 2021.

ISO (International Organization for Standardization), 2015a. ISO/TS 80004-1:2015, Nanotechnologies - Vocabulary - Part 1: Core terms. Disponível em: https://www.iso.org/obp/ui/#iso:std:iso:ts:80004:-1:ed-2:v1:en. Acesso em: 23 jun. de 2021.

ISO (International Organization for Standardization), 2015b. ISO/TS 80004-1:2015, Nanotechnologies - Vocabulary - Part 2: Nano-objects. Disponível em: https://www.iso.org/obp/ui/#iso:std:iso:ts:80004:-2:ed-1:v1:en. Acesso em: 23 jun. 2021.

KAUSHAL, M. Role of Microbes in Plant Protection Using Intersection of Nanotechnology and Biology. In: ABD-ELSALAM, K. A.; PRASAD, R. (Eds.). . **Nanobiotechnology Applications in Plant Protection**. Cham, Switzerland: Springer International Publishing, 2018. p. 111–135.

KESWANI, C. et al. Unraveling the efficient applications of secondary metabolites of various *Trichoderma* spp. **Applied Microbiology and Biotechnology**, v. 98, n. 2, p. 533–544, 2014.

KREDICS, L. et al. Biodiversity of the Genus Hypocrea/Trichoderma in Different Habitats. In: GUPTA, V. K. et al. (Eds.). . **Biotechnology and Biology of Trichoderma**. 1. ed. Oxford: Elsevier, 2014. p. 3–24.

KUMAR, C. G.; MAMIDYALA, S. K. Extracellular synthesis of silver nanoparticles using culture supernatant of Pseudomonas aeruginosa. **Colloids and Surfaces B: Biointerfaces**, v. 84, n. 2, p. 462–466, 1 jun. 2011.

LAURANCE, W. F.; SAYER, J.; CASSMAN, K. G. Agricultural expansion and its impacts on tropical nature. **Trends in Ecology and Evolution**, v. 29, n. 2, p. 107–116, 2014.

LOAYZA-MURO, R.; ELÍAS-LETTS, R. Responses of the mussel *Anodontites trapesialis* (Unionidae) to environmental stressors: Effect of pH, temperature and metals on filtration rate. **Environmental Pollution**, v. 149, n. 2, p. 209–215, 2007.

LORITO, M. et al. Chitinolytic Enzymes Produced by Trichoderma harzianum: Antifungal Activity of Purified Endochitinase and Chitobiosidase. **Phytopathology**, v. 83, n. 3, p. 302–307, 1993.

LUSHCHAK, V. I. Contaminant-induced oxidative stress in fish: a mechanistic approach. **Fish Physiology and Biochemistry**, v. 42, n. 2, p. 711–747, 2016.

MARTINEZ, C. B. R.; SIMONATO ROCHA, J. D.; MELETTI, P. C. Metals. In: KIBENGE, F. S. B.; BALDISSEROTTO, B.; CHONG, R. S.-M. (Eds.). . **Aquaculture Toxicology**. 1. ed. London: Academic Press, 2021. p. 59–78.

MARUYAMA, C. R. et al. Encapsulation of *Trichoderma harzianum* Preserves Enzymatic Activity and Enhances the Potential for Biological Control. **Frontiers in Bioengineering and Biotechnology**, v. 8, n. March, p. 1–14, 2020.

MAZON, A. F. et al. Hematological and physiological changes induced by short-term exposure to copper in the freshwater fish, Prochilodus scrofa. **Brazilian Journal of Biology**, v. 62, n. 4a, p. 621–631, 2002.

MIRANDA, R.R., DAMASO DA SILVEIRA, A.L.R., DE JESUS, I.P., GRÖTZNER, S.R., VOIGT, C.L., CAMPOS, S.X., GARCIA, J.R.E., RANDI, M.A.F., RIBEIRO, C.A.O., FILIPAK NETO, F. Effects of realistic concentrations of TiO_2 and ZnO nanoparticles in *Prochilodus lineatus* juvenile fish. Environmental Science and Pollution Research, v. 23, 5179–5188, 2016.

NASTIS, S.; MICHAILIDIS, A.; CHATZITHEODORIDIS, F. Climate change and agricultural productivity. **African Journal of Agricultural Reseearch**, v. 7, n. 35, 2012.

NEWMAN, M. C.; CLEMENTS, W. H. **Ecotoxicology: a comprehensive treatment**. Boca Raton, FL: CRC Press, Taylor & Francis Group, 2008.

NIKINMAA, M. Effects on Organisms. In: NIKINMAA, M. (Ed.). . **An Introduction to Aquatic Toxicology**. Oxford: Academic Press, 2014a. p. 111–146.

NIKINMAA, M. Detoxification. In: NIKINMAA, M. (Ed.). . **An Introduction to Aquatic Toxicology**. Oxford: Academic Press, 2014b. p. 87–98.

OLIVEIRA, L. F. DE et al. Triple-mixture of Zn, Mn, and Fe increases bioaccumulation and causes oxidative stress in freshwater neotropical fish. **Environmental Toxicology and Chemistry**, v. 37, n. 6, p. 1749–1756, 2018a.

OLIVEIRA, L. F. et al. Single and combined effects of Zn, Mn and Fe on the Neotropical freshwater bivalve *Anodontites trapesialis*: Bioaccumulation and biochemical biomarkers. **Ecotoxicology and Environmental Safety**, v. 161, p. 735–745, 2018b.

PASQUOTO-STIGLIANI, T. **Nanopartículas biogênicas de titânio a partir de *Trichoderma harzianum* para aplicação na área agrícola: síntese, caracterização, avaliação da toxicidade, e bioatividade**. [s.l.] Universidade de Sorocaba (UNISO), 2019.

PEREIRA NAVARRO LINS, J. A. et al. Uso de peixes como biomarcadores para monitoramento ambiental aquático. **Revista Acadêmica: Ciência Animal**, v. 8, n. 4, p. 469, 2017.

PÉREZ, D. J. et al. Ecological risk assessment of current-use pesticides and biocides in soils, sediments and surface water of a mixed land-use basin of the Pampas region, Argentina. **Chemosphere**, v. 263, p. 128061, jan. 2021.

PONDER, W. F.; LINDBERG, D. R.; PONDER, J. M. Shell, Body, and Muscles. In: **Biology and Evolution of the Mollusca**. 1. ed. Boca Raton, FL: CRC Press, 2019.

p. 55–132.

PORTO MARTINS MEDEIROS, I. **Homeostase osmoiônica em moluscos bivalves habitantes de diferentes nichos osmóticos: padrões fisiológicos e evolutivos**. [s.l.] Universidade Federal do Rio Grande (FURG), 2019.

PRASAD, R. **Microbial Nanobionics**. 1. ed. Cham: Springer International Publishing, 2019. v. 1

ROCHA, T. L. et al. Ecotoxicological impact of engineered nanomaterials in bivalve molluscs: An overview. **Marine Environmental Research**, v. 111, p. 74–88, 2015.

RODRIGUES, E. S. et al. Are nanomaterials making agriculture more productive? outputs from a metadata analysis of 2009-2020 research. **Agrirxiv**, 2021.

SALDAJENO, M. G. B. et al. Enhanced Resistance of Plants to Disease Using *Trichoderma* spp. In: GUPTA, V. K. et al. (Eds.). . **Biotechnology and Biology of Trichoderma**. 1. ed. Oxford: Elsevier, 2014. p. 477–493.

SAYER, J.; CASSMAN, K. G. Agricultural innovation to protect the environment. **Proceedings of the National Academy of Sciences of the United States of America**, v. 110, n. 21, p. 8345–8348, 2013.

SINGH, A. et al. Trichoderma: A Silent Worker of Plant Rhizosphere. In: GUPTA, V. K. et al. (Eds.). . **Biotechnology and Biology of Trichoderma**. 1. ed. Oxford: Elsevier, 2014. p. 533–542.

SINGH, P. et al. Biological Synthesis of Nanoparticles from Plants and Microorganisms. **Trends in Biotechnology**, v. 34, n. 7, p. 588–599, 2016.

SMITH, W. H. Forest occurrence of Trichoderma species: Emphasis on potential organochlorine (xenobiotic) degradation. **Ecotoxicology and Environmental Safety**, v. 32, n. 2, p. 179–183, 1995.

SOLOMON, K. R. et al. Effects of Herbicides on Fish. In: TIERNEY, K. B.; FARRELL, A. P.; BRAUNER, C. J. (Eds.). . **Fish Physiology**. 1. ed. Boca Raton, FL: Elsevier Inc., 2013. v. 33p. 369–409.

STEWART, A.; HILL, R. Applications of Trichoderma in Plant Growth Promotion. In: GUPTA, V. K. et al. (Eds.). . **Biotechnology and Biology of Trichoderma**. 1. ed. Oxford: Elsevier, 2014. p. 415–428.

TILMAN, D. et al. Agricultural sustainability and intensive production practices. **Nature**, v. 418, n. 6898, p. 671–677, 2002.

TOMITA, R. . Y.; BEYRUTH, Z. Toxicologia de agrotóxicos em ambiente aquático. **Biológico**, v. 4, n. 2, p. 135–142, 2002.

VASSEUR, P. Ecotoxicology, revisiting its pioneers. **Environmental Science and Pollution Research**, v. 28, p. 3852–3857, 2021.

VIEIRA, C. E. D. et al. Multiple biomarker responses in *Prochilodus lineatus* subjected to short-term in situ exposure to streams from agricultural areas in Southern Brazil. **Science of the Total Environment**, v. 542, p. 44–56, 2016.

VIEIRA, C. E. D. et al. An integrated approach in subtropical agro-ecosystems: Active biomonitoring, environmental contaminants, bioaccumulation, and multiple biomarkers in fish. **Science of the Total Environment**, v. 666, 2019.

WANG, Y.; XIA, Y. Bottom-Up and Top-Down Approaches to the Synthesis of Monodispersed Spherical Colloids of Low Melting-Point Metals. **Nano Letters**, v. 4, n. 10, p. 2047–2050, 2004.

WANG, Y. et al. Are engineered nano iron oxide particles safe? An environmental risk assessment by probabilistic exposure, effects and risk modeling. **Nanotoxicology**, v. 10, p. 1-23, 2016.

WENDELAAR BONGA, S. E. **Hormone Response to Stress**, 2011. (Nota técnica).

WINKALER, E. U. et al. Biomarcadores histológicos e fisiológicos para o monitoramento da saúde de peixes de ribeirões de Londrina, Estado do Paraná. **Acta Scientiarum**, v. 23, p. 507–514, 2001.

WOLF, J. C.; WOLFE, M. J. A Brief Overview of Nonneoplastic Hepatic Toxicity in Fish. **Toxicologic Pathology**, v. 33, n. 1, p. 75–85, 2005.

WOOD, C. M. An introduction to metals in fish physiology and toxicology: basic principles. In: WOOD, C. M.; FARRELL, A. P.; BRAUNER, C. J. (Eds.). . **Homeostasis and Toxicology of Essential Metals**. Fish Physiology. London: Academic Press, 2011. v. 31p. 1–51.

WOOD, C. M. Silver. In: CHRIS M. WOOD, A. P. F. AND C. J. B. (Ed.). . **Homeostasis and Toxicology of Non-Essential Metals**. London: Academic Press, 2012. p. 1–54.

YANCHEVA, V. et al. Fish in Ecotoxicological Studies. **Ecologia Balkanica**, v. 7, n. 1, p. 149–169, 2015.

4 MANUSCRITO I

Biogenic metallic nanoparticles (Ag, TiO_2, Fe) as potential fungicides for agriculture: are they safe for the freshwater mussel *Anodontites trapesialis*?

Maria Eduarda Tesser[1], Mariana Guilger[2,3], Wagner Ezequiel Risso[1], Renata de Lima[3], Claudia Bueno dos Reis Martinez[1]

[1] Laboratory of Animal Ecophysiology, Department of Physiological Sciences, State University of Londrina (UEL), Londrina, Paraná, Brazil.
[2] Laboratory of Environmental Nanotechnology, São Paulo State University (UNESP), Sorocaba, São Paulo, Brazil.
[3] Laboratory of Bioactivity Assessment and Toxicology of Nanomaterials, University of Sorocaba (UNISO), Sorocaba, São Paulo, Brazil.

ABSTRACT

Silver (Ag), titanium dioxide (TiO_2), and iron (Fe) nanoparticles (NPs) synthesized using the fungus *Trichoderma harzianum* are effective against the agriculture pathogen *Sclerotinia sclerotiorum.* However, their potential effects should be evaluated in aquatic organisms, as agriculture practices can contaminate the aquatic environment. Thus, this work aimed to evaluate sublethal effects of the short-term exposure (24 h) to silver nanoparticles (AgNP), rutile titanium dioxide nanoparticles (TiO_2NP) and iron nanoparticles (FeNP), all synthesized with *T. harzianum*, on the Neotropical freshwater bivalve *Anodontites trapesialis*, considering the hypothesis that suspension-feeding bivalves would be more susceptible to NPs toxicity. Individuals of *A. trapesialis* were divided into four groups (n = 8/group): a control group, kept in water only; a group exposed to AgNP (3 x 10^9 NPs mL^{-1} - 355.96 µg Ag L^{-1}); a group exposed to TiO_2NP (1 x 10^8 NPs mL^{-1} - 38.94 µg Ti L^{-1}); and a group exposed to FeNP (3 x 10^7 NPs mL^{-1} - 123.98 µg Fe L^{-1}). After the exposure, the bioaccumulation of Ag, Ti, and Fe was evaluated in the gills, hemolymph, mantle, digestive gland, and muscle (foot). Lipoperoxidation, activities of the glutathione S-transferase, catalase, and superoxide dismutase, and glycogen concentration were quantified in the gills, mantle, and digestive gland. The concentration of Na^+, K^+, Cl^-, Ca^{+2}, and Mg^{+2} ions, and glucose concentration were quantified in the hemolymph. Na^+/K^+-ATPase, H^+-ATPase, Ca^{+2}-ATPase, and carbonic anhydrase activities were assessed in the gills and mantle. Acetylcholinesterase activity was determined in the foot and adductor muscle. The mussels exposed to AgNP accumulated Ag in the gills, hemolymph, and foot, and showed a decrease in the concentrations of Na^+ and Cl^- ions in the hemolymph, which was associated with the action of Ag ion (Ag^+). The exposures to TiO_2NP and FeNP led to the accumulation of Ti and Fe, respectively, in the hemolymph of mussels, but these increases in metal concentration did not promote additional effects. Thus, *A. trapesialis* showed bioaccumulation potential and susceptibility to AgNP, but was not susceptible to TiO_2NP and FeNP. Based on the results, the preferential agricultural use of TiO_2NP and FeNP over AgNP is highlighted. In addition, the effects of the NPs presented should be tested with other species, concentrations, and exposure times, to further verify their safe use in agriculture.

Key-words: Ecotoxicology. Green synthesis. Pesticides. Ionoregulation. Bivalve.

4.1 INTRODUCTION

Latin America is expected to face great agricultural expansion and intensification in the 21st century (Dias et al., 2016; Laurance et al., 2014; Pimenta et al., 2021). For decades now, the expansion and intensification of agriculture have been accompanied by pesticide use (Carriquiriborde et al., 2014; de Almeida et al., 2017). Brazil consumed 620,000 tons of pesticides in 2019, which is 12.97% more than 2018, and 282% more than 2000 (IBAMA, 2020). The detection of pesticides in surface waters reflects their intensive use, and the impact on resident biota raises concerns (Brodeur et al., 2020; Pérez et al., 2021; Vieira et al., 2019, 2017). In light of this, research has focused on developing formulations that increase agricultural efficiency while having a less ecological impact than the most commonly used pesticides (Bonomo et al., 2020; Fraceto et al., 2016). This is the case of biogenic (also known as biological or green) metallic nanoparticles (NPs) synthesized using the filamentous fungus *Trichoderma harzianum* (Fraceto et al., 2018).

In general, the biological route for synthesis of NPs uses living organisms, or their extracts, as reducing and stabilizing agents (Zhu et al., 2019). This approach is considered to be less hazardous to the environment and more cost-effective than traditional physical-chemical methods (Singh et al., 2016; Taheriniya and Behboodi, 2016). Besides that, the organism employed for the synthesis may alter the composition of NPs, influencing their activity and toxicity (Guilger et al., 2017). The synthesis of NPs mediated by *T. harzianum* used silver (Ag), titanium dioxide (TiO_2), and iron (Fe) as metal precursors, forming silver nanoparticles (AgNP), titanium dioxide nanoparticles (TiO_2NP), and iron nanoparticles (FeNP), respectively.[1] These NPs are effective in the control of the agriculture pathogen *Sclerotinia sclerotiorum* (Bilesky-José et al., 2021; Guilger et al., 2017, Pasquoto-Stigliani et al., to be published), a fungus that causes white mold disease in soybean and several others plant species (Bolton et al., 2006).

AgNP, TiO_2NP, and FeNP have a metallic core composed of, respectively, elemental silver (Ag^0), TiO_2, and hematite (α-Fe_2O_3), although the additional presence of elemental iron (Fe^0) and maghemite (γ-Fe_2O_3) is possible in

[1] For the comprehension of this text, NPs from other studies will be referred as nano-Ag, nano-TiO_2, and nano-Fe.

the case of FeNP. The metallic core is stabilized by a capping of biomolecules secreted by the fungus, among which the hydrolytic enzymes β-1,3-glucanase, N-acetylglucosaminidase (NAGase), chitinase and acid protease have already been identified (Bilesky-José et al., 2021; Guilger-Casagrande et al., 2019; Pasquoto-Stigliani et al., to be published). Therefore, the activity and toxicity of NPs can be associated with the metal, the capping of biomolecules, or the synergy of both. In fact, Casagrande et al. (2021) demonstrated that the capping is essential for AgNP action against *S. sclerotiorum,* and hypothesized that its mechanism of toxic action results from the synergy between the metal and the capping. Another difference among the suspensions of NPs is that *T. harzianum* reproductive structures are not present in AgNP suspension, but remains in TiO_2NP and FeNP suspensions. Furthermore, FeNP stimulate *T. harzianum* proliferation, which contributes to the control of the pathogenic fungus, in addition to nanoparticle action (Bilesky-José et al., 2021).

The concentrations of AgNP, TiO_2NP, and FeNP that are intended to be applied on crops are, respectively, 3 x 10^9, 1 x 10^8, and 3 x 10^7 NPs mL^{-1}. At these concentrations, AgNP (3 x 10^9 NPs mL^{-1}) showed low cytotoxicity but were genotoxic to human and rodent cell lines, while TiO_2NP (1 x 10^8 NPs mL^{-1}) and FeNP (5 x 10^7 NPs mL^{-1}) were not cytotoxic or genotoxic to the same cell lines. AgNP, TiO_2NP, and FeNP did not affect the germination and growth of common bean seeds (*Phaseolus vulgaris*), but AgNP and TiO_2NP had effects on the mitotic index and the chromosomal alteration index of onion (*Allium cepa*) roots (Bilesky-José et al., 2021; Guilger-Casagrande et al., 2019; Guilger et al., 2017; Pasquoto-Stiagliani et al., to be published).

Once applied on crops, NPs may reach water bodies and interact with aquatic organisms. Suspension-feeding bivalves have been described as potential targets of NPs toxicity, because these animals process particles as part of their feeding habit (Canesi et al., 2012). The Neotropical freshwater mussel *Anodontites trapesialis* is a suitable biological model for the present work, because it is abundant, easy to sample, and sensitive to metals (Loayza-Muro and Elías-Letts, 2007; Oliveira et al., 2018). In addition, the effects of NPs to bivalves are mostly studied in seawater species, with few studies conducted in the freshwater (Rocha et al., 2015).

For aquatic animals, metal toxicity is often associated with

ionoregulatory disturbances (e.g.: copper, Chowdhury et al., 2016; silver, Morgan et al., 2004) and the induction of oxidative stress (Stohs and Bagchi, 1995). Ag is a non-essential metal that can be an ionoregulatory toxicant, as its acute toxicity to freshwater animals results from an impairment of Na^+ uptake (Bianchini et al., 2002). Both nano-sized and ionic Ag are absorbed and accumulated by freshwater mussels (Zimmermann et al., 2017), and similar effects caused by both forms have been reported (Volker et al., 2014). Titanium (Ti) is a non-essential metal most commonly found in nature as titanium dioxide (TiO_2) and rarely as an ion (Antignano and Manning, 2008). For some time, TiO_2 was considered biologically inert, but with the development of nanotechnology and the increasing use of TiO_2 in the nano-size range, research has been focusing on the potential adverse effects of nano-TiO_2, with emphasis in the induction of oxidative stress (Girardello et al., 2016; Skocaj et al., 2011). Fe is an essential metal that can induce oxidative stress at higher concentrations, because it participates in the Fenton reaction (Bury et al., 2011). For bivalves, the immunotoxicity of nano-Fe_2O_3 has been assessed (Zha et al., 2019). However, nano-sized Fe has been also used for environmental remediation. For instance, recoverable magnetic ferroferric oxide nanoparticles (nano-Fe_3O_4) are an environmentally friendly alternative to mitigate mussel biofouling (Li et al., 2021).

Taking into account that studies assessing the effects of biogenic nanoparticles on freshwater animals are incipient, and that the NPs presented in this work have a promising use in agriculture, this work aimed to evaluate potential sublethal effects on the freshwater mussel *A. trapesialis* after short-term exposure to AgNP, TiO_2NP, and FeNP, synthesized using the fungus *T. harzianum*.

4.2 Material and Methods

4.2.1 Biogenic Synthesis and Physiochemical Characterization of Nanoparticles

Nanoparticles were synthesized as described by Guilger et al. (2017). For the culture of *T. harzianum*, Ecotrich™ was plated onto Potato Dextrose Agar (PDA) medium and maintained for 6 days in the dark, at room temperature. Then, mycelium discs were transferred to Potato-Dextrose Broth (PD) and stirred at 150 rpm for 12 days. The biomass was filtered, transferred to ultrapure water, and

kept under agitation for 72 h. After this period, it was vacuum filtered, and the dry material was discarded. Silver nitrate (1 mM), titanium dioxide rutile (1 mM) or iron (III) chloride (1 mM) were added to the filtrate for the formation of silver, titanium and iron nanoparticles, respectively.

The hydrodynamic diameters and polydispersities of the nanoparticles were measured by dynamic light scattering (DLS), and the zeta potentials were determined by microelectrophoresis, using a ZS90 particle analyzer (Malvern Panalytical). The concentrations (NPs mL^{-1}) of the nanoparticles were obtained by nanoparticle tracking analysis (NTA), using a NanoSight LM10 cell coupled to a camera and controlled with NanoSight v. 2.3 software (Malvern Panalytical). The pH was measured using a pH meter (HMMPB-210).

Suspensions were also analyzed through atomic absorption spectrophotometry coupled to a graphite furnace (GFAAS) (AAnalyst, 700, Perkin Elmer, USA), against reference standard solutions (Specsol, Brazil), to determine the concentration of Ag, Ti and Fe, considering that metal concentration could decrease from the nominal concentration, if metals were sequestered by the fungus. After nanoparticles synthesis, suspensions were not filtered, as intended for agricultural use.

4.2.2 Collection and Acclimation of Mussels

Individuals of *A. trapesialis* (n = 32, mass: 182.8 ± 26.4 g, length: 128.7 ± 12.3 mm, width: 63.6 ± 3.5 mm, mean ± SD) were manually collected from the bottom of a fishing pond (located in Londrina, Parana State, Brazil) and transported to the laboratory inside plastic bags containing water from the pond. The mussels were acclimated for 8 days in a tank containing dechlorinated tap water under continuous aeration, constant temperature and a 12h:12h light/dark photoperiod. Every day, 40% of the water was renewed. Throughout acclimation, the mussels were fed every two days with microalgae of the species *Raphidocelis subcapitata* (~10.000 cells mL^{-1}). Water parameters were measured using a multi-parameter meter (HoribaU52), and corresponded to (n = 6, mean ± SD): temperature, 26.4 ± 0.2 °C; dissolved oxygen, 5.9 ± 0.5 mg L^{-1}; pH, 7.2 ± 0.3; turbidity, 0.5 ± 0.8 NTU.

4.2.3 Experimental Design

Following acclimation, mussels were randomly divided into four groups (n = 8 individuals/group): a control group, kept in water only; a group exposed to silver nanoparticles (AgNP) at the concentration of 3 x 10^9 NPs mL^{-1} (355.96 µg Ag L^{-1}); a group exposed to titanium dioxide nanoparticles (TiO_2NP) at the concentration of 1 x 10^8 NPs mL^{-1} (38.94 µg Ti L^{-1}); and a group exposed to iron nanoparticles (FeNP) at the concentration of 3 x 10^7 NPs mL^{-1} (123.98 µg Fe L^{-1}). All nanoparticles were biologically synthesized with the fungus *T. harzianum,* as previously described. The concentrations chosen are those that control the target organism, and therefore are intended to be applied on crops. The animals were kept individually in beakers containing 1 L of the exposure medium, and the exposure occurred for 24 h.

At initial (0 h) and final (24 h) times, water samples from each beaker were collected to determine total (15 mL of not filtered water) and dissolved (15 mL of water filtered with a 0.45 µm mesh filter) concentrations of Ag, Ti and Fe. Samples were acidified with HNO_3 1% (final concentration) and analyzed through GFAAS. The dissolved fraction encompasses metal ions, complexes, nanoparticles, and other colloids, while the total fraction includes the dissolved fraction in addition to forms of metal bounded to organic matter and larger aggregates/agglomerates of nanoparticles, but excludes sedimentation.

The same samples were also used for the determination of the electrolyte composition of water. The concentration of Cl^- was measured by the mercury thiocyanate method using a commercial kit (Quibasa-Bioclin, Brazil) at 470 nm. The concentrations of Na^+ and K^+ were measured using a flame photometer (DM-62, Digmed, Brazil), and the concentration of Ca^{+2} was measured using flame atomizer AAS. Temperature, pH, dissolved oxygen, and turbidity were measured using a multi-parameter meter (HoribaU52). Water hardness was determined by titration.

4.2.4 Mussels Handling After Exposure and Tissue Sampling

Following exposure, individual samples of hemolymph were collected from the adductor muscle of the animals and stored at -20°C. Then the mussels were

killed by sectioning the adductor muscle. Individual samples of gills, mantle, digestive gland, foot and adductor muscle were collected and stored at -80°C for the assays described below.

4.2.5 Bioaccumulation of Ag, Ti and Fe

Samples of gills, mantle, digestive gland and foot were proceeded as described by Alves and Wood (2006). Tissues were dried completely at 60°C, and then submitted to acidic digestion in suprapure nitric acid (5 N) at 60°C for 48 h. Tissue digests and the hemolymph were analyzed for Ag, Ti, and Fe concentrations through GFAAS.

4.2.6 Ions in the Hemolymph and Activity of Related Enzymes

The concentrations of Na^+, K^+, Cl^- and Ca^{+2} was determined in hemolymph samples as described for the quantification of the electrolyte composition of the exposure medium (Topic 3.2.3). Additionally, Mg^{+2} was measured using flame atomizer AAS.

Samples of gills and mantle were homogenized (1 g: 5 mL) in SEID buffer (150 mM sucrose, 10 mM EDTA, 50 mM imidazole, 2.4 mM sodium deoxycholate, pH 7.5), centrifuged (10000 g, 20 min, 4°C), and the supernatants were used for determination of the activities of Na^+/K^+-ATPase and H^+-ATPase (Gibbs and Somero, 1989), Ca^{2+}-ATPase (Vijayavel et al., 2007), and carbonic anhydrase (Vitale et al., 1999). Adaptations of protocols are described in de Paula et al. (2021).

4.2.7 Antioxidant Defenses and Oxidative Damage

Samples of gills, mantle and digestive gland were homogenized in a potassium phosphate buffer (0.1 M, pH = 7.0, 1 g:8 mL), centrifuged (16000 g, 20 min, 4 °C), and the supernatants were used for determining lipoperoxidation (LPO)

and the activities of the enzymes glutathione S-transferase (GST), catalase (CAT), and superoxide dismutase (SOD). LPO was determined by the thiobarbituric acid reactive substances (TBARS) assay, according to Camejo et al. (1998). Before TBARS assay, samples of digestive gland were treated with TCA (Oliveira et al., 2016). GST activity was determined according to Keen et al. (1976), with adaptations for a microplate reader (Gagné, 2014). CAT activity was determined according to Beutler (1972), and SOD activity was determined according to McCord and Fridovich (1969). Data was normalized by the protein concentration (Bradford, 1976) in each supernatant.

4.2.8 Glycogen and Glucose Concentrations

Glycogen was quantified in gills, mantle and digestive gland. Samples were prepared as described by Bidinotto et al. (1997), with a reduction in the volumes used. Samples (100 mg) were dissolved with 500 µL of KOH 6 N in a boiling water bath for five minutes. After that, a 125 µL aliquot was transferred to microtubes in duplicate, and mixed with 1.5 mL of ethanol 100% and 50 µL of K_2SO_4 10%. The mixture was centrifugated (8500 g, 3 min, 25°C), and the supernatant was discarded. Ultrapure water (1.250 mL) was added to re-suspend the precipitate. The final reaction was prepared according to Dubois et al. (1956), using 250 µL of the sample, 250 µL phenol 4.1%, and 1 mL H_2SO_4. Readings were performed in a microplate at 480 nm.

Hemolymph glucose was determined by the glucose oxidase method using a commercial kit (Laborclin, Brazil) at 505 nm.

4.2.9 Acetylcholinesterase (AChE) Activity

Samples of foot and adductor muscle were homogenized in a potassium phosphate buffer (0.1 M, pH 8.0, 1 g:8 mL) and centrifugated (16000 g, 20 min, 4°C). Supernatants were used for the determination of AChE activity as described in Oliveira et al. (2016), following the method described by Ellman et al. (1961) and modified by Mora et al. (1999).

4.2.10 Statistical Analysis

Normality and homoscedasticity of variance were verified using Shapiro-Wilk and Levene's test, respectively. For bioaccumulation analysis, experimental groups (AgNP, TiO_2NP, and FeNP) were compared to control group using t-test or Mann-Whitney test. For analysis of biological effects and water physiochemical parameters, data obtained for control, AgNP, TiO_2NP, and FeNP groups were compared using ANOVA or Kruskal-Wallis test, followed by the Student-Newman-Keuls (SNK) or Dunn's test, respectively, when it was necessary to locate the differences. The intend of comparing the differences of biological effects among groups, and not only compared to control, was to determine which type of biogenic nanoparticle would be less harmful to mussels and thus safer to use in agriculture. Water physiochemical parameters were also compared at initial and final times of exposure using paired t-test or Wilcoxon Signed Rank Test. Values of $P < 0.05$ were considered significant.

4.3 RESULTS

4.3.1 Physiochemical Characterization of Nanoparticles

AgNP were the smallest NPs, followed by FeNP and TiO_2NP. The PDI of AgNP and FeNP were similar, and the PDI of TiO_2NP was the lowest, indicating greater homogeneity of sizes for TiO_2NP. The zeta potentials obtained for AgNP and TiO_2NP were negative, while the zeta potential of FeNP was positive. The pH for AgNP and TiO_2NP suspension was approximately neutral, but acid for FeNP suspension. The concentrations obtained in NPs mL^{-1} were used to calculate the dilutions for the exposures (Table 1).

Table 1 – Physiochemical characterization of silver (AgNP), titanium dioxide (TiO_2NP), and iron (FeNP) nanoparticles synthesized with *Trichoderma harzianum*.

	AgNP	TiO_2NP	FeNP
Diameter (nm)	50.11 ± 0.34	233.13 ± 6.38	138.17 ± 2.00
PDI	0.32 ± 0.00	0.17 ± 0.02	0.35 ± 0.00
Zeta potential (mV)	-19.47 ± 1.15	-10.42 ± 4.98	3.37 ± 0.28

pH	7.3	7.4	5.0
Concentration (NPs mL^{-1})	9.09 x 10^{11}	1.23 x 10^{11}	1.35 x 10^{10}

Data are expressed as mean ± SD (n = 3). PDI = polydispersity index.

4.3.2 Metal Concentration and Physiochemical Conditions of the Exposure

The concentration of Ag quantified in the stock suspension of AgNP through GFAAS (92.05 mg L^{-1}) was consistent with the nominal concentration (1 mM = 107.87 mg L^{-1}). The same occurred for FeNP stock suspension (measured: 49.40 mg L^{-1}; nominal: 1 mM = 55.845 mg L^{-1}). However, the concentration of Ti measured in the TiO_2NP stock suspension (13.09 mg Ti L^{-1}) was lower than expected (nominal: 1 mM = 47.9 mg Ti L^{-1}). The presence of *T. harzianum* mycelia on the suspensions could have modified the concentration of Ti measured, due to the absorption and/or adsorption of the metal by *T. harzianum.* Indeed, it was possible to see *T. harzianum* and micron-sized TiO_2 in the TiO_2NP stock suspension under a light microscope, while the stock suspension of FeNP revealed only *T. harzianum* (Figure 1).

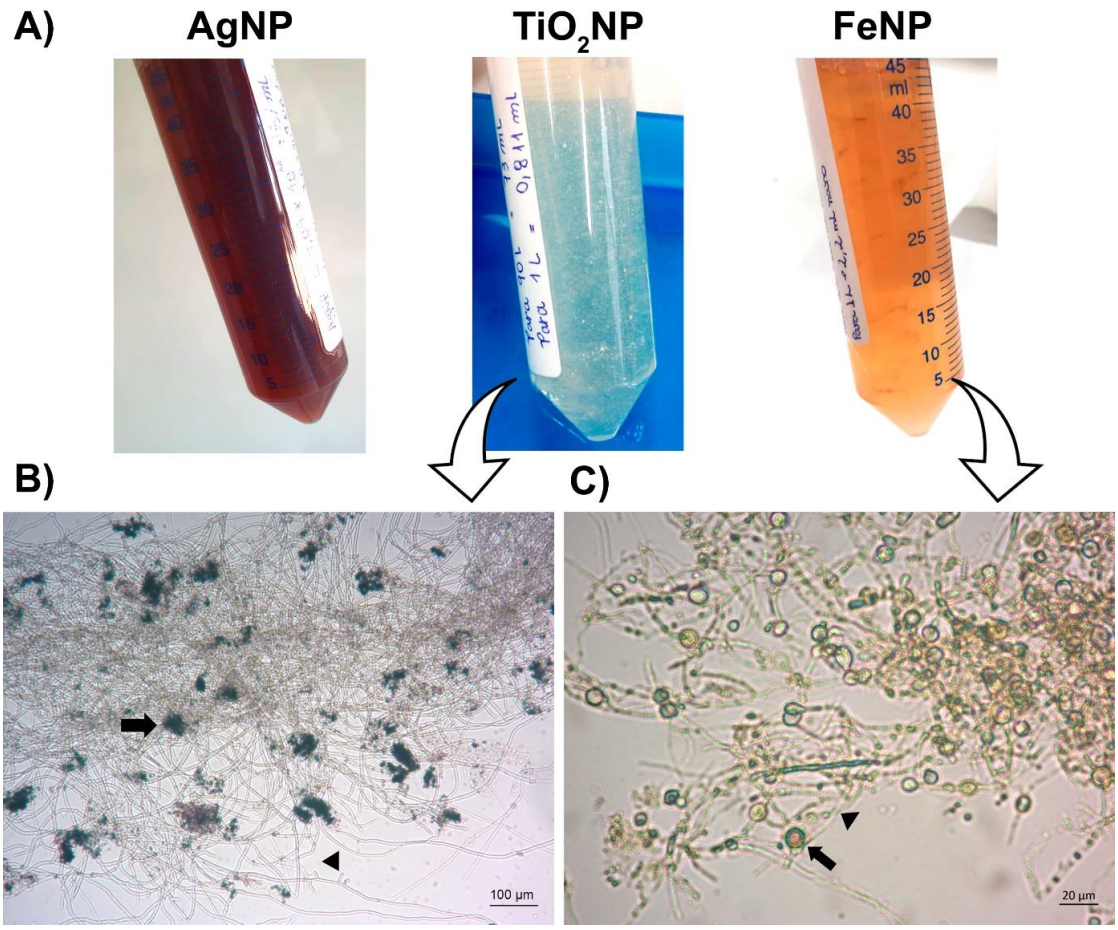

Figure 1 – **A)** Stock suspensions of AgNP (homogenous appearance), TiO_2NP (visible mycelia of *T. harzianum* and TiO_2), and FeNP (visible mycelia of *T. harzianum*). **B)** TiO_2NP stock suspension under the light microscope. Arrow: TiO_2 particles. Arrowhead: Hyphae. **C)** FeNP stock suspensions under the light microscope. Arrow: conidia. Arrowhead: hyphae.

Ag, Ti and Fe concentrations in the exposure medium are shown in Table 2. At 0 h, the total (374.9 ± 90.4 µg L^{-1}) and dissolved (157.3 ± 19.5 µg L^{-1}) concentrations of Ag measured in the exposure medium of AgNP group represented a recovery of 105.3% and 44.2%, respectively, of the nominal concentration (355.96 µg L^{-1}). After 24 h, total and dissolved Ag decreased 50.0% and 24.9%, respectively, from 0 h.

At 0 h, total Ti measured in the exposure medium of TiO_2NP (32.78 ± 10.14 µg L^{-1}) represented a recovery of 84.2% from the nominal concentration (38.94 µg L^{-1}). Dissolved Ti was not detected. At 24 h, total Ti was not measured due to technical reasons. However, dissolved Ti was detected and corresponded to 13.95 ± 3.57 µg L^{-1}.

The total (54.61 ± 14.44 µg L^{-1}) and dissolved (23.63 ± 0.92 µg L^{-1}) concentrations of Fe measured in the exposure medium of FeNP, at 0 h, represented

recoveries of, respectively, 44.0% and 19.1% from the nominal concentration (123.98 µg Fe L^{-1}). After 24 h, total and dissolved Fe decreased 26.9% and 38.6%, respectively.

Table 2 – Silver (Ag), titanium (Ti), and iron (Fe) concentrations (µg L^{-1}) measured in the exposure medium of control and experimental groups at initial (0 h) and final (24 h) times of the exposure.

	0 h	0 h	24 h
	Control	**AgNP**	
Ag total	< DL	374.9 ± 90.4 [a]	187.6 ± 60.2 [a*]
Ag dissolved	< DL	157.3 ± 19.5 [b]	118.1 ± 31.4 [b*]
	Control	**TiO_2NP**	
Ti total	< DL	32.78 ± 10.14	not measured
Ti dissolved	< DL	< DL	13.95 ± 3.57
	Control	**FeNP**	
Fe total	2.37 ± 1.72	54.61 ± 14.44 [a]	39.89 ± 10.81 [a*]
Fe dissolved	< DL	23.63 ± 0.92 [b]	14.50 ± 4.82 [b*]

Data are expressed as mean ± SD (n = 8). DL means detection limit. DL for each metal correspond to Ag: 0.005 µg L^{-1}, Ti: 0.1 µg L^{-1}, Fe: 0.06 µg L^{-1}.

Water temperature and dissolved oxygen were similar among groups at initial and final times, corresponding to 26.0 ± 0.1 ºC and 6.5 ± 0.7 mg L^{-1} (n = 64, mean ± SD). Turbidity, pH, and electrolyte composition varied among groups and between times (Table 3). At 0 h, the pH in the exposure medium of experimental groups was higher than control due to the addition of NPs. Also, at 0h, turbidity was higher in FeNP group in relation to control, AgNP, and TiO_2NP groups, which could be due to the presence of *T. harzianum*. After 24 h, the pH and Ca^{+2} concentration increased in the exposure medium of all groups, which is related to the presence of the mussels. In AgNP group, turbidity, Na^+, and Cl^- increased after 24 h (Table 2). Hardness corresponded to 29.3 ± 1.5 $CaCO_3.L^{-1}$ at 0 h.

Table 3 – Water parameters measured in the exposure medium of control and experimental groups at initial (0 h) and final (24 h) times of the exposure.

	C	AgNP	TiO_2NP	FeNP

pH	**0 h**	7.1 ± 0.2 [a]	7.4 ± 0.2 [b]	7.5 ± 0.3 [b]	7.7 ± 0.3 [b]
	24 h	8.2 ± 0.3 [a**]	8.2 ± 0.1 [a**]	8.2 ± 0.2 [a**]	8.3 ± 0.2 [a**]
Turbidity (NTU)	**0 h**	1.9 ± 1.0 [ab]	0.8 ± 1.4 [a]	3.1 ± 1.7 [b]	4.9 ± 1.76 [c]
	24 h	2.8 ± 1.9 [a]	10.2 ± 5.4 [b*]	3.3 ± 1.0 [a]	3.8 ± 2.5 [a]
Na^+ (mM)	**0 h**	0.1 ± 0.0	0.1 ± 0.0	0.1 ± 0.0	0.1 ± 0.0
	24 h	0.1 ± 0.0	0.4 ± 0.0 **	0.1 ± 0.0	0.2 ± 0.0 *
Cl^- (mM)	**0 h**	0.9 ± 0.0	0.8 ± 0.0	0.8 ± 0.0	0.9 ± 0.0
	24 h	0.8 ± 0.1	1.1 ± 0.1 **	0.8 ± 0.1 *	0.8 ± 0.1
K^+ (mM)	**0 h**	0.02 ± 0.00	0.02 ± 0.00	0.02 ± 0.00	0.02 ± 0.00
	24 h	0.03 ± 0.01 **	0.03 ± 0.00 **	0.05 ± 0.03 *	0.03 ± 0.00 **
Ca^{+2} (mM)	**0 h**	0.1 ± 0.0	0.1 ± 0.0	0.1 ± 0.0	0.1 ± 0.0
	24 h	0.3 ± 0.0 **	0.3 ± 0.1 **	0.3 ± 0.1 **	0.3 ± 0.0 **

Data are expressed as mean ± SD (n = 8). * and ** indicate significant differences between 0 h and 24 h within the same group (Paired t-test or Wilcoxon Signed Rank Test, * $P < 0.05$, **$P < 0.001$). Different letters indicate significant differences among groups at the same time (ANOVA or Kruskal Wallis, $P < 0.05$).

4.3.3 Bioaccumulation of Ag, Ti and Fe

Ag concentration increased in the hemolymph (Mann-Whitney, $P < 0.001$), gills (t-test, $P = 0.009$), and foot (Mann-Whitney, $P = 0.002$) of mussels exposed to AgNP, in relation to control. Mantle and digestive gland were not affected by AgNP exposure (Figure 2A). Ti concentration increased in the hemolymph of mussels exposed to TiO_2NP (Mann-Whitney, $P = 0.002$), but did not change in the gills, mantle, digestive gland and foot (Figure 2B). Fe concentration also increased only in the hemolymph (Mann-Whitney, $P < 0.001$) of mussels exposed to FeNP (Figure 2C).

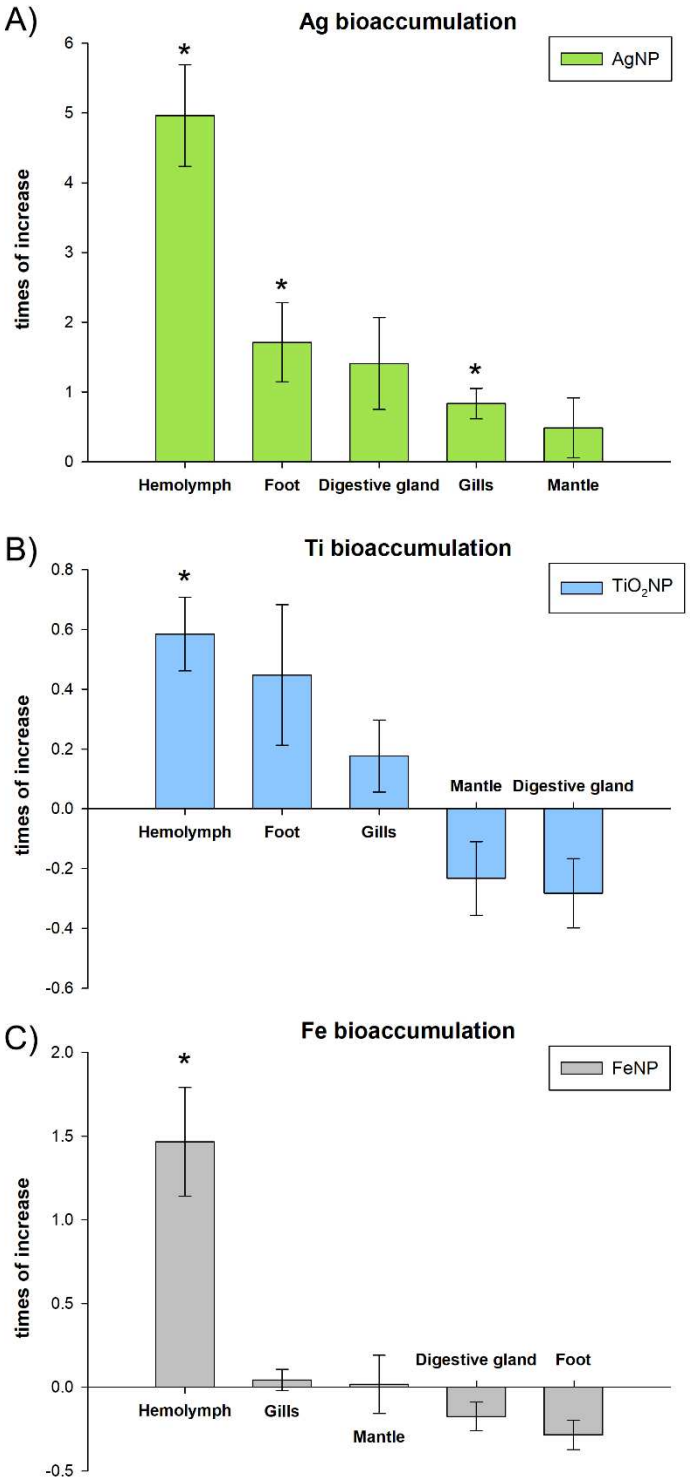

Figure 2 – Times of increase of metal concentration (Ag, Ti, Fe) in the hemolymph, gills, mantle, digestive gland, and foot of *Anodontites trapesialis* exposed to A) silver nanoparticles (AgNP), B) titanium dioxide nanoparticles (TiO_2NP), and C) iron nanoparticles (FeNP), in relation to control. Data are expressed as mean ± SE (n= 7-8). Asterisks (*) indicate differences in relation to control ($P < 0.05$).

4.3.4 Ions in the Hemolymph and Activity of Related Enzymes

Na^+ concentration decreased in the hemolymph of mussels exposed to AgNP compared to control, TiO_2NP, and FeNP (ANOVA, P = 0.005) (Figure 3A). Cl^- concentration also decreased in the hemolymph of mussels exposed to AgNP compared to control, TiO_2NP, and FeNP (ANOVA, P = 0.007) (Figure 3B). Na^+ concentration decreased 22.9% in AgNP group compared to control (from 18.15 ± 0.89 to 13.99 ± 0.76 mM, mean ± SE, n=7-8), while Cl^- concentration decreased 8.5% in AgNP group compared to control (from 37.48 ± 0.37 to 34.28 ± 0.79 mM, mean ± SE, n=7-8). K^+, Ca^{+2}, and Mg^{+2} concentrations were not affected by any exposure (Figure 3C-E).

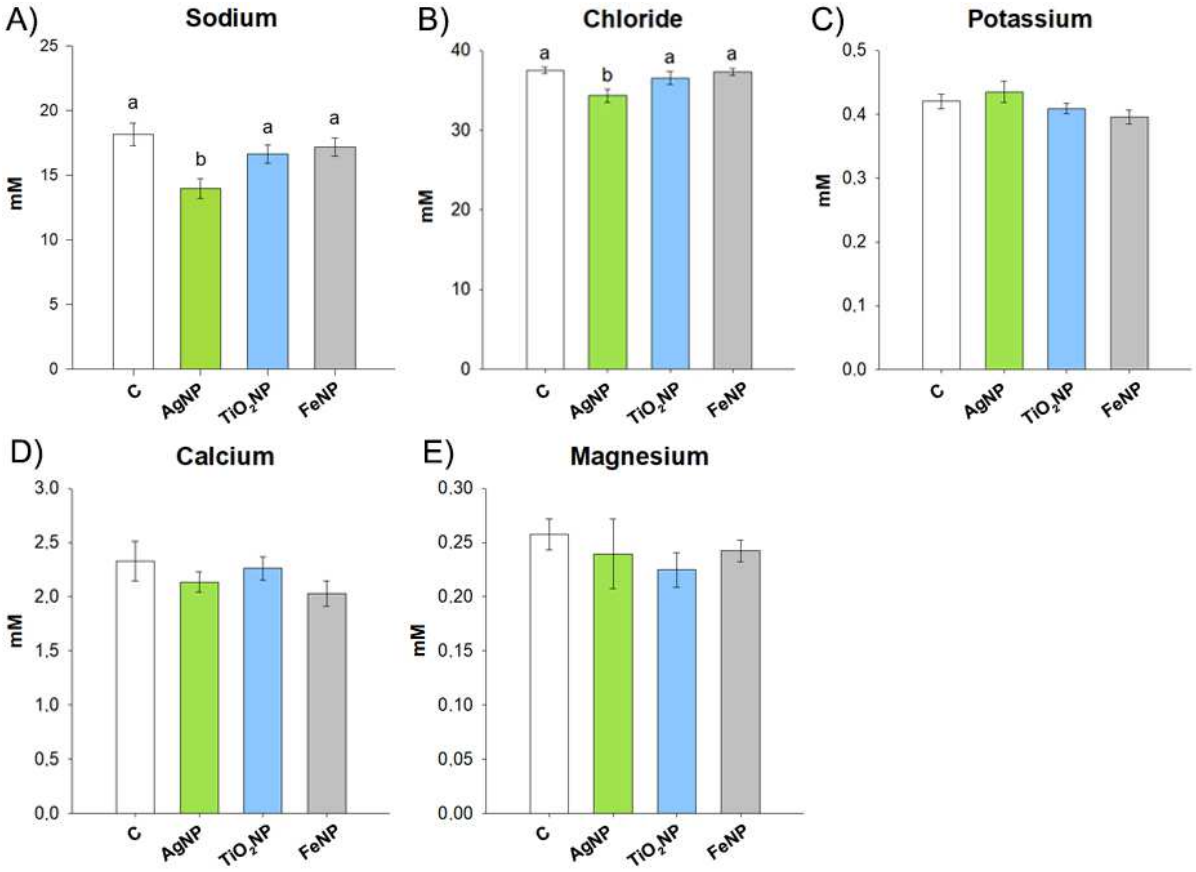

Figure 3 – Ion concentration in the hemolymph of *Anodontites trapesialis* exposed to water (C), silver nanoparticles (AgNP), titanium dioxide nanoparticles (TiO_2NP), and iron nanoparticles (FeNP). Data are expressed as mean ± SE (n= 7-8). Different letters indicate significant differences between groups (P < 0.05).

Activities of Na^+/K^+-ATPase, H^+-ATPase, and carbonic anhydrase in the gills and mantle did not change among groups (Figure 4). Activity of Ca^{2+}-ATPase increased in the gills of mussels exposed to TiO_2NP compared to AgNP (ANOVA, P = 0.023) (Figure 4C).

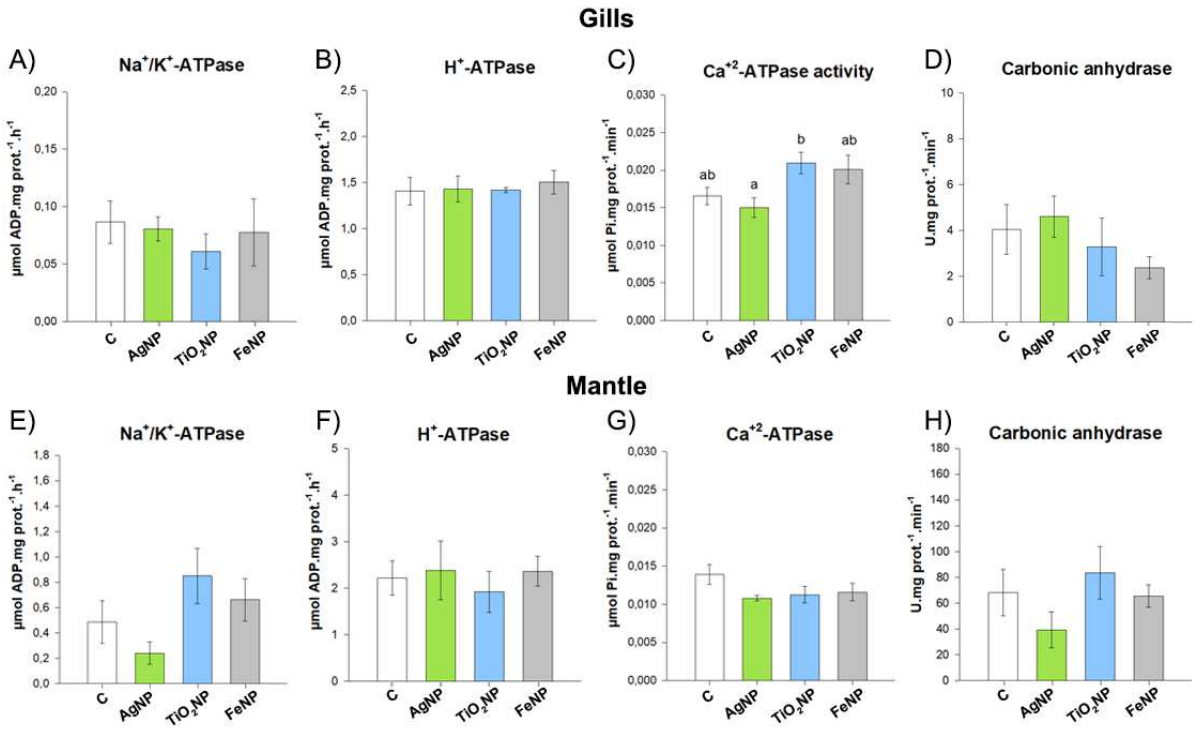

Figure 4 – Activities of Na^+/K^+-ATPase, H^+-ATPase, Ca^{2+}-ATPase, and carbonic anhydrase in the gills (A-D) and mantle (E-H) of *Anodontites trapesialis* exposed to water (C), silver nanoparticles (AgNP), titanium dioxide nanoparticles (TiO_2NP), and iron nanoparticles (FeNP). Data are expressed as mean ± SE (n= 5-8). Different letters indicate significant differences between groups (P < 0.05).

4.3.5 Antioxidant Defenses and Oxidative Damage

Activities of GST, CAT, SOD, and levels of LPO in gills, digestive gland, and mantle were not affected by any exposure (Figure 5).

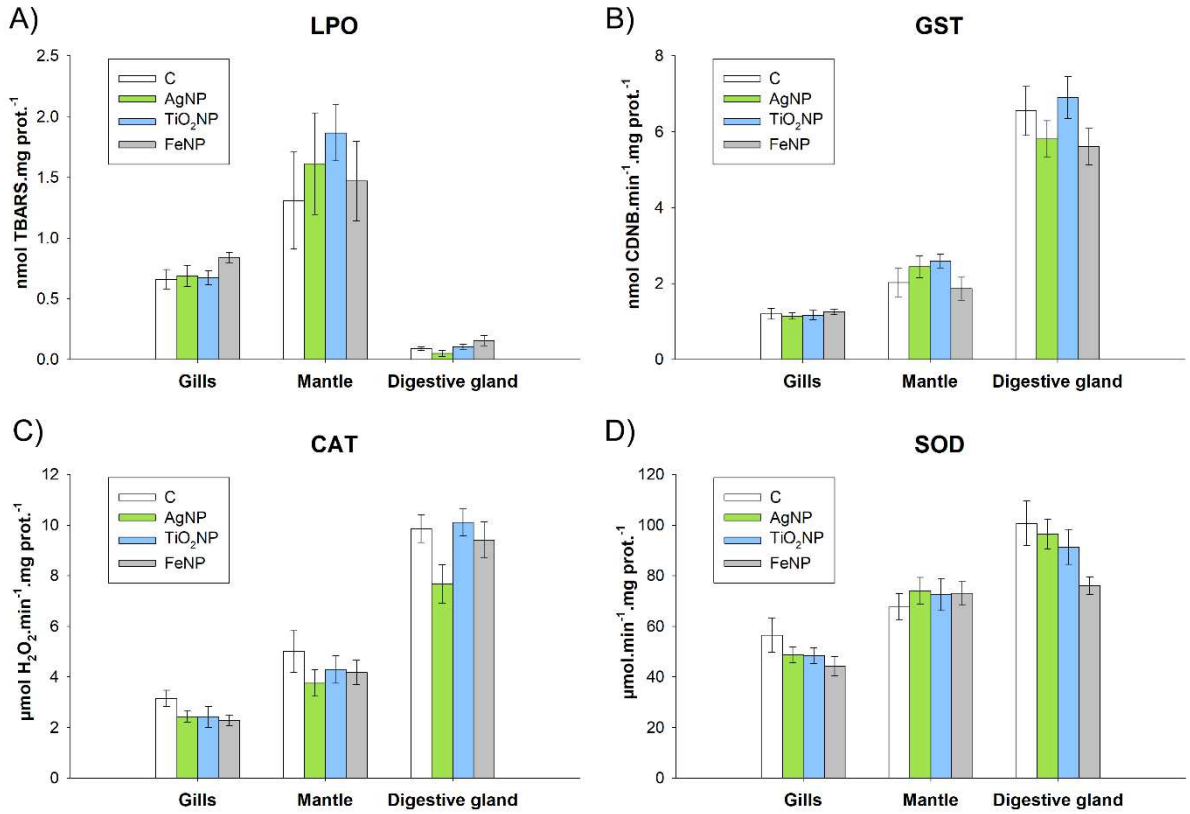

Figure 5 – A) Lipoperoxidation (LPO) and activity of B) glutathione S-transferase (GST), C) catalase (CAT) and D) superoxide dismutase (SOD) in the gills, digestive gland, and mantle of *Anodontites trapesialis* exposed to water (C), silver nanoparticles (AgNP), titanium dioxide nanoparticles (TiO_2NP), and iron nanoparticles (FeNP). Data are expressed as mean ± SE (n=5-8).

4.3.6 Glycogen and Glucose Concentrations

Glucose concentration in the hemolymph and glycogen concentration in the digestive gland, mantle and gills of mussels were not affected by any exposure (Figure 6).

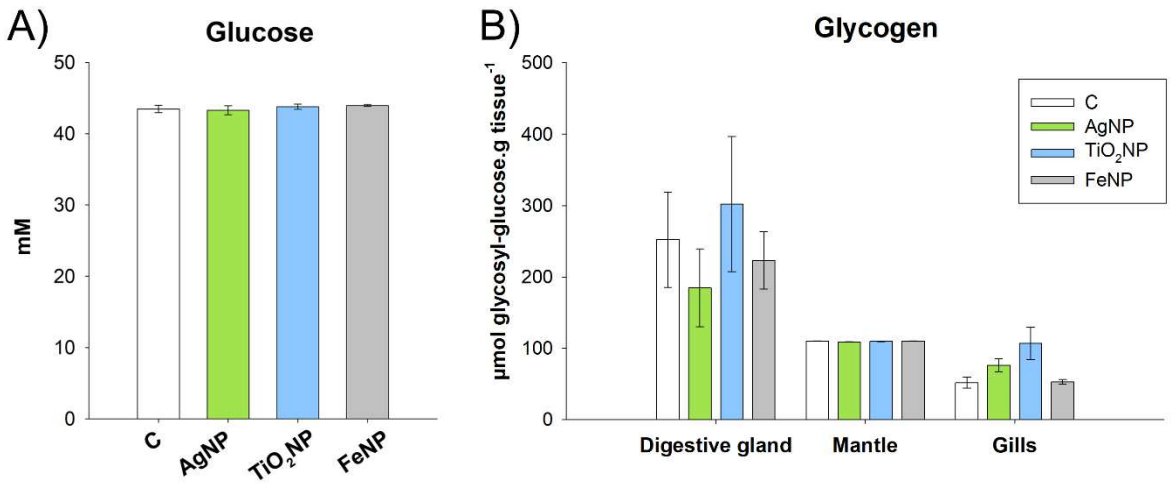

Figure 6 – A) Glucose concentration in the hemolymph and B) glycogen concentration in the digestive gland, mantle and gills of *Anodontites trapesialis* exposed to water (C), silver nanoparticles (AgNP), titanium dioxide nanoparticles (TiO_2NP), and iron nanoparticles (FeNP). Data are expressed as mean ± SE (n= 4-8).

4.3.7 Acetylcholinesterase (AChE) Activity

AChE activity in foot and adductor muscle did not change among groups (ANOVA; foot, P = 0.070; adductor muscle, P = 0.085) (Figure 7).

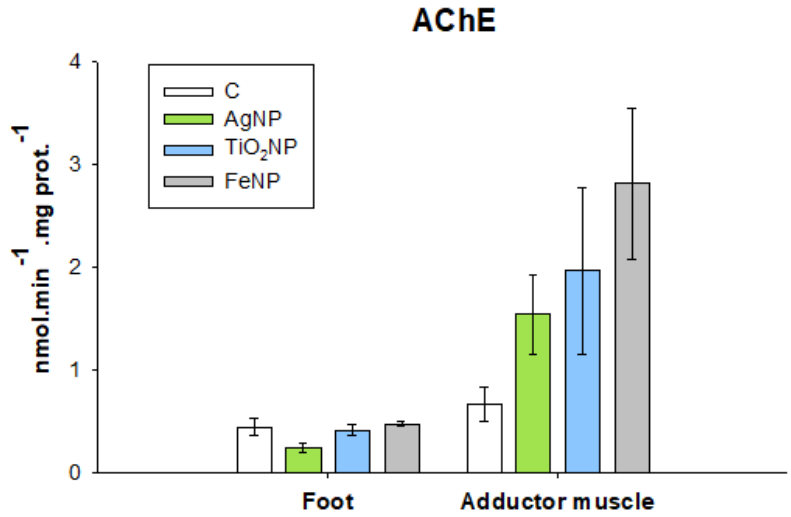

Figure 7 – Acetylcholinesterase (AChE) activity in the foot and adductor muscle of *Anodontites trapesialis* exposed to water (C), silver nanoparticles (AgNP), titanium dioxide nanoparticles (TiO_2NP), and iron nanoparticles (FeNP). Data are expressed as mean ± SE (n= 6-8).

4.4 Discussion

The physiochemical properties of each type of nanoparticle evaluated in the present work are different. AgNP are the smallest nanoparticles, followed by FeNP and TiO_2NP. In general, smaller nanoparticles are more toxic than their larger counterparts (Cazenave et al., 2019). The PDI values obtained indicate that all three types of nanoparticles have a broad size range, with TiO_2NP having the narrowest size range compared to AgNP and FeNP. Zeta potential values indicate that AgNP and TiO_2NP are weakly anionic, while FeNP are approximately neutral (Clogston and Patri, 2011). For biogenic NPs, the surface charge depends on the biomolecules present in the capping, therefore the proteins and amino acids should be conferring the negative charge. However, pH influences zeta potential. For instance, lowering the pH can make a negatively charged nanoparticle became neutralized or positively charge. Fish were exposed at neutral pH, which could have changed the FeNP zeta potential, since FeNP suspension had pH 5.0. In general, positively charged nanoparticles are more easily internalized by cells than neutral and negatively charged nanoparticles (Foroozandeh and Aziz, 2018), while phagocytic cells preferentially interact with negatively charged particles (Fröhlich, 2012). In the case of biogenic synthesis, zeta potential values do not provide information on the stability of the nanoparticles, and the suspensions used in the present work can be considered stable (Bilesky-José et al., 2021; Casagrande et al., 2021). In addition, the suspensions of NPs from the present work also differ in metal composition, nanoparticle concentration, and the remaining fungus content. All these differences can account for their effects on organisms. However, in the present work, the main effect observed (reduced Na^+ and Cl^- in the hemolymph of AgNP-exposed mussels) seems to be associated with the metal itself, as it will be further discussed.

At 0 h, the lower concentration of dissolved Ag compared to total Ag could be related to the binding of Ag to organic and inorganic ligands, such as dissolved organic matter, organic colloids, sulfide and chloride (Wood et al., 2011). It was not possible to verify if aggregation/agglomeration processes were related to the decline in the dissolved Ag quantified. After 24 h, mussels exposed to AgNP seemed to have released slightly more mucus and excretion material compared to the other groups (observational data), which could explain the increase in turbidity observed only in this group. Suspension-feeding bivalves reject particles by the mouth, labial

palps, and gills, and expel them by the mantle as pseudofeces (Cummings and Graf, 2015). It is possible that AgNP were rejected, forming pseudofeces that were released in the exposure medium. Additionally, at 0 h, water from all the beakers were transparent, except for the water from AgNP group, which assumed a yellowish color after adding the nanoparticles. The color diminished through time and was not visible after 24 h, indicating that AgNP were eliminated from the water column. Elimination could have happened due to the absorption of NPs by animals, dissolution into Ag ions, and/or binding of NPs to organic matter. The decrease in total and dissolved Ag could also be associated with the uptake of Ag by animals.

Mussels exposed to AgNP accumulated Ag in the gills, hemolymph, and foot. Suspension-feeding bivalves have ciliated gills that generate the water flow that passes through the animal, directing food particles to the mouth and then to the digestive system, where food is digested by the digestive gland (Cummings and Graf, 2015). In the present work, Ag absorption and accumulation in the gills may have occurred during this process. From the gills, Ag may have entered hemolymph, and then reached the foot. In the foot, Ag did not interfere with AChE activity.

Another difference observed on the physiochemical parameters of the exposure medium was the increase of Na^+ and Cl^- concentrations in the AgNP group, after 24 h of exposure. Such increase correlates with the decrease of Na^+ and Cl^- concentrations in the hemolymph of the mussels exposed to AgNP compared to control, TiO_2NP and FeNP groups. This effect seems to be associated with Ag action.

Ag ion (Ag^+) is known to inhibit Na^+/K^+-ATPase activity in freshwater teleosts and crustaceans, reducing Na^+ and Cl^- in blood plasma of teleosts, and Na^+ in the hemolymph and whole-body of crustaceans (Bianchini and Wood, 2003; Grosell et al., 2002; Wood, 2012). Besides decreasing Na^+ influx, Ag also increases Na^+ efflux in a crayfish species (Grosell et al., 2002). For freshwater and seawater bivalves, decreases in Na^+/K^+-ATPase activity have been reported after Ag exposure. Na^+/K^+-ATPase activity decreased in the whole-body of the freshwater bivalve *Sphaerium corneum* exposed for 28 days to nano-Ag (500 μg L^{-1}) and $AgNO_3$ (318 μg L^{-1}) (Volker et al., 2014), and in gill cells (*in vitro*) of the marine bivalve *Mytilus galloprovincialis* exposed to ionic (0.06 – 0.5 mg L^{-1}), nano-Ag (1.25 – 2.5 mg L^{-1}) and bulk-Ag (5 – 10 mg L^{-1}) for 24 h (Katsumiti et al., 2015). Furthermore, decreased activities of Na^+/K^+-ATPase, Ca^{+2}-ATPase, and Mg^{+2}-ATPase were reported in the gills, hepatopancreas, ovary, and adductor muscle of the seawater green mussel

(*Perna viridis*) exposed to $AgCl_2$ (2 mg L^{-1}) for 96 h.

However, in the present work, Na^+ e Cl^- decreased in the hemolymph without changes in the evaluated enzymes (Na^+/K^+-ATPase, H^+-ATPase, Ca^{+2}-ATPase, and carbonic anhydrase), both in the gills and in the mantle, at the time assessed (24 h). Thus, the mechanism that led to the decrease in Na^+ and Cl^- was not clarified, but the occurrence of an ionoregulatory disturbance could be evidenced. Additionally, the present work shows that both Na^+ and Cl^- were affected by Ag in the bivalve species evaluated, which is similar to the effect observed in teleost fish.

In regard to TiO_2NP exposure, Ti concentration increased in the hemolymph of mussels. Nano-TiO_2 can be internalized into hemocytes within a short period of exposure, as demonstrated by Couleau et al. (2012) on zebra mussels (*Dreissena polymorpha*) exposed to 1 mg L^{-1} of nano-TiO_2 for 24 h, and on golden mussels (*Limnoperna fortunei*) exposed to the same concentration of nano-TiO_2 for 2 h (Girardello et al., 2016). The presence of nano-TiO_2 inside hemocytes was related to the inhibition of phagocytosis in these cells (Couleau et al., 2012), and to the cell damage observed later at a higher concentration (50 mg L^{-1}, 4 h of exposure), in which larger aggregates were internalized (Girardello et al., 2016).

Although nano-TiO_2 can be internalized into hemocytes and promote damage, TiO_2NP (from the present work) are likely composed of a very small metallic core of TiO_2, stabilized by a thick layer of molecules derived from the fungus employed in the synthesis. The metal analysis of the exposure medium indicated a concentration of total Ti consistent with the nominal concentration, but dissolved Ti was not detected at 0 h. This finding indicates that most Ti found in the exposure medium was in the bulk form, and that mussels were exposed to NPs composed mainly of the fungal molecules. Therefore, the increased concentration of Ti observed in the hemolymph can be a result of the uptake of bulk TiO_2 that remained in the suspension, instead of TiO_2NP. Nevertheless, both nano and bulk forms of TiO_2 led to increases in the volume and proliferation of hemocytes on the marine clam *Ruditapes phlippinarum* exposed to 10 µg L^{-1} TiO_2 (bulk and nano forms) for 24 h, although additional effects were seen for nano-TiO_2. In the present work, within the parameters evaluated, no effects besides Ti bioaccumulation were found on mussels exposed to TiO_2NP. Considering the above mentioned, adverse effects on hemocytes are possible and could be further investigated.

The concentration of Fe measured in the exposure medium of FeNP

group was below the nominal concentration, and decreased after 24 h of exposure. This decrease, in part, is associated with the uptake of Fe by mussels. Similar to TiO_2NP, exposure to FeNP affected only the bioaccumulation in the hemolymph of mussels, with an increase in Fe concentration. This accumulation could be transient, since the exposure of *A. trapesialis* to 5 mg Fe L^{-1} for 96 h did not result in the increase of Fe concentration in any analyzed tissue (hemolymph, gills, mantle, digestive gland and foot) (Oliveira et al., 2018).

Although NPs had no effect on the parameters of oxidative stress evaluated, the activities of the antioxidant enzymes and levels of LPO in the control group varied among different tissues. The digestive gland presented a higher activity of GST, SOD and CAT enzymes, with lower LPO levels, when compared to gills and mantle. This pattern can also be seen in the work of Oliveira et al. (2018) with the same bivalve species, and indicates that the digestive gland is the main tissue involved in the detoxification process on *A. trapesialis*. Also, the digestive gland seems to be an important site for glycogen storage, given that the concentration of glycogen evaluated in the present study was highest in this organ, followed by the mantle and then the gills. It was also possible to note different activities of the enzymes related to ionoregulation. Carbonic anhydrase activity was higher in the mantle of control mussels, compared to the gills. This is in accordance with the fact that the outer mantle epithelium of bivalves is involved in shell formation (Zhao et al., 2017).

4.5 Conclusion

This work is part of an integrative assessment of the toxicity of biogenic NPs synthesized for agricultural use. Biochemical and physiological parameters were evaluated on the Neotropical freshwater mussel *A. trapesialis*, considering the hypothesis that suspension-feeding bivalves would be more susceptible to NPs toxicity. *A. trapesialis* showed bioaccumulation potential, but was not highly sensitive to the NPs used in the present work. On the concentration and time of exposure tested, AgNP promoted Ag accumulation and ionoregulatory disturbances, whereas FeNP led to Fe accumulation, and TiO_2NP led to Ti accumulation. It is highlighted the preferential use of TiO_2NP and FeNP over AgNP.

In addition, the effects of these NPs should be tested with other species, concentrations, and exposure times, to further verify their safe use in agriculture.

REFERENCES

Alves, L.C., Wood, C.M., 2006. The chronic effects of dietary lead in freshwater juvenile rainbow trout (*Oncorhynchus mykiss*) fed elevated calcium diets. Aquat. Toxicol. 78, 217–232. https://doi.org/https://doi.org/10.1016/j.aquatox.2006.03.005

Antignano, A., Manning, C.E., 2008. Rutile solubility in H_2O, H_2O-SiO_2, and H_2O-$NaAlSi_3O_8$ fluids at 0.7-2.0 GPa and 700-1000 °C: Implications for mobility of nominally insoluble elements. Chem. Geol. 255, 283–293. https://doi.org/10.1016/j.chemgeo.2008.07.001

Beutler, E., 1972. Red cell metabolism. Biochimie 54, 759–764. https://doi.org/10.1016/S0300-9084(72)80181-0

Bianchini, A., Grosell, M., Gregory, S.M., Wood, C.M., 2002. Acute silver toxicity in aquatic animals is a function of sodium uptake rate. Environ. Sci. Technol. 36, 1763–1766. https://doi.org/10.1021/es011028t

Bianchini, A., Wood, C.M., 2003. Mechanism of acute silver toxicity in *Daphnia magna*. Environ. Toxicol. Chem. 22, 1361. https://doi.org/10.1897/1551-5028(2003)022<1361:MOASTI>2.0.CO;2

Bidinotto, P.M., Moraes, G., Souza, R.H.S., 1997. Hepatic glycogen and glucose in eight tropical fresh water teleost fish: a procedure for field determinations of micro samples. B. Téc. CEPTA 10, 53–60.

Bilesky-José, N., Maruyama, C., Germano-Costa, T., Campos, E., Carvalho, L., Grillo, R., Fraceto, L.F., De Lima, R., 2021. Biogenic α-Fe_2O_3 Nanoparticles Enhance the Biological Activity of *Trichoderma* against the Plant Pathogen *Sclerotinia sclerotiorum*. ACS Sustain. Chem. Eng. 9, 1669–1683. https://doi.org/10.1021/acssuschemeng.0c07349

Bolton, M.D., Thomma, B.P.H.J., Nelson, B.D., 2006. *Sclerotinia sclerotiorum* (Lib.) de Bary: Biology and molecular traits of a cosmopolitan pathogen. Mol. Plant Pathol. https://doi.org/10.1111/j.1364-3703.2005.00316.x

Bonomo, M.M., Fernandes, J.B., Carlos, R.M., Fernandes, M.N., 2020. Biochemical

and genotoxic biomarkers and cell cycle assessment in the zebrafish liver (ZF-L) cell line exposed to the novel metal-insecticide magnesium-hespiridin complex. Chemosphere 250, 126416. https://doi.org/10.1016/J.CHEMOSPHERE.2020.126416

Bradford, M.M., 1976. A rapid and sensitive method for the quantitation of microgram quantities of protein utilizing the principle of protein-dye binding. Anal. Biochem. 72, 248–254. https://doi.org/10.1016/0003-2697(76)90527-3

Brodeur, J.C., Poletta, G.L., Simoniello, M.F., Carriquiriborde, P., Cristos, D.S., Pautasso, N., Paravani, E., Poliserpi, M.B., D'Andrea, M.F., Gonzalez, P. V., Aca, V.L., Curto, A.E., 2020. The problem with implementing fish farms in agricultural regions: A trial in a pampean pond highlights potential risks to both human and fish health. Chemosphere 262, 128408. https://doi.org/10.1016/j.chemosphere.2020.128408

Bury, N.R., Boyle, D., Cooper, C.A., 2011. Iron, in: Homeostasis and Toxicology of Essential Metals. pp. 202–253.

Camejo, G., Wallin, B., Enojärvi, M., 1998. Analysis of Oxidation and Antioxidants Using Microtiter Plates, in: Armstrong, D. (Ed.), Free Radical and Antioxidant Protocols. pp. 377–388. https://doi.org/10.1385/0-89603-472-0:377

Canesi, L., Ciacci, C., Fabbri, R., Marcomini, A., Pojana, G., Gallo, G., 2012. Bivalve molluscs as a unique target group for nanoparticle toxicity. Mar. Environ. Res. 76, 16–21. https://doi.org/10.1016/j.marenvres.2011.06.005

Carriquiriborde, P., Mirabella, P., Waichman, A., Solomon, K., Van den Brink, P.J., Maund, S., 2014. Aquatic risk assessment of pesticides in Latin America. Integr. Environ. Assess. Manag. 10, 539–542. https://doi.org/10.1002/ieam.1561

Casagrande, G., Casagrande, M.G., Costa, T.G., José, N.B., Stigliani, T.P., Carvalho, L., Fraceto, L.F., Lima, R. De, 2021. Influence of the capping of biogenic silver nanoparticles on their toxicity and mechanism of action towards *Sclerotinia sclerotiorum*. J. Nanobiotechnology 5, 1–19. https://doi.org/10.1186/s12951-021-00797-5

Cazenave, J., Ale, A., Bacchetta, C., Rossi, A.S., 2019. Nanoparticles Toxicity in Fish Models. Curr. Pharm. Des. 25, 3927–3942. https://doi.org/10.2174/1381612825666190912165413

Chowdhury, M.J., Girgis, M., Wood, C.M., 2016. Revisiting the mechanisms of copper toxicity to rainbow trout: Time course, influence of calcium, unidirectional

Na^+ fluxes, and branchial Na^+, K^+ ATPase and V-type H^+ ATPase activities. Aquat. Toxicol. 177, 51–62. https://doi.org/10.1016/j.aquatox.2016.05.009

Clogston, J.D., Patri, A.K., 2011. Zeta potential measurement. Methods Mol. Biol. 697, 63–70. https://doi.org/10.1007/978-1-60327-198-1_6

Couleau, N., Techer, D., Pagnout, C., Jomini, S., Foucaud, L., Laval-Gilly, P., Falla, J., Bennasroune, A., 2012. Hemocyte responses of Dreissena polymorpha following a short-term in vivo exposure to titanium dioxide nanoparticles: Preliminary investigations. Sci. Total Environ. 438, 490–497. https://doi.org/10.1016/j.scitotenv.2012.08.095

Cummings, K.S., Graf, D.L., 2015. Class Bivalvia, in: Thorp, J.H., Rogers, D.C. (Eds.), Thorp and Covich's Freshwater Invertebrates: Ecology and General Biology. Academic Press, London, pp. 423–506. https://doi.org/10.1016/B978-0-12-385026-3.00019-X

de Almeida, V.E.S., Friedrich, K., Tygel, A.F., Melgarejo, L., Carneiro, F.F., 2017. Use of genetically modified crops and pesticides in Brazil: growing hazards. Cienc. e Saude Coletiva 22, 3333–3339. https://doi.org/10.1590/1413-812320172210.17112017

de Paula, A.A., Risso, W.E., Martinez, C.B. dos R., 2021. Effects of copper on an omnivorous (*Astyanax altiparanae*) and a carnivorous fish (*Hoplias malabaricus*): A comparative approach. Aquat. Toxicol. 237. https://doi.org/10.1016/j.aquatox.2021.105874

Dias, L.C.P., Pimenta, F.M., Santos, A.B., Costa, M.H., Ladle, R.J., 2016. Patterns of land use, extensification, and intensification of Brazilian agriculture. Glob. Chang. Biol. 22, 2887–2903. https://doi.org/10.1111/gcb.13314

Dubois, M., Gilles, K.A., Hamilton, J.K., Rebers, P.A., Smith, F., 1956. Colorimetric Method for Determination of Sugars and Related Substances. Anal. Chem. 28, 350–356. https://doi.org/10.1021/ac60111a017

Ellman, G.L., Courtney, K.D., Andres, V., Feather-Stone, R.M., 1961. A new and rapid colorimetric determination of acetylcholinesterase activity. Biochem. Pharmacol. 7, 88–95.

Foroozandeh, P., Aziz, A.A., 2018. Insight into Cellular Uptake and Intracellular Trafficking of Nanoparticles. Nanoscale Res. Lett. 13. https://doi.org/10.1186/s11671-018-2728-6

Fraceto, L.F., Grillo, R., de Medeiros, G.A., Scognamiglio, V., Rea, G., Bartolucci, C.,

2016. Nanotechnology in agriculture: Which innovation potential does it have? Front. Environ. Sci. 4, 1–5. https://doi.org/10.3389/fenvs.2016.00020

Fraceto, L.F., Maruyama, C.R., Guilger, M., Mishra, S., Keswani, C., Singh, H.B., de Lima, R., 2018. *Trichoderma harzianum*-based novel formulations: potential applications for management of Next-Gen agricultural challenges. J. Chem. Technol. Biotechnol. 93, 2056–2063. https://doi.org/10.1002/jctb.5613

Fröhlich, E., 2012. The role of surface charge in cellular uptake and cytotoxicity of medical nanoparticles. Int. J. Nanomedicine. https://doi.org/10.2147/IJN.S36111

Gagné, F., 2014. Xenobiotic Biotransformation, in: Biochemical Ecotoxicology. Academic Press, pp. 117–130. https://doi.org/10.1016/B978-0-12-411604-7.00007-6

Gibbs, A., Somero, G., 1989. Pressure adaptation of Na^+/K^+-ATPase in gills of marine teleost fishes. J. Exp. Biol. 143, 475–492.

Girardello, F., Leite, C.C., Branco, C.S., Roesch-Ely, M., Fernandes, A.N., Salvador, M., Henriques, J.A.P., 2016. Antioxidant defences and haemocyte internalization in *Limnoperna fortunei* exposed to TiO_2 nanoparticles. Aquat. Toxicol. 176, 190–196. https://doi.org/10.1016/j.aquatox.2016.04.024

Grosell, M., Brauner, C.J., Kelly, S.P., McGeer, J.C., Bianchini, A., Wood, C.M., 2002. Physiological responses to acute silver exposure in the freshwater crayfish (*Cambarus diogenes diogenes*) - A model invertebrate? Environ. Toxicol. Chem. 21, 369–374. https://doi.org/10.1002/etc.5620210220

Guilger-Casagrande, M., Germano-Costa, T., Pasquoto-Stigliani, T., Fraceto, L.F., Lima, R. de, 2019. Biosynthesis of silver nanoparticles employing *Trichoderma harzianum* with enzymatic stimulation for the control of *Sclerotinia sclerotiorum*. Sci. Rep. 9, 14351. https://doi.org/https://doi.org/10.1038/s41598-019-50871-0

Guilger, M., Pasquoto-Stigliani, T., Bilesky-Jose, N., Grillo, R., Abhilash, P.C., Fraceto, L.F., De Lima, R., 2017. Biogenic silver nanoparticles based on *Trichoderma harzianum*: Synthesis, characterization, toxicity evaluation and biological activity. Sci. Rep. 7, 1–13. https://doi.org/10.1038/srep44421

Katsumiti, A., Gilliland, D., Arostegui, I., Cajaraville, M.P., 2015. Mechanisms of toxicity of Ag nanoparticles in comparison to bulk and ionic Ag on mussel hemocytes and gill cells. PLoS One 10, 1–30. https://doi.org/10.1371/journal.pone.0129039

Keen, J.H., Habig, W.H., Jakoby, W.B., 1976. Mechanism for the several activities of

the glutathione S transferases. J. Biol. Chem. 251, 6183–6188.

Laurance, W.F., Sayer, J., Cassman, K.G., 2014. Agricultural expansion and its impacts on tropical nature. Trends Ecol. Evol. 29, 107–116. https://doi.org/10.1016/j.tree.2013.12.001

Li, S., Li, X., Cheng, J., Zhan, A., 2021. Effectiveness and mechanisms of recoverable magnetic nanoparticles on mitigating golden mussel biofouling. Environ. Sci. Technol. 55, 2500–2510. https://doi.org/10.1021/acs.est.0c08014

Loayza-Muro, R., Elías-Letts, R., 2007. Responses of the mussel *Anodontites trapesialis* (Unionidae) to environmental stressors: Effect of pH, temperature and metals on filtration rate. Environ. Pollut. 149, 209–215. https://doi.org/10.1016/j.envpol.2007.01.003

McCord, J.M., Fridovich, I., 1969. Superoxide dismutase. An enzymic function for erythrocuprein (hemocuprein). J. Biol. Chem.

Mora, P., Michel, X., Narbonne, J.F., 1999. Cholinesterase activity as potential biomarker in two bivalves. Environ. Toxicol. Pharmacol. 7, 253–260. https://doi.org/10.1016/S1382-6689(99)00019-8

Morgan, T.P., Grosell, M., Gilmour, K.M., Playle, R.C., Wood, C.M., 2004. Time course analysis of the mechanism by which silver inhibits active Na+ and Cl- uptake in gills of rainbow trout. Am. J. Physiol. - Regul. Integr. Comp. Physiol. 287, 234–242. https://doi.org/10.1152/ajpregu.00448.2003

Oliveira, L.F. de, Cabral, M.T., Vieira, C.E.D., Antoniazzi, M.H., Risso, W.E., Martinez, C.B. dos R., 2016. Metals bioaccumulation and biomarkers responses in the Neotropical freshwater clam *Anodontites trapesialis*: Implications for monitoring coal mining areas. Sci. Total Environ. 571, 983–991. https://doi.org/10.1016/j.scitotenv.2016.07.086

Oliveira, L.F., Cabral, M.T., Risso, W.E., Martinez, C.B. dos R., 2018. Single and combined effects of Zn, Mn and Fe on the Neotropical freshwater bivalve *Anodontites trapesialis*: Bioaccumulation and biochemical biomarkers. Ecotoxicol. Environ. Saf. 161, 735–745. https://doi.org/10.1016/j.ecoenv.2018.06.029

Pérez, D.J., Iturburu, F.G., Calderon, G., Oyesqui, L.A.E., De Gerónimo, E., Aparicio, V.C., 2021. Ecological risk assessment of current-use pesticides and biocides in soils, sediments and surface water of a mixed land-use basin of the Pampas region, Argentina. Chemosphere 263, 128061.

https://doi.org/10.1016/j.chemosphere.2020.128061

Pimenta, F.M., Speroto, A.T., Costa, M.H., Dionizio, E.A., 2021. Historical changes in land use and suitability for future agriculture expansion in Western Bahia, Brazil. Remote Sens. 13, 1–31. https://doi.org/10.3390/rs13061088

Rocha, T.L., Gomes, T., Sousa, V.S., Mestre, N.C., Bebianno, M.J., 2015. Ecotoxicological impact of engineered nanomaterials in bivalve molluscs: An overview. Mar. Environ. Res. 111, 74–88. https://doi.org/10.1016/j.marenvres.2015.06.013

Singh, P., Kim, Y.J., Zhang, D., Yang, D.C., 2016. Biological Synthesis of Nanoparticles from Plants and Microorganisms. Trends Biotechnol. 34, 588–599. https://doi.org/10.1016/j.tibtech.2016.02.006

Skocaj, M., Filipic, M., Petkovic, J., Novak, Sasa, Novak, Saša, Stefan, J., 2011. Titanium dioxide in our everyday life; is it safe? Radiol Oncol 45, 227–247. https://doi.org/10.2478/v10019-011-0037-0

Stohs, S.J., Bagchi, D., 1995. Oxidative mechanisms in the toxicity of metal ions. Free Radic. Biol. Med. 18, 321–336.

Taheriniya, S., Behboodi, Z., 2016. Comparing Green Chemical Methods and Chemical Methods for the synthesis of tianium dioxide nanoparticles. Int. J. Pharm. Sci. Res. 7, 4927–4932. https://doi.org/10.13040/IJPSR.0975-8232.7(12).4927-32

Vieira, C.E.D., Costa, P.G., Cabrera, L.C., Primel, E.G., Fillmann, G., Bianchini, A., Bueno dos Reis Martinez, C., 2017. A comparative approach using biomarkers in feral and caged Neotropical fish: Implications for biomonitoring freshwater ecosystems in agricultural areas. Sci. Total Environ. https://doi.org/10.1016/j.scitotenv.2017.02.026

Vieira, C.E.D., Costa, P.G., Caldas, S.S., Tesser, M.E., Risso, W.E., Escarrone, A.L.V., Primel, E.G., Bianchini, A., dos Reis Martinez, C.B., 2019. An integrated approach in subtropical agro-ecosystems: Active biomonitoring, environmental contaminants, bioaccumulation, and multiple biomarkers in fish. Sci. Total Environ. 666. https://doi.org/10.1016/j.scitotenv.2019.02.209

Vijayavel, K., Gopalakrishnan, S., Balasubramanian, M.P., 2007. Sublethal effect of silver and chromium in the green mussel *Perna viridis* with reference to alterations in oxygen uptake, filtration rate and membrane bound ATPase system as biomarkers. Chemosphere 69, 979–986.

https://doi.org/10.1016/j.chemosphere.2007.05.011

Vitale, A.M., Monserrat, J.M., Castilho, P., Rodriguez, E.M., 1999. Inhibitory effects of cadmium on carbonic anhydrase activity and ionic regulation of the estuarine crab *Chasmagnathus granulata* (Decapoda, Grapsidae). Comp. Biochem. Physiol. Part C Pharmacol. Toxicol. Endocrinol. 122, 121–129. https://doi.org/10.1016/S0742-8413(98)10094-4

Volker, C., Kampken, I., Boedicker, C., Oehlmann, J., Oetken, M., 2014. Toxicity of silver nanoparticles and ionic silver: Comparison of adverse effects and potential toxicity mechanisms in the freshwater clam *Sphaerium corneum*. Nanotoxicology 5390, 1–9. https://doi.org/10.3109/17435390.2014.963723

Wood, C.M., 2012. Silver, in: Chris M. Wood, A.P.F. and C.J.B. (Ed.), Homeostasis and Toxicology of Non-Essential Metals. Academic Press, London, pp. 1–54.

Wood, C.M., Farrell, A.P., Brauner, C.J., 2011. Homeostasis and Toxicology of Non-Essential Metals, Homeostasis and Toxicology of Non-Essential Metals. Elsevier Inc. https://doi.org/10.1016/s1546-5098(11)31032-1

Zha, S., Rong, J., Guan, X., Tang, Y., Han, Y., Liu, G., 2019. Immunotoxicity of four nanoparticles to a marine bivalve species, *Tegillarca granosa*. J. Hazard. Mater. 377, 237–248. https://doi.org/10.1016/j.jhazmat.2019.05.071

Zhao, L., Schöne, B.R., Mertz-Kraus, R., 2017. Delineating the role of calcium in shell formation and elemental composition of *Corbicula fluminea* (Bivalvia). Hydrobiologia 790, 259–272. https://doi.org/10.1007/s10750-016-3037-7

Zhu, X., Pathakoti, K., Hwang, H.-M., 2019. Green synthesis of titanium dioxide and zinc oxide nanoparticles and their usage for antimicrobial applications and environmental remediation, in: Green Synthesis, Characterization and Applications of Nanoparticles. Elsevier Inc., pp. 223–263.

Zimmermann, S., Ruchter, N., Loza, K., Epple, M., Sures, B., 2017. Nanoparticulate versus ionic silver: Behavior in the tank water, bioaccumulation, elimination and subcellular distribution in the freshwater mussel *Dreissena polymorpha*. Environ. Pollut. 222, 251–260. https://doi.org/10.1016/j.envpol.2016.12.048

5 MANUSCRITO II

Biogenic metallic nanoparticles (Ag, TiO_2, Fe) effects on the freshwater fish *Prochilodus lineatus*: bioaccumulation and multiple biomarkers

Maria Eduarda Tesser[1], Mariana Guilger[2,4], Wagner Ezequiel Risso[1], Adalto Bianchini[3], Renata de Lima[4], Claudia Bueno dos Reis Martinez[1]

[1] Laboratory of Animal Ecophysiology, Department of Physiological Sciences, State University of Londrina (UEL), Londrina, Paraná, Brazil.
[2] Laboratory of Environmental Nanotechnology, São Paulo State University (UNESP), Sorocaba, São Paulo, Brazil
[3] Institute of Biological Sciences, Federal University of Rio Grande (FURG), Rio Grande, Rio Grande do Sul, Brazil
[4] Laboratory of Bioactivity Assessment and Toxicology of Nanomaterials, University of Sorocaba (UNISO), Sorocaba, São Paulo, Brazil

ABSTRACT

Silver (Ag), titanium dioxide (TiO_2), and iron (Fe) nanoparticles (NPs) synthesized using the fungus *Trichoderma harzianum* have promising agricultural use. However, possible effects must be evaluated on aquatic organisms, which may encounter agricultural contaminants. Thus, this work aimed to evaluate the sublethal effects of the short-term exposure (24 h) to silver nanoparticles (AgNP), rutile titanium dioxide nanoparticles (TiO_2NP) and iron nanoparticles (FeNP), all synthesized using *T. harzianum*, on the freshwater teleost *Prochilodus lineatus,* a Neotropical fish species that has shown to be sensitive to metals and nanoparticles. Juveniles were divided into four groups (n = 8/group): a control group, kept in water only; a group exposed to AgNP at the concentration of 3 x 10^8 NPs mL^{-1} (35.60 µg Ag L^{-1}); a group exposed to TiO_2NP at a concentration of 1 x 10^8 NPs mL^{-1} (38.94 µg Ti L^{-1}); and a group exposed to FeNP at a concentration of 3 x 10^7 NPs mL^{-1} (123.98 µg Fe L^{-1}). After the exposure, bioaccumulation of metals and multiple biomarkers were evaluated. AgNP caused silver accumulation, histological changes in the gills (hyperplasia and hypertrophy of epithelial cells, lamellar adhesion and lamellar fusion, with increased DTC), increased plasma glucose, lactate and potassium, decreased plasma calcium, decreased circulating white blood cells count and decreased glutathione and glutathione S-transferase (GST) activity in the liver. TiO_2NP caused titanium accumulation, decreased plasma calcium, decreased GST and increased liver glycogen. FeNP caused Fe accumulation in all tissues and fluids evaluated, increased circulating white blood cells count, decreased glutathione and increased lipoperoxidation in the gills, decreased GST and increased liver glycogen. Histological changes in the gills are related to the increase in plasma glucose, lactate and K^+, and indicate respiratory toxicity associated with AgNP. In this group, the decrease in glutathione may be related to silver binding with sulfhydryl groups. On the other hand, the decrease in glutathione and increase in lipoperoxidation evidences oxidative stress in the gills of teleosts exposed to FeNP, and the accumulation of Fe indicates bioavailability of Fe as FeNP. All NPs lead to a decrease in GST in the liver, which can compromise biotransformation. Among tissues, AgNP and FeNP affected mainly the gills, while TiO_2NP affected mainly the liver. All nanoparticles caused metal accumulation in the posterior kidney, plasma, and hemolymph, which points to the sensitivity of this tissue and fluids to accumulation of NPs. Mutagenicity (micronucleus and nuclear erythrocytic alterations) and neurotoxicity (acetylcholinesterase enzyme activity) were not observed. The results indicate that the NPs evaluated were not safe at the concentrations tested, with AgNP being the most harmful. More studies are needed for the environmentally safe use of these NPs in agriculture.

Key-words: Ecotoxicology. Green synthesis. Pesticides. Fish. Oxidative stress. Respiratory toxicity.

5.1 INTRODUCTION

Sclerotinia sclerotiorum is a cosmopolitan fungal pathogen that causes white mold disease in more than 400 plant species, including several species of economical relevance (Bolton et al., 2006). *Trichoderma harzianum* is a filamentous fungus widely used for biological control: in Brazil in 2019, the most produced and marketed microbiological products for application in agriculture and other sectors were *Trichoderma* species (IBAMA, 2020). *T. harzianum* effectively acts against *S. sclerotiorum*, but its use is limited due to its low persistence in crops (Fraceto et al., 2018). This limitation can be overcome with new application technologies, such as microencapsulation (Maruyama et al., 2020) and the synthesis of metallic nanoparticles using *T. harzianum* (Guilger et al., 2017).

Nanoparticles (NPs) can be synthesized by physical, chemical, and biological processes. The biological (also known as biogenic or green) synthesis, which employs microorganisms and plant extracts, presents advantages over physical and chemical methods, including a more environmentally sustainable, faster, and cost-effective production. Additionally, biogenic NPs can possess a capping of biomolecules derived from the organism employed in the synthesis. The capping provides stability and can also have bioactive compounds that enhance nanoparticle efficacy. Thus, the capping formation during biological synthesis removes additional steps required in physiochemical synthesis, such as the addition of stabilizing agents and biologically active compounds (Singh et al., 2016).

Silver (Ag), titanium dioxide (TiO_2), and iron (Fe) NPs[2] synthesized using *T. harzianum* are effective in the control of white mold (Bilesky-José et al., 2021; Guilger et al., 2017; Pasquoto-Stigliani, to be published). The chemical composition of AgNP, TiO_2NP, and FeNP consists in a metallic core stabilized by a capping of biomolecules derived from *T. harzianum*. AgNP synthesis occurs by the reduction of silver ions (Ag^+), resulting in a metallic core composed of elemental silver (Ag^0) (Guilger et al., 2017). In contrast, TiO_2NP formation does not occur by redox mechanisms, but it most likely occurs by the dispersion of TiO_2 in *T. harzianum* enzyme content, followed by adsorption of fungal proteins on the particles surface

[2] These nanoparticles are referred in the present work as AgNP, TiO_2NP, and FeNP, respectively, while NPs from other studies are referred as nano-Ag, nano-TiO_2, and nano-Fe, for the clear understanding of the text.

(data to be published, Pasquoto Stigliani et al.). Lastly, X-ray diffraction indicates that FeNP are composed of hematite (α-Fe_2O_3). The proposed mechanism for FeNP synthesis consists of hydrolysis of $FeCl_3$, followed by the association of Fe^{3+} with oxygen, forming α-Fe_2O_3. However, it is possible that more than one type of iron nanoparticle could be formed during the synthesis, such as zero-valent iron and maghemite (Bilesky-José et al., 2021).

The analysis of AgNP, TiO_2NP, and FeNP capping revealed functional groups of biomolecules, protein bands and the hydrolytic enzymes N-acetylglucosaminidase (NAGase), β-1,3-glucanase, chitinase and acid protease (AgNP, Casagrande et al., 2021; FeNP, Bilesky-José et al., 2021, TiO_2NP: to be published, Pasquoto Stigliane et al.). Casagrande et al. (2021) demonstrated that the capping is crucial for AgNP action against *S. sclerotiorum*. A hypothesis for AgNP mechanism of action is the degradation of carbohydrates by hydrolytic enzymes from *T. harzianum* capping, followed by cytotoxic action of Ag (Casagrande et al., 2021). Such mechanism seems to be different for FeNP. In this case, the effects of the suspension against *S. sclerotiorum* occurs not only because of nanoparticle action, but also because after formed, FeNP promotes the development of *T. harzianum* reproductive structures such as mycelium, conidia, and conidiospores, stimulating fungal proliferation, which in turn acts against the phytopathogen (Bilesky-José et al., 2021).

The application of NPs on crops may result in their entrance in aquatic ecosystems, which are the final receptors of most contaminants. The effects of biogenic NPs for freshwater fish have been evaluated in some studies. The acute toxicity and sublethal effects of nano-Ag synthesized using plants and fungi were assessed mainly in *Danio rerio* (Krishnaraj et al., 2016; Ottoni et al., 2020; Rheder et al., 2018; Samrot et al., 2019; Sarkar et al., 2014), but also in *Labeo rohita* (Shobana et al., 2018), and *Oreochromis niloticus* (Girilal et al., 2015). In these studies, the median lethal concentration (LC_{50}-96h) of nano-Ag reported was 25 μg L^{-1} (Shobana et al., 2018), 142.2 μg L^{-1} (Krishnaraj et al., 2016) and 400 μg L^{-1} (Sarkar et al., 2014). The variation of toxicity found may originate from the fact that each study assessed the effects of unique NPs, with different composition and physiochemical proprieties, due to the different extracts employed in the biological synthesis. Along with that, different species and water physiochemical characteristics were used.

The Neotropical freshwater teleost *Prochilodus lineatus* is a sensitive

species to contaminants. In this species, as demonstrated by Ale et al. (2018a), nano-Ag (2.5 and 25 μg L^{-1}, 5 and 15 days) modified the composition of skin mucus and stimulated the proliferation of mucus cells in the gills. In the gills, the authors also found that nano-Ag promoted Ag accumulation and oxidative stress, with decreased activity of antioxidant enzymes (superoxide dismutase, SOD, catalase, CAT, glutathione S-transferase, GST, glutathione reductase, GR, and glutathione peroxidase, GPx), decreased total antioxidant capacity (ACAP), and increased LPO (Ale et al., 2018a). In the liver, under the same exposure conditions, nano-Ag increased the activity of antioxidant enzymes, but decreased ACAP, suggesting increased ROS levels (Ale et al., 2018b). In this latter work, Ag accumulated in the liver, intestine, and brain, but the increased activity of antioxidants in these organs prevented oxidative damage. Hematological and metabolic changes were also reported by the authors (Ale et al., 2018b, 2018a).

Nano-TiO_2 (1-50 mg L^{-1}, 2 and 14 days) affected the osmotic and ionic balance of *P. lineatus* after short-term exposure, but homeostasis was restored after sub-chronic exposure due to morphological changes in the gills (Carmo et al., 2018b). The liver and kidney were considered responsible for eliminating nano-TiO_2, however, degenerative changes and necrosis were found in both organs, and oxidative damage was found in the kidney. Nano-TiO_2 also led to bioaccumulation of Ti and affected hematology parameters and AChE activity (Carmo et al., 2019, 2018a).

Nano-Fe_2O_3 (1 and 25 mg/L for 96 h) caused hematological and ionoregulatory changes in the Indian major carp (*L. rohita*), such as decreased hemoglobin, hematocrit, plasma protein, Na^+, K^+, and Cl^-, and Na^+/K^+-ATPase activity in the gills, but increased white blood cell count and plasma glucose (Saravanan et al., 2015). In Mozambique tilapia (*Oreochromis mossambicus*), nano-Fe_3O_4 (15 mg L^{-1} for 96 h and 60 days) induced histological changes in the gills, liver, and brain. These changes were irreversible, since they were found even after 60 days of recovery in clean water (Vidya and Chitra, 2019).

In light of the above mentioned, the hypothesis of the present work was that the bioaccumulation and the biological effects caused by each type of nanoparticle (AgNP, TiO_2NP or FeNP) would be different due to the different modes of toxic action of each metal. Thus, this work aimed to evaluate the sublethal effects of a short-term exposure to AgNP, TiO_2NP, and FeNP, all synthesized using the

fungus *T. harzianum*, for the teleost *Prochilodus lineatus*.

5.2 Material and Methods

5.2.1 Biogenic Synthesis and Characterization of Nanoparticles

Nanoparticle synthesis is described in Guilger et al. (2017). Silver, titanium, and iron nanoparticles were synthesized using silver nitrate (1 mM), titanium dioxide rutile (1 mM) or iron (III) chloride (1 mM). After the synthesis, dynamic light scattering (DLS) and microelectrophoresis were performed to obtain the hydrodynamic diameter, polydispersity index (PDI), and zeta potential of the suspensions, using ZS90 particle analyzer (Malvern Panalytical). The concentrations (NPs mL^{-1}) were obtained by nanoparticle tracking analysis (NTA), using NanoSight LM10 cell and NanoSight v.2.3 software (Malvern Panalytical). The pH was measured using a pH meter (HMMPB-210).

5.2.2 Acclimation and Exposure of Fish

Juveniles of *P. lineatus* (n = 32; weight: 72.9 ± 12 g; total length: 19.3 ± 1.2 cm, mean ± SD) were purchased from a local fish farming and acclimated for one month in a 500 L tank containing dechlorinated tap water under continuous aeration, controlled temperature and a 14 h:10 h light/dark photoperiod. Temperature, pH, and dissolved oxygen were measured using a multi-parameter meter (HoribaU52), and corresponded to 26.36 ± 0.19 °C, 7.23 ± 0.30, and 5.85 ± 0.47, respectively (mean ± SD, n = 6). Every 48 h, water from the fish tank was renewed and the fish were fed with commercial fish feed (Guabi, Brazil), which was interrupted 24 h prior to the beginning of the experiment and during the experiment.

Following acclimation, fish were randomly divided into four groups (n = 8 individuals/group): a control group, kept in water only; a group exposed to silver nanoparticles (AgNP) at the concentration of 3 x 10^8 NPs.mL^{-1} (35.60 µg Ag L^{-1}); a group exposed to titanium dioxide nanoparticles (TiO_2NP) at the concentration of 1 x 10^8 NPs.mL^{-1} (38.94 µg Ti L^{-1}); and a group exposed to iron nanoparticles (FeNP) at

the concentration of 3 x 10^7 NPs.mL^{-1} (123.98 µg Fe L^{-1}). All nanoparticles were biologically synthesized with the fungus *T. harzianum,* as previously described. The chosen concentrations for TiO_2NP and FeNP exposures are those that control the target organism and therefore are intended to be applied on crops. The chosen concentration for AgNP is ten times lower than the concentration intended to be applied on crops. We assumed that the concentration of AgNP that controls the target organism (3 x 10^9 NPs mL^{-1}, 355.96 µg Ag L^{-1}) would be lethal to *P. lineatus*, based on the LC_{50}-96h of commercial nano-Ag for *P. lineatus* (53.84 µg L^{-1}) (Ale et al., 2018b).

Fish were kept individually in glass aquaria containing 10 L of the exposure medium for 24 h. Temperature, pH, and dissolved oxygen were measured at initial (0 h) and final (24 h) times of exposure using a multi-parameter meter (HoribaU52). Parameters did not differ between times and among groups, so data were pooled and corresponded to (mean ± SD, n = 32): temperature, 25 ± 0.47 °C; pH, 7.12 ± 0.24; dissolved oxygen, 5.16 ± 0.73. Water hardness was determined by titration and corresponded to 30.8 ± 2.1 $CaCO_3$ L^{-1} (mean ± SD, n = 8). At initial (0 h) and final (24 h) times, water samples from each aquarium were collected to determine total (not filtered) and dissolved (filtered with a 0.45 µm mesh filter) concentrations of Ag, Ti, and Fe. Samples were acidified with HNO_3 1% (final concentration) and analyzed through atomic absorption spectrophotometry coupled to a graphite furnace (GFAAS) (AAnalyst, 700, Perkin Elmer, USA), against reference standard solutions (Specsol, Brazil). The dissolved fraction comprises metal ions, complexes, nanoparticles, and other colloids. The total fraction comprises the dissolved fraction in addition to forms of metal bounded to organic matter and larger aggregates/agglomerates of nanoparticles, and excludes sedimentation.

Following exposure, fish were anesthetized with benzocaine (0.1 g L^{-1}) to collect blood samples, then fish were killed by medullar sectioning to collect organs. The conducted assays are described below.

5.2.3 Bioaccumulation of Metals

Samples of gills, liver, posterior kidney, muscle, and brain were completely dried at 60°C, and then submitted to acidic digestion with suprapure nitric

acid (5 N) at 60°C for 48 h, according to Alves and Wood (2006). Bile samples were not dried, but submitted to acidic digestion along with the other tissues. Tissue digests and blood plasma samples were analyzed for Ag, Ti, and Fe concentrations through GFAAS.

5.2.4 Biomarkers of Oxidative Stress

Samples of gills, liver, and brain were homogenized in a potassium phosphate buffer (100 mM, pH 7.0, 1 g:5 mL for gills, 1 g:10 mL for liver and brain), centrifuged (16000 g, 20 min, 4 °C), and the supernatants were used for the assays described below.

Glutathione (GSH) concentration was determined using the method by Beutler et al. (1963), which quantifies non-protein thiols. Samples were acidified with trichloroacetic acid (TCA 6%, 1:1 dilution) and centrifuged (1500 g, 5 min, 4 ºC). The reaction consisted of the supernatants, potassium phosphate buffer, and 0.5 mM 5,5-dithio-bis-(2-nitrobenzoic acid) (DTNB). Thiolate formation was measured at 412 nm and quantified based on a GSH standard curve (5-400 mM). Glutathione S-transferase (GST) activity was determined by the conjugation of GSH with the substrate 1-chloro-2,4-dinitrobenzene (CDNB) every minute for 10 min at 340 nm (Gagné, 2014; Keen et al., 1976). Catalase (CAT) activity was determined by the decomposition of H_2O_2 every minute at 240 nm (Beutler, 1972). Superoxide dismutase (SOD) activity was determined by the inhibition of cytochrome c reduction rate by the superoxide radical, at 550 nm (McCord and Fridovich, 1969). Lipoperoxidation (LPO) was measured by the quantification of thiobarbituric acid reactive substances (TBARS assay) against a MDA standard curve (Camejo et al., 1998). The protein concentration in each sample was quantified to normalize data (Bradford, 1976).

5.2.5 Biomarkers of Hematology

Aliquots of blood were used for the determination of hematocrit, hemoglobin concentration, red blood cells count, hematimetric indices, and the total

and differential counts of white blood cells. For hematocrit (Hct, %), heparinized microcapillaries filled with blood were centrifuged (1200 g, 7 min) and read using a standardized card. Hemoglobin (Hb, g dL^{-1}) was quantified by the cyanmethemoglobin method using a commercial kit (Labtest, Brazil) at 540 nm. For red blood cells count (RBC, x 10^6 μL^{-1}), blood was diluted in a formol-citrate buffer (1:200) and analyzed using a Neubauer chamber under a light microscope. The hematimetric indices mean corpuscular hemoglobin concentration (MCHC, g dL^{-1}), mean corpuscular hemoglobin (MCH, pg $cell^{-1}$) and mean corpuscular volume (MCV, fL), were calculated as MCHC = (Hb x 100)/Hct, MCH = (Hb x 10)/RBC, MCV = (Hct x 10)/RBC. For the total and differential counts of white blood cells (WBC, x 10^3 μL^{-1}), blood smears were stained with Diff-Quik kit (New Prov, Brazil). WBC was determined by counting 2000 cells and differentiating red blood cells, white blood cells and thrombocytes. For differential count of WBC, 200 cells were evaluated. Blood samples were centrifuged (1870 x g, 10 min) to obtain plasma samples, which were stored at -20°C for further analysis.

5.2.6 Plasma Ions Concentrations and Enzyme Activity in Gills

For analysis of plasma ions, Na^+ and K^+ were quantified using a flame photometer (DM-62, Digmed, Brazil), Ca^{2+} was quantified using flame atomizer AAS (AAnalyst 700, PerkinElmer, USA), and Cl^- was quantified by the mercury thiocyanate method using a commercial kit (Quibasa-Bioclin, Brazil) at 470 nm.

Gill filaments were homogenized (1 g: 5 mL) in SEID buffer (150 mM sucrose, 10 mM EDTA, 50 mM imidazole, 2.4 mM sodium deoxycholate, pH 7.5) and centrifuged (10000 g, 20 min, 4°C). Supernatants were used for determination of Na^+/K^+-ATPase, H^+-ATPase, Ca^{2+}-ATPase, and carbonic anhydrase activities. For Na^+/K^+-ATPase and H^+-ATPase activities, Gibbs and Somero (1989) protocol was adapted for a microplate reader. Enzyme activity was measured by the disappearance rate of NADH, at 340 nm, in a reaction medium containing N-ethylmaleimide (NEM, H^+-ATPase inhibitor), ouabain (Na^+/K^+-ATPase inhibitor), or without inhibitors (total ATPase activity). Ca^{2+}-ATPase activity was determined according to Vijayavel et al. (2007), with modifications. Samples were incubated in a reactive solution (189 mM NaCl, 5 mM $MgCl_2$, 20 mM Tris, 5 mM $CaCl_2$, 2 mM

ouabain, pH 7.6) with (3 mM ATP) and without ATP, at 30°C for 30 min. The reaction was stopped by leaving the microplate on ice for 10 min. Then, inorganic phosphate (Pi) formation was estimated according to Ames (1966). Readings were performed at 620 nm based on a phosphate standard curve (0.08-0.65 mM). Carbonic anhydrase activity was determined according to Vitale et al. (1999), based on the pH decay immediately after adding water saturated with CO_2 to the samples. The protein concentration in each sample was quantified to normalize data (Bradford, 1976).

5.2.7 Biomarkers of Energy Metabolism

Samples of liver and muscle were used for glycogen quantification, using the method described by Bidinotto et al. (1997), with a reduction in the volumes. The method consists in the precipitation of glycogen by ethanol and subsequent quantification of glucose by the phenol-sulfuric acid hydrolysis, at 480 nm (Dubois et al., 1956). Plasma glucose was quantified by an enzymatic method using glucose oxidase (commercial kit, Laborclin, Brazil) at 505 nm. Plasma lactate was quantified by an enzymatic method using lactate oxidase (commercial kit, Labtest, Brazil).

5.2.8 Frequency of Micronuclei and Nuclear Abnormalities in Erythrocytes

The frequencies of micronuclei (MN) and erythrocytic nuclear abnormalities (ENA) were evaluated according to Ueda et al. (1992). Blood smears were fixed with methanol and stored at 4°C. Immediately prior to analysis, slides were stained with acridine orange (0.003%) in Sorenson's buffer (KH_2PO_4, $NaHPO_4$, pH 6.8), and examined under fluorescence at 1000x magnification. For each fish, 3000 erythrocytes were count. Classification of MN and ENA were based on Carrasco et al. (1990) and Carrola et al. (2014). ENA were classified as: kidney-shaped nucleus, segmented nucleus, lobed, blebbed, and notched nucleus, vacuolated nucleus, and binucleated cells. The frequencies of MN, frequencies of each nuclear abnormality, and frequencies of the sum of ENA, were calculated for each group.

5.2.9 Acetylcholinesterase (AChE) Activity

Samples of muscle and brain were homogenized in a potassium phosphate buffer (100 mM, pH 7.5, 1 g:10 mL) and centrifugated (16000 g, 20 min, 4°C). Supernatants were used for the determination of AChE activity according to Ellman et al. (1961) and adapted by Alves-Costa et al. (2007).

5.2.10 Histopathology of Gills

Gills arches were fixed in formalin-aceto-alcohol (FAA) and included in paraffin. Sections of 5 µm were stained with hematoxylin and eosin (H&E) and analyzed under a light microscope. Damage was evaluated semi-quantitatively by the Degree of Tissue Change (DTC), according to Poleksic and Mitrovic-Tutundzic (1994). Tissue changes were classified as stage I, which do not alter the normal functioning of the tissue; stage II, which impair the normal functioning of the tissue and are reversible; and stage III, which cause irreparable damage. DTC values were calculated as follows: $DTC = (1 \times \sum I) + (10 \times \sum II) + (100 \times \sum III)$, where the sum of I, II, and III correspond respectively to the number of changes in stages I, II, and III.

5.2.11 Statistical Analysis

Shapiro-Wilk and Levene's test were adopted to verify the normality and homoscedasticity of variance, respectively. Paired t-test or Wilcoxon Signed Rank Test were used to compared the concentrations of total and dissolved metals at the same time and at initial and final times of exposure. Bioaccumulation data from exposures were compared to control using t-test or Mann-Whitney test. Data from biomarkers (control x AgNP x TiO_2NP x FeNP) were analyzed using One Way ANOVA or Kruskal-Wallis test, followed by Student–Newman–Keuls (SNK) or Dunn's test, respectively, when necessary. Data from biomarkers were compared among groups to determine which type of nanoparticle would be less harmful to fish and thus safer to use in agriculture. Values of $P < 0.05$ were considered significant.

5.3 RESULTS

5.3.1 Physiochemical Characterization of Nanoparticle Suspensions

AgNP were the smallest NPs, followed by FeNP and TiO_2NP. The PDI of AgNP and FeNP were similar, and the PDI of TiO_2NP was the lowest, indicating greater homogeneity of sizes for TiO_2NP. The zeta potentials obtained for AgNP and TiO_2NP were negative, while the zeta potential of FeNP was positive. The pH for AgNP and TiO_2NP suspension was approximately neutral, but acid for FeNP suspension. The concentrations obtained in NPs mL^{-1} were used to calculate the dilutions for the exposures (Table 1).

Table 1 – Physiochemical characterization of silver (AgNP), titanium dioxide (TiO_2NP), and iron (FeNP) nanoparticles synthesized with *Trichoderma harzianum*.

	AgNP	TiO_2NP	FeNP
Diameter (nm)	50.11 ± 0.34	233.13 ± 6.38	138.17 ± 2.00
PDI	0.32 ± 0.00	0.17 ± 0.02	0.35 ± 0.00
Zeta potential (mV)	-19.47 ± 1.15	-10.42 ± 4.98	3.37 ± 0.28
pH	7.3	7.4	5.0
Concentration (NPs mL^{-1})	9.09×10^{11}	1.23×10^{11}	1.35×10^{10}

Data are expressed as mean ± SD (n = 3). PDI = polydispersity index.

5.3.2 Concentration of Metals in Exposure Medium and Tissues

The concentrations of Ag and Fe measured in the water from AgNP and FeNP exposures, respectively, are shown in Table 2. The total concentration of Ag measured in the water from AgNP exposure immediately before adding the fish (0 h) represented a 95.0% recovery from the nominal concentration (35.60 µg L^{-1}), and did not differ from the dissolved (<0.45 µm) concentration measured at the same time. After the exposure (24 h), total Ag concentration decreased 27.6%, and dissolved Ag concentration decreased 53.6%. Total and dissolved concentrations of Ag were quantified in the control water, but represented only 1.27% of the concentration from AgNP exposure.

The total concentration of Fe measured in the water from FeNP at 0 h represented a 75.0% recovery from the nominal concentration (123.98 µg L^{-1}),

while the dissolved fraction of Fe at 0 h represented a 39.0% recovery from the nominal concentration. After 24 h of exposure, total Fe concentration decreased 23.6%, and dissolved Fe concentration decreased 53.7%. Total and dissolved concentrations Fe were quantified in the control water and represented 15.6% and 18.2% of the total and dissolved concentrations measured in the of FeNP exposure, respectively.

The quantification of Ti was not possible due to technical reasons.

Table 2 – Concentration of metals (μg L^{-1}) in the water from control (C), silver nanoparticles exposure (AgNP), and iron nanoparticles exposure (FeNP), at initial and final times of exposure.

	0 h	24 h	0 h	24 h
	Control		**AgNP**	
Ag total	0.43 ± 0.04	0.05 ± 0.02*	33.81 ± 1.69	24.48 ± 2.36[a]*
Ag dissolved	0.48 ± 0.04	0.05 ± 0.03*	34.19 ± 2.21	15.86 ± 3.18[b]*
	Control		**FeNP**	
Fe total	14.46 ± 1.26[a]	12.73 ± 0.53[a]*	92.92 ± 12.38[a]	71.03 ± 11.56[a]*
Fe dissolved	8.81 ± 1.04[b]	8.51 ± 2.41[b]	48.34 ± 5.84[b]	22.38 ± 10.28[b]*

Data are expressed as mean ± SD (n = 8). Detection limit of Ag: 0.005 μg L^{-1}, Fe: 0.06 μg L^{-1}. Asterisk (*) indicates significant difference between 0 h and 24 h within the same row and group. Different letters indicate significant difference between total and dissolved within the same time. Statistics applied were paired t-test or Wilcoxon Signed Rank Test ($P < 0.05$).

5.3.3 Bioaccumulation of Metals

Ag concentration increased in the gills (Mann-Whitney, $P < 0.001$), posterior kidney (t-test, $P < 0.001$), and plasma (t-test, $P < 0.001$), but decreased in the bile (t-test, $P = 0.009$), of fish exposed to AgNP (Fig. 1A). Ti concentration increased in the plasma (t-test, $P < 0.001$), liver (Mann-Whitney, $P = 0.002$), and posterior kidney (Mann-Whitney, $P = 0.013$), but decreased in the bile (Mann-Whitney, $P = 0.038$), of fish exposed to TiO_2NP (Fig. 1B). Overall, there was a net increase of Ag and Ti concentrations in fish exposed to AgNP and TiO_2NP, respectively. Fe concentration increased in all tissues (and blood plasma) analyzed: liver, posterior kidney, gills, brain, bile, plasma (all Mann-Whitney, $P < 0.001$), and muscle (t-test, $P = 0.001$) (Figure 1C). The increases in Fe concentrations were the highest among metals (49.6-fold higher in the liver of FeNP-exposed fish), followed by Ag and Ti, which increased more than 6-fold in the gills of AgNP-exposed fish and

plasma of TiO_2NP-exposed fish, respectively.

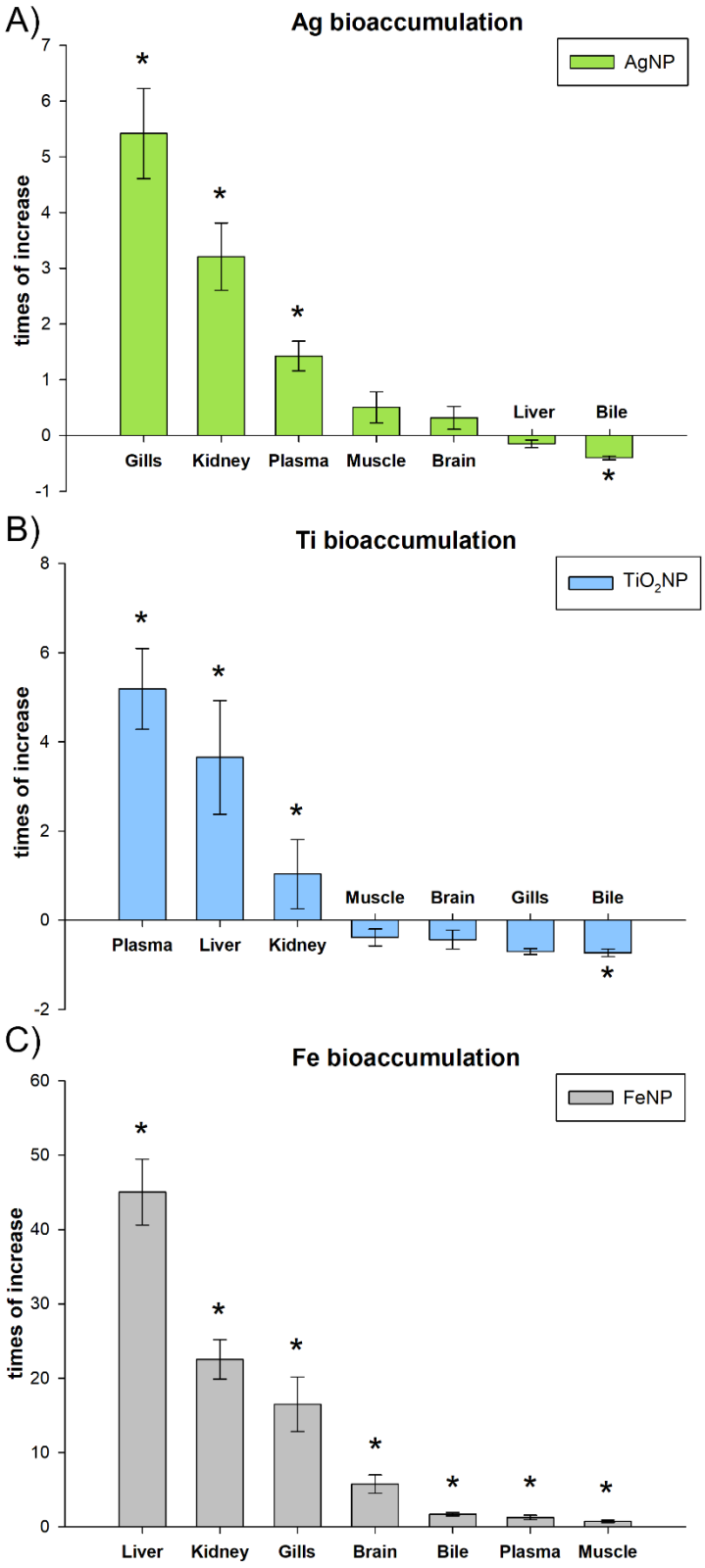

Fig. 1 – Times of increase in metal concentrations (Ag, Ti, and Fe) in multiple tissues and plasma of *Prochilodus lineatus* from A) silver nanoparticles exposure (AgNP), B) titanium

dioxide nanoparticles exposure (TiO_2NP), and C) iron nanoparticles exposure (FeNP), in relation to the control. Data are expressed as mean ± SE (n=6-8). Asterisks (*) indicate significant differences in relation to control (P < 0.05, t-test or Mann-Whitney).

5.3.4 Biomarkers of Oxidative Stress

In the liver, GSH concentration decreased in AgNP exposure compared to control, TiO_2NP, and FeNP (ANOVA, P = 0.003) (Fig. 2A), and GST activity decreased in all exposures compared to control (ANOVA, P = 0.002) (Fig. 2C).

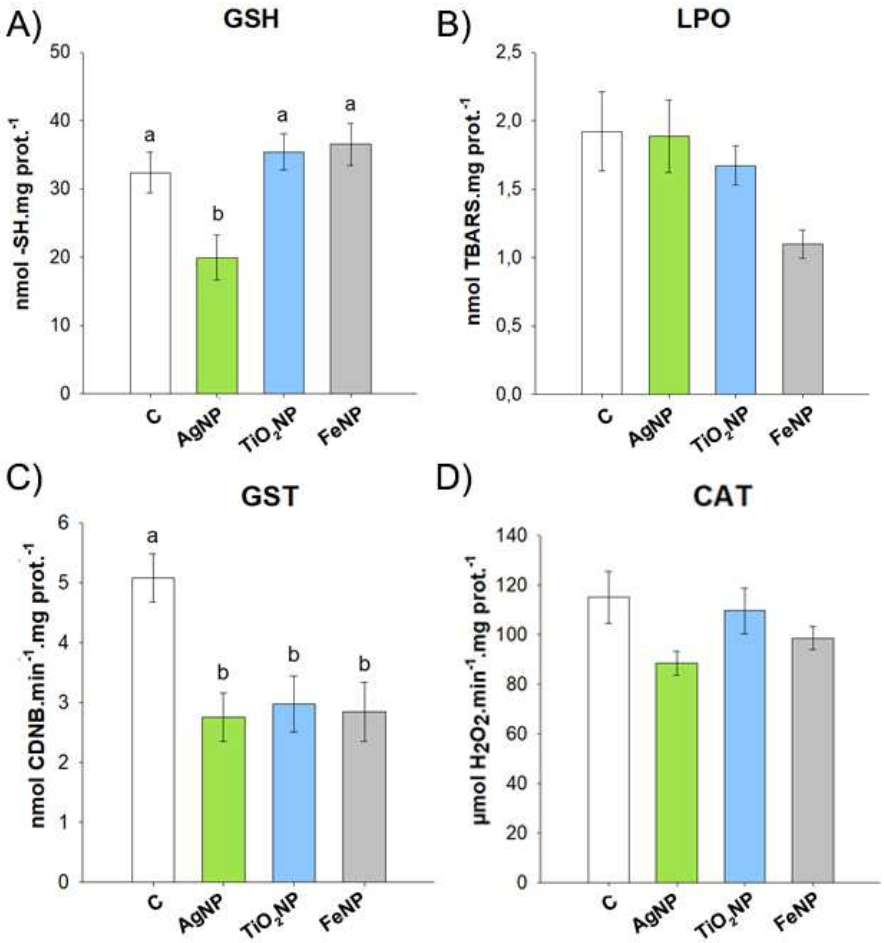

Fig. 2 – Biomarkers of oxidative stress in the liver of *Prochilodus lineatus* from control (C), silver nanoparticles exposure (AgNP), titanium dioxide nanoparticles exposure (TiO_2NP), and iron nanoparticles exposure (FeNP). Data are expressed as mean ± SE (n=7-8). Different letters indicate significant differences between groups (P < 0.05, ANOVA). GSH = glutathione, LPO = lipoperoxidation, GST = glutathione S-transferase, CAT = catalase.

In the gills, FeNP exposure decreased the concentration of GSH (ANOVA, P = 0.011) and increased LPO (ANOVA, P = 0.018), compared to control (Fig. 3A,B).

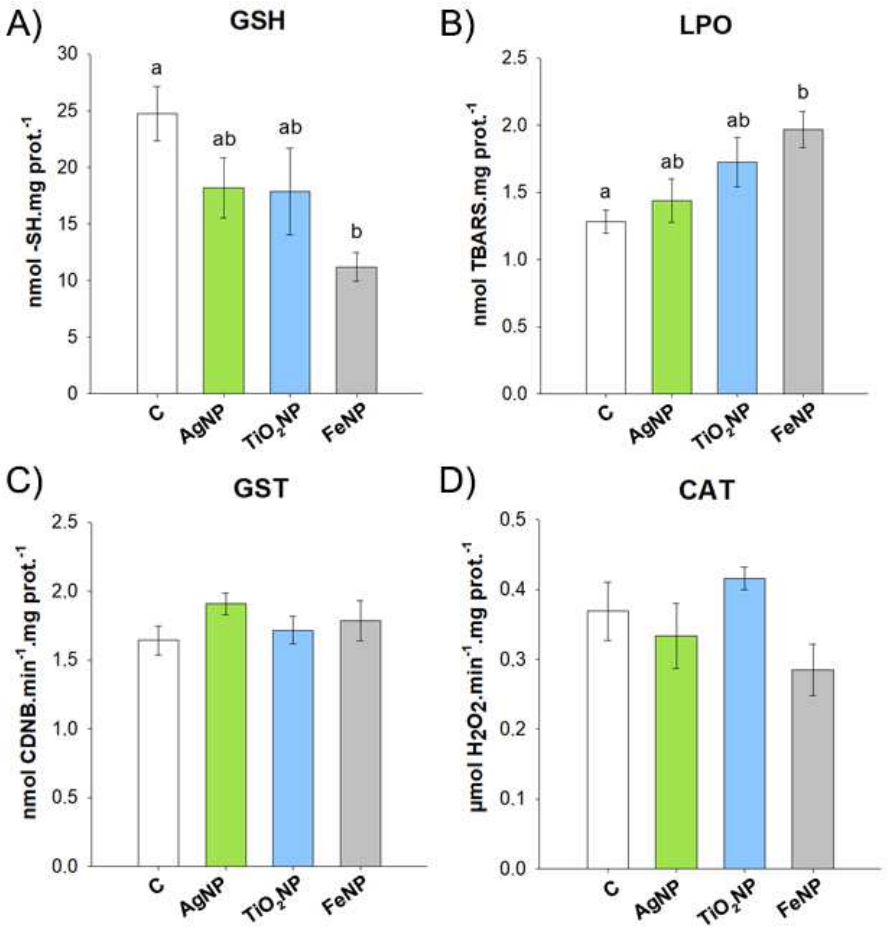

Fig. 3 – Biomarkers of oxidative stress in the gills of *Prochilodus lineatus* from control (C), silver nanoparticles exposure (AgNP), titanium dioxide nanoparticles exposure (TiO_2NP), and iron nanoparticles exposure (FeNP). Data are expressed as mean ± SE (n=6-8). Different letters indicate significant differences between groups (P < 0.05, ANOVA). GSH = glutathione, LPO = lipoperoxidation, GST = glutathione S-transferase, CAT = catalase.

In the brain, none of the exposures affected GSH and GST, but LPO increased in fish exposed to AgNP compared to FeNP (Fig. 4).

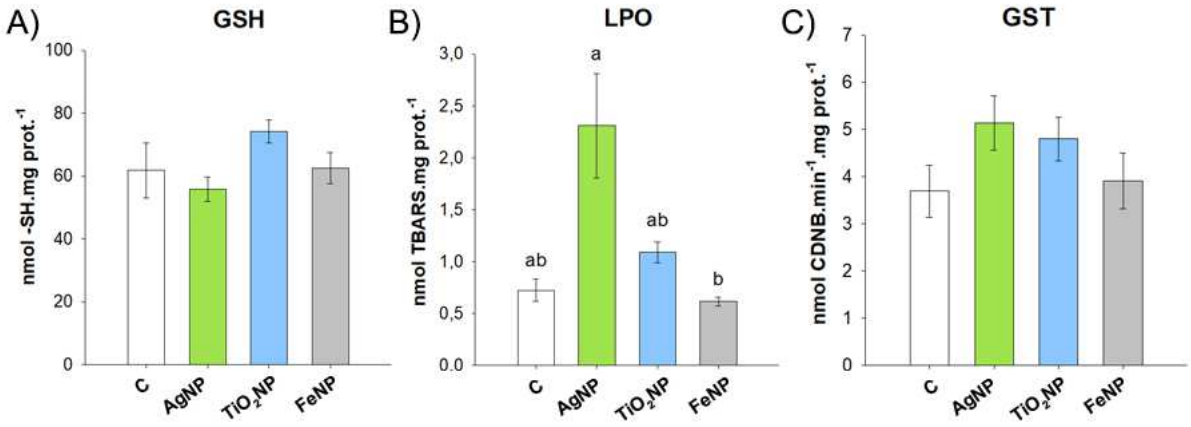

Fig. 4 – Biomarkers of oxidative stress in the brain of *Prochilodus lineatus* from control (C), silver nanoparticles exposure (AgNP), titanium dioxide nanoparticles exposure (TiO_2NP), and iron nanoparticles exposure (FeNP). Data are expressed as mean ± SE (n=6-8). Different letters indicate significant differences between groups ($P < 0.05$, ANOVA or Kruskal-Wallis). GSH = glutathione, LPO = lipoperoxidation, GST = glutathione S-transferase.

5.3.5 Biomarkers of Hematology

There was a tendency of increase in MCV after AgNP exposure (ANOVA, $P = 0.052$). On the other hand, AgNP decreased WBC count compared to control, TiO_2NP, and FeNP, but FeNP increased WBC count compared to control (ANOVA, $P < 0.001$) (Table 3). The relative frequency of monocytes was higher in fish exposed to AgNP compared to TiO_2NP (Kruskal-Wallis, $P < 0.05$) (Table 3). Figure 5 shows RBC, WBC, and thrombocytes. WBC were differentiated in lymphocytes, neutrophils, monocytes, and eosinophils.

Table 3 – Biomarkers of hematology in Prochilodus lineatus from control (C), silver nanoparticles exposure (AgNP), titanium dioxide nanoparticles exposure (TiO_2NP), and iron nanoparticles exposure (FeNP).

	C	AgNP	TiO_2NP	FeNP
Hemoglobin (g dL^{-1})	8.19 ± 0.60	8.61 ± 0.43	8.45 ± 0.40	9.30 ± 0.46
Hematocrit (%)	37.00 ± 0.97	33.75 ± 1.43	32.87 ± 1.09	36.50 ± 1.77
RBC (10^6 μL^{-1})	1.74 ± 0.14	1.44 ± 0.16	1.52 ± 0.07	1.81 ± 0.09
MCHC (g dL^{-1})	22.03 ± 1.15	24.98 ± 1.47	25.95 ± 1.45	25.12 ± 0.35
MCH (pg $cell^{-1}$)	48.27 ± 3.80	61.98 ± 1.56	56.56 ± 4.11	51.95 ± 2.97
MCV (fL)	207.61 ± 9.64	245.29 ± 16.17	203.07 ± 8.68	203.01 ± 10.63
WBC (10^3 μL^{-1})	**30.52 ± 5.03^{a}**	**13.36 ± 1.53^{b}**	**41.60 ± 5.31^{ac}**	**51.25 ± 3.79^{c}**
Lymphocytes (%)	89.50 ± 1.09	58.13 ± 11.90	93.43 ± 0.35	90.19 ± 1.45
Neutrophils (%)	5.25 ± 1.18	32.00 ± 10.90	4.43 ± 0.54	5.25 ± 1.57
Monocytes (%)	**5.38 ± 0.92^{ab}**	**7.69 ± 2.35^{a}**	**2.25 ± 0.51^{b}**	**3.81 ± 0.61^{ab}**
Eosinophils (%)	0.25 ± 0.13	0.57 ± 0.21	0.00 ± 0.00	0.06 ± 0.06

RBC = red blood cell count, MCHC = mean corpuscular hemoglobin concentration, MCH = mean corpuscular hemoglobin, MCV = mean corpuscular volume, WBC = white blood cell count. Data are expressed as mean ± SE (n=6-8). Different letters indicate significant differences between groups ($P < 0.05$, ANOVA or Kruskal-Wallis).

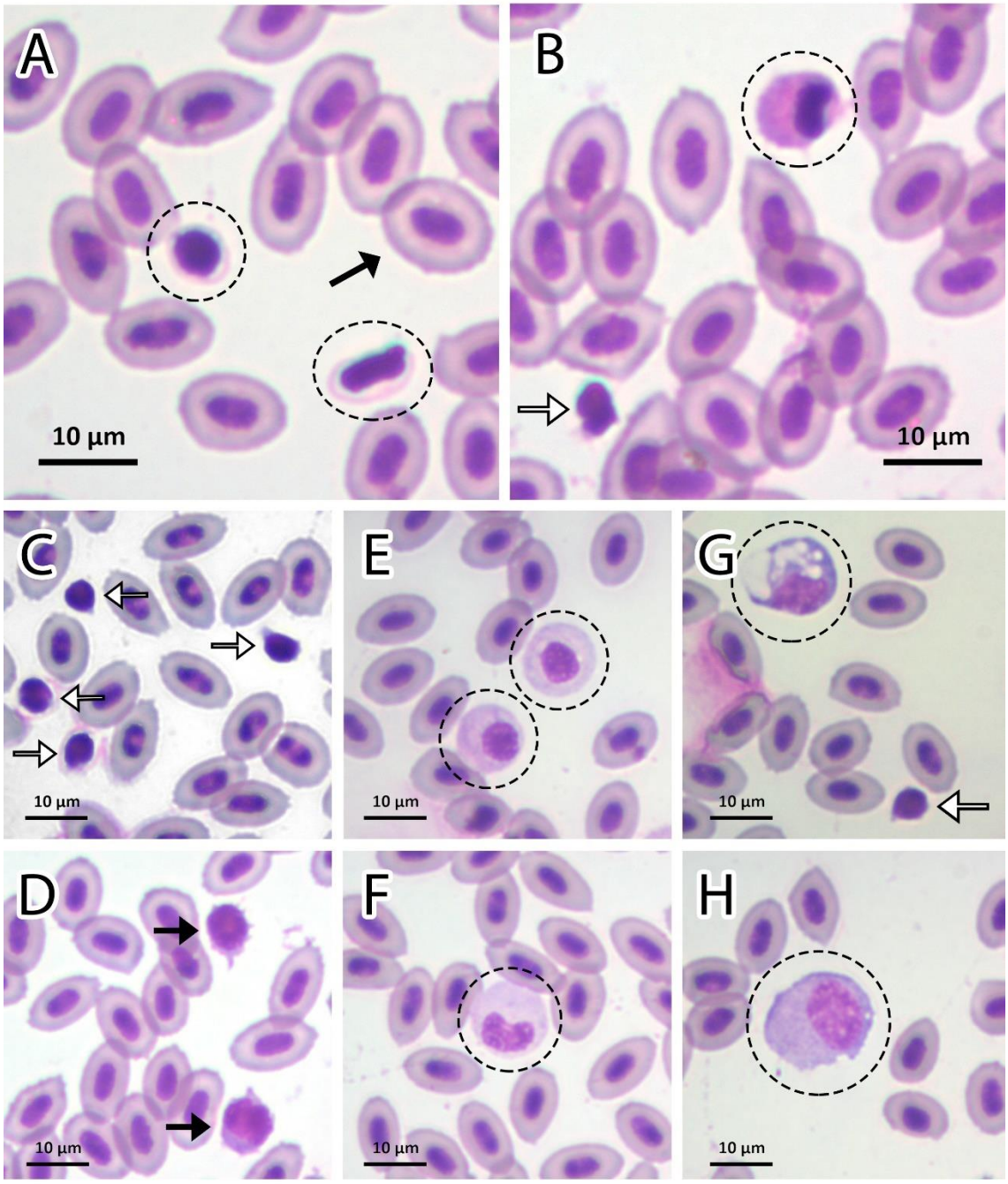

Fig. 5 – Red blood cells, white blood cells, and thrombocytes found in the peripheral blood of *Prochilodus lineatus*. A – Red blood cell (black arrow) and thrombocytes (within the circles). B – Eosinophil (within the circle) and small lymphocyte (white arrow). C – Small lymphocytes (white arrows). D – Large lymphocytes (black arrows). E, F – Neutrophils (within the circles). G, H – Monocytes (within the circles) and small lymphocyte (white arrow). Diff-Quik stain. Scale bar: 10 µm.

5.3.6 Plasma Ions Concentrations and Enzyme Activity in Gills

Plasma Na^+ concentration increased in AgNP exposure compared to control and FeNP (ANOVA, P = 0.006) (Fig. 6A). K^+ concentration increased in AgNP exposure compared to control (Kruskal-Wallis, P < 0.001) (Fig. 6B). On the other hand, Ca^{+2} concentration decreased in AgNP exposure compared to control, TiO_2NP, and FeNP exposures, and Ca^{+2} concentration decreased in TiO_2NP compared to control and FeNP (ANOVA, P < 0.001) (Fig. 6C). Cl^- increased in FeNP compared to control and AgNP (ANOVA, P = 0.005) (Fig. 6D). Na^+/K^+-ATPase, H^+-ATPase, Ca^{+2}-ATPase, and carbonic anhydrase activities in the gills were not affected (Fig. 6E-H).

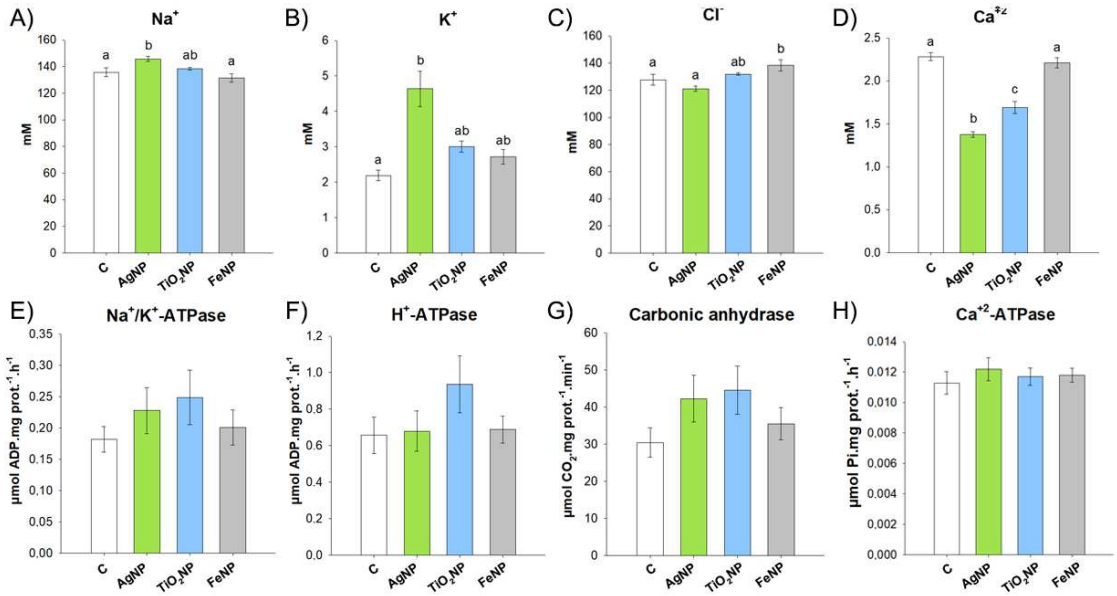

Fig. 6 – Plasma ions and enzymes activity in the gills of *Prochilodus lineatus* from control (C), silver nanoparticles exposure (AgNP), titanium dioxide nanoparticles exposure (TiO_2NP), and iron nanoparticles exposure (FeNP). Data are expressed as mean ± SE (n=5-8). Different letters indicate significant differences between groups (P < 0.05, ANOVA or Kruskal-Wallis).

5.3.7 Biomarkers of Energy Metabolism

Hepatic glycogen increased in TiO_2NP exposure compared to control and AgNP exposure, and also increased in FeNP exposure compared to control and to AgNP (ANOVA, P = 0.005) (Fig. 7B). AgNP increased plasma glucose compared

to control, TiO_2NP and FeNP (ANOVA, $P < 0.001$) (Fig. 7C). AgNP increased plasma lactate compared to control, TiO_2NP and FeNP (Mann-Whitney, $P < 0.001$) (Fig. 7D).

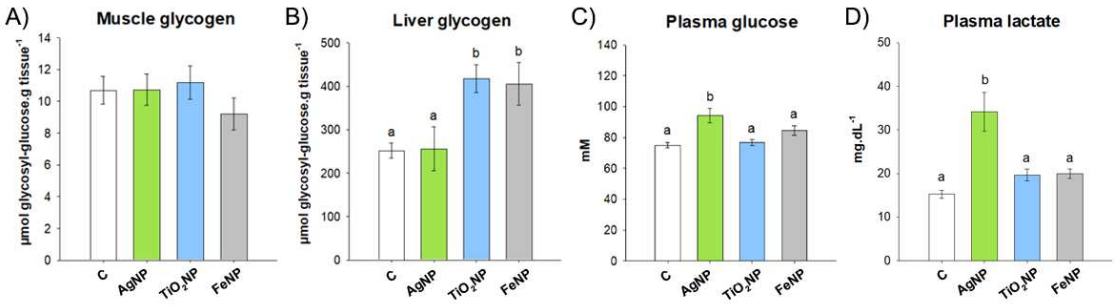

Fig. 7 – Biomarkers of energy metabolism in *Prochilodus lineatus* from control (C), silver nanoparticles exposure (AgNP), titanium dioxide nanoparticles exposure (TiO_2NP), and iron nanoparticles exposure (FeNP). Data are expressed as mean ± SE (n=7-8). Different letters indicate significant differences between groups ($P < 0.05$, ANOVA or Kruskal-Wallis).

5.3.8 Frequency of Micronuclei and Nuclear Abnormalities in Erythrocytes

Four erythrocytes with micronucleus were found in the entire experiment, one in each group. Regarding nuclear abnormalities, the following were found: kidney-shaped nucleus, segmented nucleus, lobed, blebbed, and notched nucleus, vacuolated nucleus, and binucleated cells. However, there were no significant differences in the frequency of the sum of nuclear abnormalities among groups, neither when each abnormality was tested separately (Table 4).

Table 4 – Erythrocytic nuclear abnormalities (ENA, expressed per 1000 erythrocytes - ‰) of Prochilodus lineatus from control (C), silver nanoparticles exposure (AgNP), titanium dioxide nanoparticles exposure (TiO_2NP), and iron nanoparticles exposure (FeNP).

	CTR	AgNP	TiO_2NP	FeNP
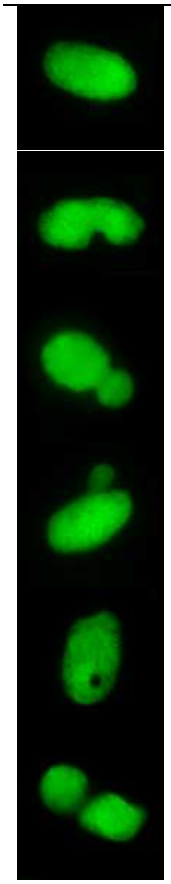 **Normal**	-	-	-	-
Kidney-shaped	0.95 ± 0.09	0.71 ± 0.29	0.33 ± 0.10	0.52 ± 0.20
Segmented	0.52 ± 0.20	1.38 ± 0.56	0.67 ± 0.27	0.96 ± 0.33
Lobed, blebbed or notched	0.52 ± 0.22	0.96 ± 0.40	0.52 ± 0.19	0.29 ± 0.14
Vacuolated	0.38 ± 0.18	0.25 ± 0.14	0.75 ± 0.34	0.05 ± 0.04
Binucleated	0.10 ± 0.06	0.05 ± 0.04	0	0.08 ± 0.05
Total ENA	2.48 ± 0.43	3.92 ± 1.31	3.33 ± 1.31	2.54 ± 0.76

Data are expressed as mean ± SE (n=7-8, Kruskal-Wallis).

5.3.9 Acetylcholinesterase (AChE) Activity

None of the exposures affected AChE activity in brain and muscle (Fig. 8).

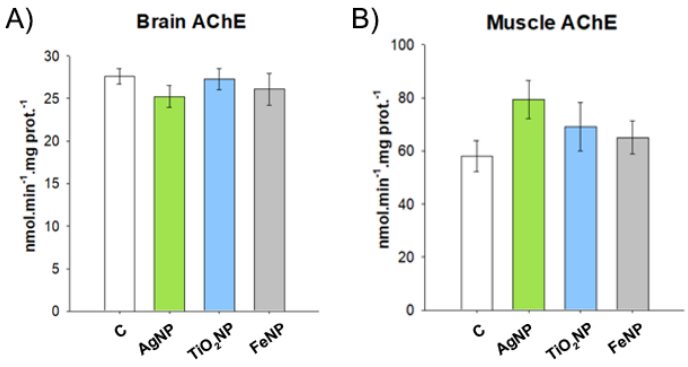

Fig. 8 – Acetylcholinesterase (AChE) activity in the A) brain and B) muscle of *Prochilodus lineatus* from control (C), silver nanoparticles exposure (AgNP), titanium dioxide nanoparticles exposure (TiO_2NP), and iron nanoparticles exposure (FeNP). Data are expressed as mean ± SE (n=7-8, ANOVA).

5.3.10 Histopathology of Gills

Table 5 shows the mean frequency of each histological change in the gills of each group, and DTC values for each group. Figure 9 shows the overall aspect of gills from each group. In general, sections of gills from control and TiO_2NP exposure presented a non-pathological architecture, with rare or few alterations. Gill sections from AgNP presented conspicuous epithelial cell hyperplasia, which could be seen in almost all filaments in most animals (not all). In some cases, epithelial cell hyperplasia was accompanied by hypertrophy of the same cells and lamellar adhesion. These changes resulted in a higher DTC value for AgNP compared to control and TiO_2NP (ANOVA, $P = 0.004$). Gills sections from FeNP presented higher frequency of epithelial cell hyperplasia than control and TiO_2NP, but it did not result in a significant higher DTC value compared to other groups.

Table 5 – Histological changes and Degree of Tissue Change (DTC) found in the gills of Prochilodus lineatus from control (C), silver nanoparticles exposure (AgNP), titanium dioxide nanoparticles exposure (TiO_2NP), and iron nanoparticles exposure (FeNP).

	Stage	C	AgNP	TiO_2NP	FeNP
Epithelial cell hypertrophy	I	0+	+	0+	0+
Epithelial lifting	I	+	+	+	+
Epithelial cell hyperplasia	I	0+	+++	0+	+
Lamellar adhesion/fusion of lamellae tips	I	0	+	0	0
Incomplete lamelar fusion	I	0+	+	0+	+
Complete lamelar fusion	I	0+	++	0+	+
Lamellar disarray	I	+	0+	+	+
Vascular congestion	I	0+	0+	0+	0+
Aneurysm	II	0+	0+	0	0+
Presence of parasites	I	0	0+	0+	0+
DTC		**5.43 ± 1.02^{a}**	**14.13 ± 2.07^{b}**	**5.50 ± 0.73^{a}**	**10.00 ± 1.93^{ab}**

Note: 0 = absent; 0+ = rare; + = fairly frequent; ++ = frequent; +++ = very frequent. DTC values are expressed as mean ± SE (n=7-8). Different letters indicate significant differences between groups ($P < 0.05$, ANOVA). Statistics were only applied to DTC values.

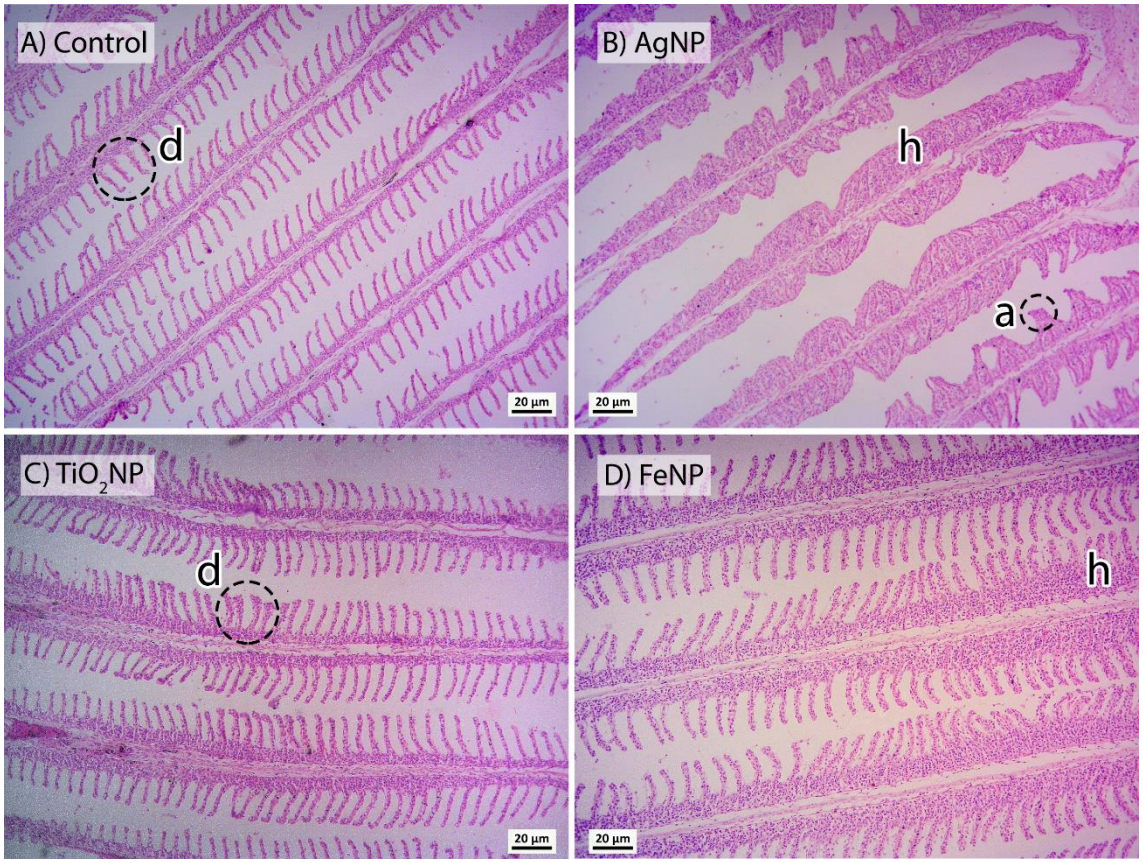

Fig. 5 – Histological sections of gills of *Prochilodus lineatus* from A) control, B) silver nanoparticles exposure (AgNP), C) titanium dioxide nanoparticles exposure (TiO_2NP), and D) iron nanoparticles exposure (FeNP). Sections from control, TiO_2NP, and FeNP present normal architecture, although some changes can be seen, such as lamellar disarray (d) and epithelial cell hyperplasia (h). Section from AgNP show extensive epithelial cell hyperplasia (h) and lamellar adhesions (a). Scale bar = 20 µm. H&E.

5.4 Discussion

The unique properties of each type of nanoparticle evaluated are responsible for the different effects observed in fish. The most notable difference is the metal composition. In fact, as it will be further discussed, several effects seem to be a result of the specific metal exposure. However, each type of nanoparticle also presents different physiochemical properties (Manuscript 1). Furthermore, the concentration of nanoparticles in each exposure is different, as well as the survival and development of *T. harzianum* in the suspensions.

The bioaccumulation of Ag, Ti, and Fe indicates that the biogenic synthesis employed did not prevent metal uptake. The most sensitive tissues (and

plasma) to metal accumulation were the kidney and blood plasma, which accumulated metals after all exposures. Thus, these tissues are indicated for future bioaccumulation analysis after exposure to the nanoparticles used in the present work. Additionally, plasma analysis has the advantage of not requiring the animal to be killed. In relation to metal accumulation in the kidney, if nanoparticles reached the organ (and not solely other forms of the metal), their excretion may be impaired, because NPs are in general larger than the glomerular filter (Handy et al., 2008). This could indeed contribute to metal accumulation, in addition to other intrinsic characteristics of the organ, such as the high blood flow. However, elimination of NPs may occur in the kidney through melanomacrophage (MM) action (Carmo et al., 2018a). The potential for the kidney to be a target organ is shown in some other studies. For example, in the Indian major carp *L. rohita* exposed for 35 days to 2.5 and 5 μg L^{-1} nano-Ag obtained using *Piper nigrum* leaf extract, Ag accumulation followed the order: kidney > liver > gill (Shobana et al., 2018). In *P. lineatus* exposed to nano-TiO_2, the kidney showed cellular and nuclear hypertrophy, focal tubule degeneration, necrosis, and melanomacrophage (MM) proliferation (Carmo et al., 2018a).

In the present work, Ag concentration increased in gills, plasma, and posterior kidney of fish exposed to AgNP, but decreased in fish bile. Such increases surpassed the decrease in bile, resulting in a net increase of Ag. This distribution pattern indicates Ag uptake by gills and distribution to the kidney via blood circulation. On the other hand, Ti concentration increased in the plasma, liver, and posterior kidney of fish exposed to TiO_2NP, and decreased in the bile of fish. Also in this case, there was a net Ti increase in the animal. It was unexpectable to obtain an increase in metal concentration in internal organs, but not in the gills, after a 24 h exposure. However, Ti accumulation in the liver corroborates the sublethal effects found mostly in this tissue after TiO_2NP exposure. Furthermore, a different pattern of bioaccumulation was found for *P. lineatus* exposed to TiO_2NP for 14 days: all concentrations tested (1, 5, 10, and 50 mg L^{-1}) led to increased Ti concentration in the gills, but only the highest concentrations promoted accumulation in other organs (10 and 50 mg L^{-1} in brain and muscle, 50 mg L^{-1} in the liver), and the concentrations of 5 and 50 mg L^{-1} resulted in Ti accumulation in the kidney (Carmo et al., 2019, 2018a). In the recently cited work, the morphological changes found in the gills were less severe than those found in the liver and kidney of fish, which showed

degenerative changes and necrosis (Carmo et al., 2019, 2018a).

AgNP and TiO_2NP exposures led to decreases in Ag and Ti, respectively, in the fish bile. This finding indicates that both exposures modified metal distribution in tissues. The mechanism underlying this result is not known, but is possible that liver function is compromised, affecting bile production and/or secretion. Besides the morphological changes cited in the last paragraph, the liver of *P. lineatus* exposed to 0.1, 1, and 10 μg L^{-1} TiO_2NP for 5 days displayed increased frequency of necrosis, leukocyte infiltration, basophilic foci, and vascular congestion, and decreased frequency of cholestasis. These histological changes may compromise liver functions, including bile production (Miranda et al., 2016).

Regarding Fe bioaccumulation, *P. lineatus* exposed to 5 mg L^{-1} Fe, as $FeSO_4.7H_2O$, for 96 h did not accumulate Fe in any analyzed tissue (muscle, blood, brain, gills, bile, liver, posterior kidney, and anterior kidney) (Oliveira et al., 2018). In the present work, fish from the FeNP group were exposed to 123.98 μg L^{-1} Fe - a much lower concentration than the previously cited work - and accumulated Fe in all tissues analyzed (gills, liver, posterior kidney, brain, muscle, plasma, and bile), with remarkable increases compared to control. Although it would be necessary to compare these results within the same exposure conditions (equal time and concentration), the increases in Fe concentration found in the present work, with a low concentration of exposure, may indicate that FeNP enhance Fe bioavailability, compared to Fe salts. In fact, nano-Fe can be used in fish aquaculture as a supplement for iron deficiency (Thangapandiyan et al., 2020).

FeNP exposure decreased GSH and increased LPO in fish gills. Fe acts as a catalyst in the Fenton reaction, an oxidation process that generates hydroxyl radical from hydrogen peroxide. Hydroxyl radical is a highly reactive molecule that along with other ROS can cause oxidative damage to cell constituents (Lushchak, 2016). To a certain extent, GSH prevents oxidative damage from metals because it chelates metal cations and also eliminates ROS. The depletion of GSH observed in the present study should be primarily related to its role as ROS scavenger. Also, GSH binds to Fe^{+2} (Berndt and Lillig, 2017), which could also decrease GSH concentration. Nevertheless, fish antioxidant system was not capable of preventing oxidative damage, as indicated by the increased LPO. GSH depletion and LPO increase in the gills of fish indicates the occurrence of oxidative stress induced by FeNP exposure.

GSH was also reduced in the liver of fish exposed to AgNP. Ag binds to biomolecules such as glutathione and metallothionein (Wood, 2012). In the liver of AgNP-exposed fish, GST activity was also decreased. Despite decreases in GSH and GST, peroxidation of lipid membranes did not occur.

All nanoparticles (AgNP, TiO_2NP, and FeNP) led to reduced GST activity of the same intensity in the liver of fish for all exposures. The only common properties among the three nanoparticles are their nanoparticulate form and the capping of fungal molecules. However, it was not possible to infer how these proprieties would affect GST activity. The glutathione S-transferases (GSTs) are a family of enzymes that participate in phase II reactions of biotransformation but also in antioxidant defense (Nikinmaa, 2014). Decreased activity of GST can negatively affect both processes.

The mechanism of acute Ag toxicity described for freshwater fish derives from ionic silver (Ag^+) action, and consists in the decrease in Na^+ and Cl^- influx due to the inhibition of Na^+/K^+-ATPase and carbonic anhydrase activities in the fish gill. Following the reduction in plasma [Na^+] and [Cl^-], blood volume decreases, and there is an increase of hematocrit, hemoglobin, and plasma protein and glucose (Wood, 2012). However, this mechanism was not evidenced in the present work.

In the present work, fish exposed to AgNP showed Ag accumulation in the gills accompanied by histological changes in this organ, namely hyperplasia and hypertrophy of epithelial cells and lamellar adhesion, resulting in incomplete or complete fusion of the lamellae and increased DTC. Several studies report hyperplasia of gill epithelial cells after exposure to AgNP or $AgNO_3$ (Abarghoei et al., 2016; Mohsenpour et al., 2020; Xiang et al., 2020). The mechanism supporting this phenomenon may be the upregulation of collagen type I alpha expression (Xiang et al., 2020).

Hyperplasia causes a decrease in the contact surface area of the gills, which decreases the passive diffusion of ions from the animal to the water but also impairs the uptake of O_2 and excretion of CO_2 and ammonia. Both the impairment in the uptake of O_2 and the excretion of CO_2 can cause acidosis. In the first case, it increases the anaerobic metabolism (metabolic acidosis), and in the second case, it increases CO_2 partial pressure (pCO_2) in the blood (respiratory acidosis). In the present work, there was an increase in anaerobic metabolism, evidenced by the increase in plasma lactate. The increase in anaerobic metabolism

and plasma lactate may also originate, in part, from the stress response. Although it was not evidenced, it is possible that pCO_2 also increased in the blood.

Acidosis can be accompanied by hyperkalemia, owing to the exchange of H^+ and K^+ in the muscle (Graham, 1983). Webb and Wood (1998) observed a continual loss of K^+ to the water without changes in plasma [K^+] in rainbow trout exposed to $AgNO_3$. The authors attributed [K^+] loss to the occurrence of metabolic acidosis in fish (interpreted with a different cause from the one in the present work), suggesting that fish were losing K^+ from tissues to plasma to water. In the present work, as plasma [K^+] doubled in fish exposed to AgNP compared to control, it is possible that K^+ excretion is compromised. In fact, [K^+] loss through gills must be decreased because of the reduced surface area, and the posterior kidney function can be impaired given the accumulation of Ag in this organ.

Hyperkalemia also occurred in *P. lineatus* exposed for 24 h to 10 µg L^{-1} $AgNO_3$ or biogenic AgNP, and was sustained after 96 h exposure to $AgNO_3$ (data to be published, Ferroni et al.). Hypoxia, acidosis, and hyperkalemia compromises heart function. In these conditions, rainbow trout is capable of maintaining myocardial function due to adrenergic stimulation (Hanson et al., 2006). However, we do not know whether this ability can be maintained in a condition of contaminant exposure (in this case, AgNP), where several physiological parameters are affected. For example, exposure to AgNP also led to hypocalcemia, which again affects heart function.

Based on the above mentioned, decreased gill contact surface area and increased plasma lactate and K^+ concentrations suggest respiratory toxicity associated with AgNP exposure in *P. lineatus*.

Although plasma [Na^+] increased in fish exposed to AgNP and plasma [Cl^-] increased in fish exposed to FeNP, both increases were small, and the absolute values remained within the normal range for *P. lineatus*. On the other hand, plasma [Ca^{+2}] decreases in fish exposed to AgNP and TiO_2NP were more severe. Hypocalcemia causes hyperexcitability of neuronal membranes, which can lead to tetanic muscle contraction, depending on how low calcium is. Conversely, hyperkalemia (observed in fish exposed to AgNP) decreases neuronal excitability, indicating that several factors can be influencing neuronal membrane excitability in AgNP-exposed fish. Hypocalcemia can also affect heart function, since myocytes are excitable cells.

The increase in plasma glucose in fish exposed to AgNP can indicate the mobilization of energy reserves that occurs during anaerobic metabolism. However, it should favor a decrease in hepatic glycogen stores, but there was no change in glycogen neither in the liver nor in the muscle of fish exposed to AgNP. Conversely, hepatic glycogen increased in fish exposed to TiO_2NP and FeNP. Toxic exposures can result in both accumulation or depletion of glycogen in the fish liver (Wolf and Wolfe, 2005). Fish were fasting for 48 h, because feeding was interrupted 24 h prior to the beginning of the experiment and lasted to the end of the experiment (24 h exposure). Increasing glycogen stores in a fasting condition indicates a disruption of normal glucose metabolism, which can be a result of either stimulated or inhibited metabolic pathways. If glycogen stores cannot be consumed during a longer period of time, effects such as poor growth may appear (Peplow and Edmonds, 2005).

Furthermore, the increase in plasma glucose in fish exposed to AgNP can be indicative of a stress response. In addition to plasma glucose and cortisol, WBC profile is useful for assessing stress in vertebrates. Cortisol increases neutrophil numbers while decreasing lymphocyte numbers, resulting in a neutrophil:lymphocyte (N:L) increased ratio (Davis et al., 2008). The reduced lymphocyte number can lead to leukopenia, i.e., low WBC count (Clauss et al., 2008). In the present work, AgNP exposure resulted in leukopenia, and although a shift towards an increase in neutrophils (%) and a decrease in lymphocytes (%) appeared in medium values, these changes were not significant. Thus, AgNP exposure did not affect WBC differential count at the time tested, but the leukopenia observed may indicate a stress response. However, the opposite effect also has been reported, with increased plasma cortisol and WBC count in fish exposed to stressors (e.g., nano-Ag exposure, Shaluei et al., 2013). Additional studies also reported increased WBC number in fish after nano-Ag exposure (Ale et al., 2018b; Imani et al., 2015), but the exposure to biogenic nano-Ag synthesized with starch also decreased WBC number (Mansour et al., 2021).

On the other hand, WBC count increased in fish exposed to FeNP. Increased WBC numbers were also observed in the Indian major carp (*L. rohita*) exposed to 1 and 25 mg L^{-1} nano-Fe_2O_3 for 96 h (Saravanan et al., 2015), but decreased WBC numbers were found in higher concentrations and longer times of exposure, with *L. rohita* (Remya et al., 2015) and common carp, *Cyprinus carpio*

(Khoei, 2021). Interestingly, in the last cited work, the same concentration of $FeCl_3$ had no effect on WBC, while exposure to $FeSO_4$ increased WBC number in *L. rohita* (Singh et al., 2019). Additionally, no effects on WBC were seen in *O. mykiss* exposed to 1, 10, and 25 mg L^{-1} α- and γ-Fe_2O_3 NPs for 4 and 10 days (Gürkan et al., 2021).

In the present work, WBC increase in fish exposed to FeNP may be a sign of inflammation, which could be triggered by ROS and tissue damage (Cazenave et al., 2019). In fact, oxidative damage was evidenced in the gills of fish exposed to FeNP, and additional organs can be affected, since Fe accumulated in all tissues analyzed. Another trigger of inflammation could be *T. harzianum* structures, which are more present in FeNP suspension. Although WBC decrease in fish exposed to AgNP may indicate that the ability of fish to fight infections is compromised, and WBC increase in fish exposed to FeNP may indicate an inflammatory response, the use of additional biomarkers of immunotoxicity, such as WBC functionality, lysozyme activity, and cytokine expression, would provide a better understanding of fish immune status in both exposures (Torrealba et al., 2019).

Nanoparticles did not affect AChE activity in brain and muscle. However, metal nanoparticles can affect AChE under certain conditions. For instance, environmental realistic concentrations as low as 10 µg L^{-1} TiO_2NP are capable of inducing decreases in muscle AChE activity in *P. lineatus* exposed for 5 days (Miranda et al., 2016). The presence of the capping in TiO_2NP may have protected *P. lineatus* from this effect.

5.5 Conclusion

The present work combined analysis of bioaccumulation with multiple biomarkers to understand the physiological process underlying the toxicity of metallic nanoparticles (AgNP, TiO_2NP, FeNP) synthesized using *T. harzianum* to the freshwater teleost *Prochilodus lineatus*. NPs promoted metal accumulation in tissues and affected hematology, plasma ions concentrations, histology of gills, energy metabolism, detoxification and redox homeostasis. Among the tissues, the gills were the main target organ for AgNP and FeNP toxicity, while the liver was the main target organ for TiO_2NP.

Taken together, the results indicate the NPs evaluated were not safe

at the concentrations tested. AgNP were responsible for most effects, and therefore can be considered more harmful, within the conditions tested, than TiO_2NP and FeNP. It is important to note that the concentration of each nanoparticle for application in agriculture is different, so the concentrations originally chosen for the present work would be those intended to be applied on crops. However, as we assumed that fish mortality would happen after AgNP exposure at the proper concentrations, fish were exposed to AgNP at a concentration ten times lower than the predicted for use in agriculture. Even so, AgNP elicited more effects than TiO_2NP and FeNP, which makes them potentially more harmful.

For the safe use of nanoparticles in agriculture, more studies are needed. Considering that *P. lineatus* was sensitive to NPs, its use as a biological model would be suitable for future evaluations, such as determining the no observed effect concentration (NOEC).

REFERENCES

Abarghoei, S., Hedayati, A., Ghorbani, R., Miandareh, H.K., Bagheri, T., 2016. Histopathological effects of waterborne silver nanoparticles and silver salt on the gills and liver of goldfish *Carassius auratus*. Int. J. Environ. Sci. Technol. 13, 1753–1760. https://doi.org/10.1007/s13762-016-0972-9

Ale, A., Bacchetta, C., Rossi, A.S., Galdopórpora, J., Desimone, M.F., de la Torre, F.R., Gervasio, S., Cazenave, J., 2018a. Nanosilver toxicity in gills of a neotropical fish: Metal accumulation, oxidative stress, histopathology and other physiological effects. Ecotoxicol. Environ. Saf. https://doi.org/10.1016/j.ecoenv.2017.11.072

Ale, A., Rossi, A.S., Bacchetta, C., Gervasio, S., de la Torre, F.R., Cazenave, J., 2018b. Integrative assessment of silver nanoparticles toxicity in *Prochilodus lineatus* fish. Ecol. Indic. 93, 1190–1198. https://doi.org/10.1016/j.ecolind.2018.06.023

Alves, L.C., Wood, C.M., 2006. The chronic effects of dietary lead in freshwater juvenile rainbow trout (*Oncorhynchus mykiss*) fed elevated calcium diets. Aquat. Toxicol. 78, 217–232. https://doi.org/https://doi.org/10.1016/j.aquatox.2006.03.005

Berndt, C., Lillig, C.H., 2017. Glutathione, Glutaredoxins, and Iron. Antioxidants Redox Signal. 27, 1235–1251. https://doi.org/10.1089/ars.2017.7132

Beutler, E., 1972. Red cell metabolism. Biochimie 54, 759–764. https://doi.org/10.1016/S0300-9084(72)80181-0

Beutler, E., Duron, O., Kelly, B.M., 1963. Improved method for the determination of blood glutathione. J. Lab. Clin. Med. 61, 882–888.

Bidinotto, P.M., Moraes, G., Souza, R.H.S., 1997. Hepatic glycogen and glucose in eight tropical fresh water teleost fish: a procedure for field determinations of micro samples. B. Téc. CEPTA 10, 53–60.

Bilesky-José, N., Maruyama, C., Germano-Costa, T., Campos, E., Carvalho, L., Grillo, R., Fraceto, L.F., De Lima, R., 2021. Biogenic α-Fe_2O_3 Nanoparticles Enhance the Biological Activity of *Trichoderma* against the Plant Pathogen *Sclerotinia sclerotiorum*. ACS Sustain. Chem. Eng. 9, 1669–1683. https://doi.org/10.1021/acssuschemeng.0c07349

Bolton, M.D., Thomma, B.P.H.J., Nelson, B.D., 2006. *Sclerotinia sclerotiorum* (Lib.) de Bary: Biology and molecular traits of a cosmopolitan pathogen. Mol. Plant Pathol. https://doi.org/10.1111/j.1364-3703.2005.00316.x

Bradford, M.M., 1976. A rapid and sensitive method for the quantitation of microgram quantities of protein utilizing the principle of protein-dye binding. Anal. Biochem. 72, 248–254. https://doi.org/10.1016/0003-2697(76)90527-3

Camejo, G., Wallin, B., Enojärvi, M., 1998. Analysis of Oxidation and Antioxidants Using Microtiter Plates, in: Armstrong, D. (Ed.), Free Radical and Antioxidant Protocols. pp. 377–388. https://doi.org/10.1385/0-89603-472-0:377

Carmo, T.L.L., Azevedo, V.C., de Siqueira, P.R., Galvão, T.D., dos Santos, F.A., dos Reis Martinez, C.B., Appoloni, C.R., Fernandes, M.N., 2018a. Reactive oxygen species and other biochemical and morphological biomarkers in the gills and kidneys of the Neotropical freshwater fish, Prochilodus lineatus , exposed to titanium dioxide (TiO_2) nanoparticles. Environ. Sci. Pollut. Res. 25, 22963–22976. https://doi.org/10.1007/s11356-018-2393-4

Carmo, T.L.L., Azevedo, V.C., Siqueira, P.R., Galvão, T.D., Santos, F.A., Martinez, C.B.R., Appoloni, C.R., Fernandes, M.N., 2018b. Mitochondria-rich cells adjustments and ionic balance in the Neotropical fish Prochilodus lineatus exposed to titanium dioxide nanoparticles. Aquat. Toxicol. 200, 168–177. https://doi.org/10.1016/j.aquatox.2018.05.006

Carmo, T.L.L., Siqueira, P.R., Azevedo, V.C., Tavares, D., Pesenti, E.C., Cestari, M.M., Martinez, C.B.R., Fernandes, M.N., 2019. Overview of the toxic effects of titanium dioxide nanoparticles in blood, liver, muscles, and brain of a Neotropical detritivorous fish. Environ. Toxicol. 34, 457–468. https://doi.org/10.1002/tox.22699

Carrola, J., Santos, N., Rocha, M.J., Fontainhas-Fernandes, A., Pardal, M.A., Monteiro, R.A.F., Rocha, E., 2014. Frequency of micronuclei and of other nuclear abnormalities in erythrocytes of the grey mullet from the Mondego, Douro and Ave estuaries-Portugal. Environ. Sci. Pollut. Res. 21, 6057–6068. https://doi.org/10.1007/s11356-014-2537-0

Casagrande, G., Casagrande, M.G., Costa, T.G., José, N.B., Stigliani, T.P., Carvalho, L., Fraceto, L.F., Lima, R. De, 2021. Influence of the capping of biogenic silver nanoparticles on their toxicity and mechanism of action towards *Sclerotinia sclerotiorum*. J. Nanobiotechnology 5, 1–19. https://doi.org/10.1186/s12951-021-00797-5

Cazenave, J., Ale, A., Bacchetta, C., Rossi, A.S., 2019. Nanoparticles Toxicity in Fish Models. Curr. Pharm. Des. 25, 3927–3942. https://doi.org/10.2174/1381612825666190912165413

Clauss, T.M., Dove, A.D.M., Arnold, J.E., 2008. Hematologic Disorders of Fish. Vet. Clin. North Am. - Exot. Anim. Pract. 11, 445–462. https://doi.org/10.1016/j.cvex.2008.03.007

Davis, A.K., Maney, D.L., Maerz, J.C., 2008. The use of leukocyte profiles to measure stress in vertebrates: A review for ecologists. Funct. Ecol. 22, 760–772. https://doi.org/10.1111/j.1365-2435.2008.01467.x

Dubois, M., Gilles, K.A., Hamilton, J.K., Rebers, P.A., Smith, F., 1956. Colorimetric Method for Determination of Sugars and Related Substances. Anal. Chem. 28, 350–356. https://doi.org/10.1021/ac60111a017

Ellman, G.L., Courtney, K.D., Andres, V., Feather-Stone, R.M., 1961. A new and rapid colorimetric determination of acetylcholinesterase activity. Biochem. Pharmacol. 7, 88–95.

Fraceto, L.F., Maruyama, C.R., Guilger, M., Mishra, S., Keswani, C., Singh, H.B., de Lima, R., 2018. *Trichoderma harzianum*-based novel formulations: potential applications for management of Next-Gen agricultural challenges. J. Chem. Technol. Biotechnol. 93, 2056–2063. https://doi.org/10.1002/jctb.5613

Gagné, F., 2014. Xenobiotic Biotransformation, in: Biochemical Ecotoxicology. Academic Press, pp. 117–130. https://doi.org/10.1016/B978-0-12-411604-7.00007-6

Gibbs, A., Somero, G., 1989. Pressure adaptation of Na^+/K^+-ATPase in gills of marine teleost fishes. J. Exp. Biol. 143, 475–492.

Girilal, M., Krishnakumar, V., Poornima, P., Mohammed Fayaz, A., Kalaichelvan, P.T., 2015. A comparative study on biologically and chemically synthesized silver nanoparticles induced Heat Shock Proteins on fresh water fish Oreochromis niloticus. Chemosphere 139, 461–468. https://doi.org/10.1016/j.chemosphere.2015.08.005

Graham, M.S., 1983. Why do 189–201.

Guilger, M., Pasquoto-Stigliani, T., Bilesky-Jose, N., Grillo, R., Abhilash, P.C., Fraceto, L.F., De Lima, R., 2017. Biogenic silver nanoparticles based on *Trichoderma harzianum*: Synthesis, characterization, toxicity evaluation and biological activity. Sci. Rep. 7, 1–13. https://doi.org/10.1038/srep44421

Gürkan, M., Gürkan, S.E., Yılmaz, S., Ateş, M., 2021. Comparative Toxicity of Alpha and Gamma Iron Oxide Nanoparticles in Rainbow Trout: Histopathology, Hematology, Accumulation, and Oxidative Stress. Water. Air. Soil Pollut. 232. https://doi.org/10.1007/s11270-021-04988-6

Handy, R.D., Henry, T.B., Scown, T.M., Johnston, B.D., Tyler, C.R., 2008. Manufactured nanoparticles: Their uptake and effects on fish - A mechanistic analysis. Ecotoxicology 17, 396–409. https://doi.org/10.1007/s10646-008-0205-1

Hanson, L.M., Obradovich, S., Mouniargi, J., Farrell, A.P., 2006. The role of adrenergic stimulation in maintaining maximum cardiac performance in rainbow trout (Oncorhynchus mykiss) during hypoxia, hyperkalemia and acidosis at 10°C. J. Exp. Biol. 209, 2442–2451. https://doi.org/10.1242/jeb.02237

Imani, M., Halimi, M., Khara, H., 2015. Effects of silver nanoparticles (AgNPs) on hematological parameters of rainbow trout, Oncorhynchus mykiss. Comp. Clin. Path. 24, 491–495. https://doi.org/10.1007/s00580-014-1927-5

Keen, J.H., Habig, W.H., Jakoby, W.B., 1976. Mechanism for the several activities of the glutathione S-transferases. J. Biol. Chem. 251, 6183–6188. https://doi.org/10.1016/s0021-9258(20)81842-0

Khoei, A.J., 2021. Evaluation of potential immunotoxic effects of iron oxide nanoparticles (IONPs) on antioxidant capacity, immune responses and tissue

bioaccumulation in common carp (Cyprinus carpio). Comp. Biochem. Physiol. Part - C Toxicol. Pharmacol. 244. https://doi.org/10.1016/j.cbpc.2021.109005

Krishnaraj, C., Harper, S.L., Yun, S. Il, 2016. In Vivo toxicological assessment of biologically synthesized silver nanoparticles in adult Zebrafish (Danio rerio). J. Hazard. Mater. 301, 480–491. https://doi.org/10.1016/j.jhazmat.2015.09.022

Lushchak, V.I., 2016. Contaminant-induced oxidative stress in fish: a mechanistic approach. Fish Physiol. Biochem. 42, 711–747. https://doi.org/10.1007/s10695-015-0171-5

Mansour, W.A.A., Abdelsalam, N.R., Tanekhy, M., Khaled, A.A., Mansour, A.T., 2021. Toxicity, inflammatory and antioxidant genes expression, and physiological changes of green synthesis silver nanoparticles on Nile tilapia (Oreochromis niloticus) fingerlings. Comp. Biochem. Physiol. Part - C Toxicol. Pharmacol. 247, 109068. https://doi.org/10.1016/j.cbpc.2021.109068

Maruyama, C.R., Bilesky-José, N., de Lima, R., Fraceto, L.F., 2020. Encapsulation of *Trichoderma harzianum* Preserves Enzymatic Activity and Enhances the Potential for Biological Control. Front. Bioeng. Biotechnol. 8, 1–14. https://doi.org/10.3389/fbioe.2020.00225

McCord, J.M., Fridovich, I., 1969. Superoxide dismutase. An enzymic function for erythrocuprein (hemocuprein). J. Biol. Chem.

Miranda, R.R., Damaso da Silveira, A.L.R., de Jesus, I.P., Grötzner, S.R., Voigt, C.L., Campos, S.X., Garcia, J.R.E., Randi, M.A.F., Ribeiro, C.A.O., Filipak Neto, F., 2016. Effects of realistic concentrations of TiO_2 and ZnO nanoparticles in Prochilodus lineatus juvenile fish. Environ. Sci. Pollut. Res. 23, 5179–5188. https://doi.org/10.1007/s11356-015-5732-8

Mohsenpour, R., Mousavi-Sabet, H., Hedayati, | Aliakbar, Rezaei, | Amir, Ahmad, |, Yalsuyi, M., Faggio, C., 2020. In vitro effects of silver nanoparticles on gills morphology of female Guppy (Poecilia reticulate) after a short-term exposure. https://doi.org/10.1002/jemt.23549

Nikinmaa, M., 2014. Detoxification, in: Nikinmaa, M. (Ed.), An Introduction to Aquatic Toxicology. Academic Press, Oxford, pp. 87–98. https://doi.org/https://doi.org/10.1016/B978-0-12-411574-3.00009-8

Oliveira, L.F. de, Santos, C., Risso, W.E., dos Reis Martinez, C.B., 2018. Triple-mixture of Zn, Mn, and Fe increases bioaccumulation and causes oxidative stress in freshwater neotropical fish. Environ. Toxicol. Chem. 37, 1749–1756.

https://doi.org/10.1002/etc.4133

Ottoni, C.A., Lima Neto, M.C., Léo, P., Ortolan, B.D., Barbieri, E., De Souza, A.O., 2020. Environmental impact of biogenic silver nanoparticles in soil and aquatic organisms. Chemosphere. https://doi.org/10.1016/j.chemosphere.2019.124698

Peplow, D., Edmonds, R., 2005. The effects of mine waste contamination at multiple levels of biological organization. Ecol. Eng. 24, 101–119. https://doi.org/10.1016/j.ecoleng.2004.12.011

Poleksic, V., Mitrovic-Tutundzic, V., 1994. Fish gills as a monitor of sublethal and chronic effects of pollution. In: Sublethal and Chronic Effects of Pollutants on Freshwater Fish. Sublethal Chronic Eff. Pollut. Freshw. Fish 339–352.

Remya, A.S., Ramesh, M., Saravanan, M., Poopal, R.K., Bharathi, S., Nataraj, D., 2015. Iron oxide nanoparticles to an Indian major carp, Labeo rohita: Impacts on hematology, iono regulation and gill Na+/K+ ATPase activity. J. King Saud Univ. - Sci. 27, 151–160. https://doi.org/10.1016/j.jksus.2014.11.002

Rheder, D.T., Guilger, M., Bilesky-José, N., Germano-Costa, T., Pasquoto-Stigliani, T., Gallep, T.B.B., Grillo, R., Carvalho, C. dos S., Fraceto, L.F., Lima, R., 2018. Synthesis of biogenic silver nanoparticles using *Althaea officinalis* as reducing agent: evaluation of toxicity and ecotoxicity. Sci. Rep. 8, 1–11. https://doi.org/10.1038/s41598-018-30317-9

Samrot, A. V., SaiPriya, C., Lavanya Agnes Angalene, J., Roshini, S.M., Jane Cypriyana, P.J., Saigeetha, S., Raji, P., Suresh Kumar, S., 2019. Evaluation of Nanotoxicity of Araucaria heterophylla Gum Derived Green Synthesized Silver Nanoparticles on Eudrilus eugeniae and Danio rerio. J. Clust. Sci. 30, 1017–1024. https://doi.org/10.1007/s10876-019-01561-4

Saravanan, M., Suganya, R., Ramesh, M., Poopal, R.K., Gopalan, N., Ponpandian, N., 2015. Iron oxide nanoparticles induced alterations in haematological, biochemical and ionoregulatory responses of an Indian major carp Labeo rohita. J. Nanoparticle Res. 17, 1–12. https://doi.org/10.1007/s11051-015-3082-6

Sarkar, B., Netam, S.P., Mahanty, A., Saha, A., Bosu, R., Krishnani, K.K., 2014. Toxicity Evaluation of Chemically and Plant Derived Silver Nanoparticles on Zebrafish (Danio rerio). Proc. Natl. Acad. Sci. India Sect. B - Biol. Sci. 84, 885–892. https://doi.org/10.1007/s40011-013-0298-z

Shaluei, F., Hedayati, A., Jahanbakhshi, A., Kolangi, H., Fotovat, M., 2013. Effect of subacute exposure to silver nanoparticle on some hematological and plasma

biochemical indices in silver carp (Hypophthalmichthys molitrix). Hum. Exp. Toxicol. 32, 1270–1277. https://doi.org/10.1177/0960327113485258

Shobana, C., Rangasamy, B., Poopal, R.K., Renuka, S., Ramesh, M., 2018. Green synthesis of silver nanoparticles using Piper nigrum: tissue-specific bioaccumulation, histopathology, and oxidative stress responses in Indian major carp Labeo rohita. Environ. Sci. Pollut. Res. 25, 11812–11832. https://doi.org/10.1007/s11356-018-1454-z

Singh, M., Barman, A.S., Devi, A.L., Devi, A.G., Pandey, P.K., 2019. Iron mediated hematological, oxidative and histological alterations in freshwater fish *Labeo rohita*. Ecotoxicol. Environ. Saf. 170, 87–97. https://doi.org/10.1016/j.ecoenv.2018.11.129

Singh, P., Kim, Y.J., Zhang, D., Yang, D.C., 2016. Biological Synthesis of Nanoparticles from Plants and Microorganisms. Trends Biotechnol. 34, 588–599. https://doi.org/10.1016/j.tibtech.2016.02.006

Thangapandiyan, S., Alif Alisha, A.S., Anidha, K., 2020. Growth performance, hematological and biochemical effects of iron oxide nanoparticles in Labeo rohita. Biocatal. Agric. Biotechnol. 25, 101582. https://doi.org/10.1016/j.bcab.2020.101582

Torrealba, D., More-Bayona, J.A., Wakaruk, J., Barreda, D.R., 2019. Innate immunity provides biomarkers of health for teleosts exposed to nanoparticles. Front. Immunol. https://doi.org/10.3389/fimmu.2018.03074

Ueda, T., Hayashi, M., Ohtsuka, Y., Nakamura, T., Kobayashi, J., Sofuni, T., 1992. A preliminary study of the micronucleus test by acridine orange fluorescent staining compared with chromosomal aberration test using fish erythropoietic and embryonic cells. Water Sci. Technol. 26, 235–240. https://doi.org/10.2166/wst.1992.0297

Vidya, P. V, Chitra, K.C., 2019. Irreversible Histopathological Modifications Induced by Iron Oxide Nanoparticles in the Fish, *Oreochromis mossambicus* (Peters, 1852). Biol. Forum-An Int. J. 11, 01–06.

Webb, N.A., Wood, C.M., 1998. Physiological analysis of the stress response associated with acute silver nitrate exposure in freshwater rainbow trout (*Oncorhynchus mykiss*). Environ. Toxicol. Chem. 17, 579–588. https://doi.org/10.1897/1551-5028(1998)017<0579:PAOTSR>2.3.CO;2

Wolf, J.C., Wolfe, M.J., 2005. A Brief Overview of Nonneoplastic Hepatic Toxicity in

Fish. Toxicol. Pathol. 33, 75–85. https://doi.org/10.1080/01926230590890187

Wood, C.M., 2012. Silver, in: Chris M. Wood, A.P.F. and C.J.B. (Ed.), Homeostasis and Toxicology of Non-Essential Metals. Academic Press, London, pp. 1–54.

Xiang, Q.Q., Gao, Y., Li, Q.Q., Ling, J., Chen, L.Q., 2020. Proteomic profiling reveals the differential toxic responses of gills of common carp exposed to nanosilver and silver nitrate. J. Hazard. Mater. 394, 122562. https://doi.org/10.1016/j.jhazmat.2020.122562

6 CONSIDERAÇÕES FINAIS

A aplicação da Nanotecnologia para a agricultura sustentável é promissora, mas os nanomateriais são contaminantes emergentes cujos efeitos e impactos para o ambiente ainda estão sendo compreendidos. Nesse contexto, esta dissertação buscou compreender os efeitos de nanopartículas metálicas de síntese biológica para duas espécies nativas de animais dulcícolas. A avalição dos efeitos dessas nanopartículas se faz necessária devido ao seu potencial uso agrícola, mas também porque os efeitos de nanopartículas metálicas de síntese biológica ainda são pouco conhecidos, ainda que se saiba que sua composição e atividade se distinguem de nanopartículas de síntese física e química.

Todas as nanopartículas causaram bioacumulação de metais em ambas as espécies. Esse resultado está de acordo com a hipótese 4, mas contradiz as hipóteses 5 e 6. O presente trabalho discutiu a bioacumulação do metal em si (incluindo íons, nanopartículas e complexos), não sendo possível determinar se o metal foi absorvido pelos animais como nanopartícula, ou se houve transformações previamente e após a absorção. No entanto, a bioacumulação de ferro em todos os tecidos avaliados de *P. lineatus* sugere que as nanopartículas foram absorvidas, pois o ferro em outras formas químicas (por exemplo, quando adicionado como sal) não se mostra tão biodisponível.

Assim, a bioacumulação de ferro em todos os tecidos avaliados de *P. lineatus* foi o resultado mais marcante, tornando evidente a biodisponibilidade das FeNP. A resolução CONAMA 357/05 estabelece o valor máximo de 0,3 mg L^{-1} de Fe dissolvido para corpos de água doce de classe 1, os quais podem se destinar à proteção das comunidades aquáticas. Assumindo que essa concentração de ferro esteja adequada para a proteção dos ecossistemas aquáticos, de acordo com pesquisas em que se avaliou o ferro em outras formas químicas que não nanopartículas, o presente trabalho mostra que concentrações mais baixas de ferro dissolvido podem ser tóxicas, quando na forma de nanopartícula. Assim, a toxicidade de nanopartículas se distingue daquela dos metais em outras formas químicas. É importante ressaltar que os efeitos tóxicos provocados pelas FeNP no presente trabalho ocorreram em condições de laboratório, e seu comportamento pode mudar no ambiente aquático, em que a concentração de matéria orgânica, por exemplo, é maior. No entanto, os resultados de acúmulo de ferro e de seus efeitos tóxicos, tais

como danos oxidativos, em concentrações de ferro mais baixas do que as presentes na resolução CONAMA, sugerem a necessidade de mais estudos com nanopartículas metálicas, para que seja possível rever a legislação.

Quando observados os fluidos e tecidos em que houve acúmulo, o acúmulo de metal (Ag, Ti e Fe) na hemolinfa dos bivalves e no plasma dos teleósteos foi comum a todas as nanopartículas. É possível que as características fisioquímicas das nanopartículas utilizadas neste trabalho prolonguem o seu tempo na circulação dos animais, como ocorre com algumas nanopartículas com aplicações na biomedicina.

Dentre as nanopartículas, as AgNP foram responsáveis pela maioria dos efeitos provocados em ambas as espécies. No entanto, a toxicidade provocada pela prata foi de caráter osmorregulatório em bivalves, mas respiratório em teleósteos. Além disso, a concentração de exposição para os teleósteos foi dez vezes menor do que para os bivalves, o que sugere que *P. lineatus* seja mais sensível às AgNP do que *A. trapesialis*. Apesar dos bivalves serem citados como organismos-alvo para a toxicidade de nanopartículas, a espécie utilizada neste trabalho se mostrou menos sensível às nanopartículas, em relação ao teleósteo juvenil utilizado, o que contradiz a hipótese 3.

A hipótese 2 supunha que os efeitos provocados por cada tipo de nanopartícula (AgNP, TiO_2NP ou FeNP) apresentariam similaridades e discrepâncias entre si, sendo as discrepâncias relacionadas à toxicidade do metal que compõe a nanopartícula. De fato, similaridades foram observadas, sendo elas: a) o acúmulo do respectivo metal na hemolinfa de bivalves e no plasma e rim posterior de teleósteos, como já mencionado; b) a diminuição de mesma intensidade na atividade da glutationa S-transferase no fígado de *P. lineatus*, após todas as exposições; e c) o aumento de glicogênio no fígado de *P. lineatus* após exposição às TiO_2NP e FeNP. Em relação às discrepâncias, algumas se relacionaram com a toxicidade do metal, a saber: a) a diminuição de sódio e cloreto na hemolinfa de *A. trapesialis* após exposição às AgNP, efeito conhecido da prata; e b) danos oxidativos nas brânquias de *P. lineatus* após exposição às FeNP, sendo o ferro conhecidamente pró-oxidante em concentrações acima das essenciais.

Por fim, foi possível distinguir as AgNP como as nanopartículas mais prejudiciais, em detrimento das TiO_2NP e FeNP, *in vivo*, em condições de laboratório, para espécies nativas.

7 ANEXO

UNIVERSIDADE
ESTADUAL DE LONDRINA

COMISSÃO DE ÉTICA NO USO DE ANIMAIS

OF. CIRC. CEUA Nº 05/020

Londrina, 05 de fevereiro de 2020.

Prezado (a) professor (a),

Certificamos a aprovação do projeto de pesquisa intitulado: "**Efeitos subletais de nanopartículas biológicas de dióxido de titânio, de ferro e de prata no teleósteo neotropical *Prochilodus lineatus***" protocolo CEUA nº**463.2020.75** sob a responsabilidade de **Cláudia Bueno dos Reis Martinez** que envolve a produção, manutenção e/ou utilização de animais pertencentes ao filo Chordata, subfilo Vertebrata (exceto o homem) para fins de pesquisa científica (ou ensino), encontra-se de acordo com os preceitos da Lei nº 11.794, de 8 de outubro de 2008, do Decreto nº 6.899, de 15 de julho de 2009, e com as normas editadas pelo Conselho Nacional de Controle da Experimentação Animal (CONCEA), e foi **aprovado** pela Comissão de Ética no Uso de Animais da Universidade Estadual de Londrina (CEUA/UEL) em reunião do dia **04/02/2020**.

Este projeto tem por objetivo avaliar os efeitos subletais da exposição aguda a nanopartículas biológicas de dióxido de titânio, de ferro e de prata no teleósteo *Prochilodus lineatus*. **Grau de invasividade: 2.**

Finalidade	( ) Ensino (x) Pesquisa científica
Vigência da autorização	05/02/2020 a 06/02/2021
Espécie/ linhagem/ raça	Peixe/ *Prochilodus lineatus* (Curimba)
Nº de animais	32
Peso/ Idade	10 g/ juvenis
Sexo	Machos ou fêmeas
Origem	Piscicultura Venites, localizada em Toleto (PR)
Amostras a serem coletadas	Sangue, brânquias, fígado, trato de gastrointestinal, bile, rim posterior, músculo e cérebro

Cumpre orientar que caso pretendam-se quaisquer alterações no protocolo experimental aprovado, deve-se submeter o novo protocolo à apreciação da CEUA/UEL anteriormente à execução das modificações.

Em cumprimento às exigências do CONCEA, em até 30 dias da finalização do projeto de pesquisa ou extensão, conforme vigência expressa neste ofício, encaminhar relatório da descrição de uso de animais para ceua@uel.br, conforme modelo disponível no site da CEUA/UEL (http://www.uel.br/comites/ceua/pages/relatorio-de-projetos.php).

Coloco-me à disposição para quaisquer esclarecimentos que se fizerem necessários. Sem mais para o momento, subscrevo-me, cordialmente.

Maria Fernanda R. Graciano

Profª Drª Maria Fernanda Rodrigues Graciano
Coordenadora da CEUA/UEL

Profª Drª Maria Fernanda Rodrigues Graciano
Coordenadora da Comissão de Ética no Uso de Animais
Universidade Estadual de Londrina
(43) 3371-5454

Ilmo.(a) Sr.(a)
Prof. (a) Dr (a). Cláudia Bueno dos Reis Martinez
Responsável pelo projeto
C/C para Depto. de Ciências Fisiológicas/CCB
C/C para a Direção do Centro de Ciências Biológicas